The PHILOSOPHICAL MAGAZINE

UNIVERSITY OF HAWAII LIBRARY
JAN 18 '54

FIRST PUBLISHED IN 1798

L. 44 SEVENTH SERIES No. 359 December 1953

A Journal of Theoretical Experimental and Applied Physics

EDITOR
PROFESSOR N. F. MOTT, M.A., D.Sc., F.R.S.

EDITORIAL BOARD
SIR LAWRENCE BRAGG, O.B.E., M.C., M.A., D.Sc., F R.S.
SIR GEORGE THOMSON, M.A., D.Sc., F.R.S.
PROFESSOR A. M. TYNDALL, C.B.E., D.Sc., F.R.S.

PRICE 15s. 0d.
Annual Subscription £8 0s. 0d. payable in advance

AND PUBLISHED BY TAYLOR & FRANCIS LTD., RED LION COURT, FLEET ST., LONDON, E.C.4.

ALERE FLAMMAM

THE MATHEMATICAL WORKS OF JOHN WALLIS, D.D., F.R.S.

by

J. F. SCOTT, Ph.D., B.A.

"His work will be indispensable to those interested in the early history of The Royal Society. I commend to all students of the Seventeenth Century, whether scientific or humane, this learned and lucid book."—Extract from foreword by Prof. E. N. da C. Andrade, D.Sc., Ph.D., F.R.S.

Recommended for publication by University of London

12/6 net

Printed and Published by

TAYLOR & FRANCIS, LTD.

RED LION COURT, FLEET STREET, LONDON, E.C.4.

DECADE 1941–50

We are requested by many of our clients overseas, to purchase on their behalf

PHILOSOPHICAL MAGAZINE

and all other important Scientific Journals for the years 1941–50 during which time, owing to war restrictions their supply was stopped.

YOUR OFFERS WILL BE APPRECIATED

Complete sets and longer runs also required by

THE SCIENTIFIC BOOK SUPPLY SERVICE
(T. FREDERICK DE LOCHE)
5 FETTER LANE, FLEET ST., LONDON, E.C.4.

All enquiries for Advertisements to:

ADVERTISEMENT MANAGER,
22a College Hill, Cannon Street,
London, E.C.4
Telephone: CITy 2381

CXXXVIII. *The Thickness of the Saturated Helium II Film*

By Raymond Bowers
Institute for the Study of Metals, University of Chicago*

[Received August 18, 1953]

Abstract

The average thickness of the saturated He II film on an aluminium foil has been measured by a gravimetric method. For the film in contact with the bulk liquid, values between 120 and 180 atomic layers ($4{\cdot}8\times10^{-6}$ cm and $7{\cdot}2\times10^{-6}$ cm) have been observed, depending on the height of the specimen above the bulk liquid level. The average thickness is independent of temperature except within 0·006 degrees of the lambda point. The values obtained suggest a film profile $d=11{\cdot}8\times10^{-6}/h^{1/2}$, where d is the actual film thickness in cm at a height h above the liquid level. For the He II film not in direct contact with the liquid, a thickness of 55 atomic layers ($2{\cdot}2\times10^{-6}$ cm) has been observed, independent of temperature and position of the bulk liquid level. This value is discussed in terms of a lack of temperature equilibrium. Observations of the evaporation of the film by radiation influx have been made. The possibility that the disparity between the results of various film determinations may be due to differing conditions of heat influx is considered in the discussion.

§ 1. Introduction

In spite of numerous measurements of the thickness of the saturated† helium II film, this fundamental property of the film is still not known with any certainty. The earliest experiments of Daunt and Mendelssohn (1939) and those of Kikoin and Lasarew (1938, 1939) indicated that the saturated film was approximately 100 atomic layers. Actually, the individual results at different temperatures obtained by Daunt and Mendelssohn varied in a random manner from 2·7 to $4{\cdot}9\times10^{-6}$ cm (70 to 120 atomic layers). More recent work has yielded a considerable amount of data for the thickness of the film, but there is little consistency between the data of different workers. In table 1 we have summarized the principal results of a number of investigations. For simplicity, we shall consider the general magnitudes

---

* Communicated by the Author.

† Most of the work described in the paper refers to the film in direct contact with the liquid. The special case of a film isolated from the liquid except via the vapour is discussed in the text, but it is referred to specifically as the 'isolated film'.

observed; and we have not included fine details such as variation with temperature and height of the film above the bulk liquid level. A more detailed analysis of previous work is given by Atkins (1950).

Table 1

Investigation	Method	Substrate	Thickness
Daunt and Mendelssohn 1939	Volumetric	Metal	$3{\cdot}6\times10^{-6}$ cm
Kikoin and Lasarew 1938, 1939	Volumetric	Metal	$2\text{–}3\times10^{-6}$ cm
Burge and Jackson 1949	Optical	Thin layer of barium stearate	2×10^{-6} cm, varying with height and slightly with temperature
Long and Meyer 1949	Volumetric absorption	Rouge	$6{\cdot}4\times10^{-6}$ cm
Atkins 1950	Film oscillation	Glass	2×10^{-6} cm, varying with height, temperature and nature of surface

(Helium film of 100 atomic layers is equivalent to 4×10^{-6} cm)

It is evident from the table that there are large disparities between the results of various investigations. Actually, they are larger than is immediately obvious from the table. For example, the result of Burge and Jackson is the thickness at a height of 1 cm above the liquid level; on the other hand, Daunt and Mendelssohn's value is an average over 3 to 18 cm of film above the liquid level. If the thickness (d) of the film varies with height (h) above the bulk liquid level according to the relation

$$d=k/h^{1/n} \qquad \ldots\ldots\ldots \quad (1)$$

where k is a constant and $n=2$ or 3 (Frenkel 1940, Schiff 1941, Bijl, de Boer and Michels 1941) then an extrapolation of the Burge–Jackson result to the heights involved in the experiment of Daunt and Mendelssohn results in a discrepancy of about five times.

It is not obvious that there are systematic differences between the various investigations, of a type which might explain the gross disparities. In allied studies, such as those of adsorbed films, one would immediately consider the nature of the surfaces used. However, apart from considerations such as those of Frenkel (1940) involving surface energies and those of Bowers (1953 b) for the special case of a fine powder, it is not easy to see how the substrate could determine the thickness of a film as thick as the one being considered here. The forces between a helium atom and the substrate must be of very short range compared with any of the measured values for the Helium II film thickness (see case of classical liquids, Bowden and Throssell 1951). The extent to which a substrate can affect the film is best seen from the value of E_1, the energy of adsorption of the first atomic layer. The influence of substrate on E_1 has not been studied extensively for helium and it is complicated by the fact that E_1 varies with amount adsorbed (Keesom and Schweers 1941), but it is well known that for other gases E_1 varies very little as the substrate (non-ionic) is changed (Brunauer 1945, p. 244).

In considering a possible variation of film thickness with substrate, it is tempting to use the observed independence of film transfer on the chemical nature of the substrate (Chandrasekhar and Mendelssohn 1952) as an argument for a film thickness which does not change with surface. However, the transport property is not a good criterion for considering the thickness of the film. The total mass transfer is the product of a linear velocity in the film and the thickness involved and there is some reason for believing that this product is invariant with respect to a change in linear velocity or thickness (see Dingle 1952, Equation 135).

The discussion given above indicates some of the difficulties in understanding the disparity between the results of different investigations. The investigation to be described in this paper was undertaken to obtain further data for a resolution of these difficulties. The film thickness has been measured by a gravimetric method. This method is direct, there being no corrections necessary to the observed weight of the helium II film apart from the evaluation of the surface roughness factor of the specimen. The technique used was the same as for similar studies of unsaturated films (Bowers 1953 a, 1953 b). The microbalance assembly has been described elsewhere (Bowers and Long 1953). A summary of the results has already been published (Bowers 1953 c).

§ 2. METHOD

The measurements were made on an aluminium foil 7·6 cm × 5 cm and 0·002 cm in thickness. The shape of the specimen is of great importance in this investigation since it must have no folds or pores of a type that would retain bulk liquid. Since the thickness of the film forming on it is determined from the effective increase in weight of the specimen, it is essential that no drops of bulk liquid be included in the total weight. The form shown in fig. 1 was the one found most suitable for our work. The foil was folded into a series of smooth ‘ s ’ bends. Care was taken to ensure that the folds of the foil did not touch each other and that no sharp bends appeared in it.

In order to support the specimen from the wires which hang from the beam of the microbalance, holes were cut into the top of the foil. The holes had a diameter of 1 mm and were large enough so that a sheet of liquid would not be maintained across them by surface tension. A narrow tail (diameter 0·002 in.) was attached to the bottom of the specimen in order that contact could be made between the specimen and the liquid below.

The design of a suitable specimen has been the greatest single difficulty in this investigation. For our work on unsaturated films, it was sufficient to use a loosely wound coil, but at saturation the formation and retention of liquid between the folds rendered a precise determination of the film thickness impossible. Experiments at saturation, using such a specimen, yielded very high values for the film thickness with little consistency both above and below the lambda point. It was observed that the apparent thickness could be increased by tightening the windings of the coil, indicating the presence of bulk liquid. After numerous experiments with specimens of this kind, it was concluded that the specimen must approximate more closely the conditions of a plane sheet. In using the specimen shown in fig. 1, it was necessary to reduce the area of the foil by a factor 4 since it is not as compact as the coils mentioned. Hence a fourfold decrease in the sensitivity was expected.

Fig. 1

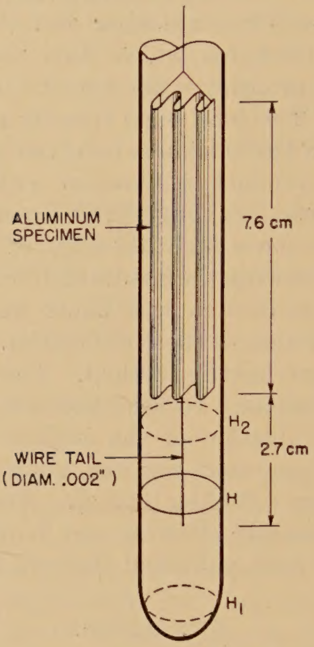

The specimen was cleaned and outgassed as in the work on unsaturated films. Its effective area was determined from a measurement of the nitrogen isotherm. The effective area was found to be 97 cm^2, giving a roughness factor of 1·3, in agreement with our previous work. Thus 1 atomic layer of helium on the specimen weighs 0·40 μg, assuming the liquid spacing of 4 Å. (The balance sensitivity is 0·0158 mm/μg.)

With the exception of the specimen and some alterations in the radiation shielding, the arrangement used was precisely the same as that used in the earlier work (Bowers 1953 a, 1953 b). We have improved the radiation shielding by placing an extra shield on the specimen support wire itself at 10 cm above the specimen. (See fig. 4, Bowers and Long 1953.)

The liquid in the specimen chamber is condensed in at a slight over-pressure. While this is being done, drops form on the specimen, but they appear to evaporate or fall off in a few minutes ; the fact that measurements of the saturated film of He I and also that of liquid nitrogen gave about 10 atomic layers confirms our belief that no appreciable amount of bulk liquid adhered to the specimen. In the case of He II, the measurements made were as follows : the change in weight of the specimen was observed as the liquid helium level (H) in the specimen chamber was raised from a height H_1 at the bottom of the chamber to a height H_2 within 3 mm of the bottom of the foil. It can be seen from fig. 1 that until the liquid level touches the tail of the specimen, the liquid and the foil are not in direct contact ; on touching the tail, contact is made via the mobile film on this tail. The zero position for the balance is determined as in our previous work by observing the position of the balance beam at 15% saturation.

The film thickness obtained on dividing the change in weight of the specimen by the product of its area and the density of the film, is an average thickness over the specimen. In considering the values obtained, we must take account of the film profile, i.e., the variation of the actual film thickness with height above the liquid level. If the profile of the film is given by eqn. (1) above, then the weight of film is obtained by integrating (1) over the height of the specimen. It is easily shown that the weight w is given by

$$w=\frac{n}{n-1}\frac{\rho AK}{a}[h_2^{n-1/n}-h_1^{n-1/n}] \quad . \quad . \quad . \quad . \quad . \quad . \quad (2)$$

where ρ is the density of the film, A is the total effective area of the foil (97 cm²) and a is the vertical length of the foil (7·6 cm). The limiting heights h_1 and h_2 are shown in the inset of fig. 2. Expressed in another form, the average number of layers (N)

$$N=\frac{W}{\rho At}=\frac{n}{n-1}\frac{K}{at}[h_2^{n-1/n}-h_1^{n-1/n}] \quad . \quad . \quad . \quad . \quad (3)$$

where t is the atomic spacing (4 Å for all but the first few layers). Hence the film profile can be decided from our observations.

§ 3. RESULTS

The first measurements made with liquid helium were to check our data on the unsaturated film. The principal observations were repeated and verified ; close to saturation ($p/p_0=0{\cdot}9992$) the film is only 20 atoms thick. When this had been established, liquid helium II was condensed into the specimen chamber and the average film thickness was observed as the liquid helium level was raised from the bottom of the specimen chamber (H_1 in fig. 1) until it touched the tail of the specimen. This thickness of the isolated film was found to be 55 atomic layers, independent of temperature and also independent of the level of the liquid.

These observations will be discussed later, but it is convenient to mention some aspects of the observations which concern the sensitivity of our method. In our work on the unsaturated film, using a specimen of four times the area, it was possible to measure thicknesses to within one atomic layer. In this case, the accuracy seemed to be limited by the ultimate sensitivity of the balance. However, when measuring the film thickness in the presence of bulk liquid, we have found the scatter was higher than the four atomic layers expected. When liquid is present, the balance is less stable ; small fluctuations in temperature produce large spurious deflections of the balance. Even when controlling the temperature to 1/1000 of a degree, we have not found it possible to reduce the scatter below 5–10 atomic layers. The greater instability observed when bulk liquid is present is probably due to the fact that when a slight temperature change occurs, a small amount of helium evaporates or condenses in the liquid below the specimen. The resulting movement of gas disturbs the balance. This type of instability might ultimately limit the extent to which the sensitivity of the gravimetric method can be increased.

Fig. 2

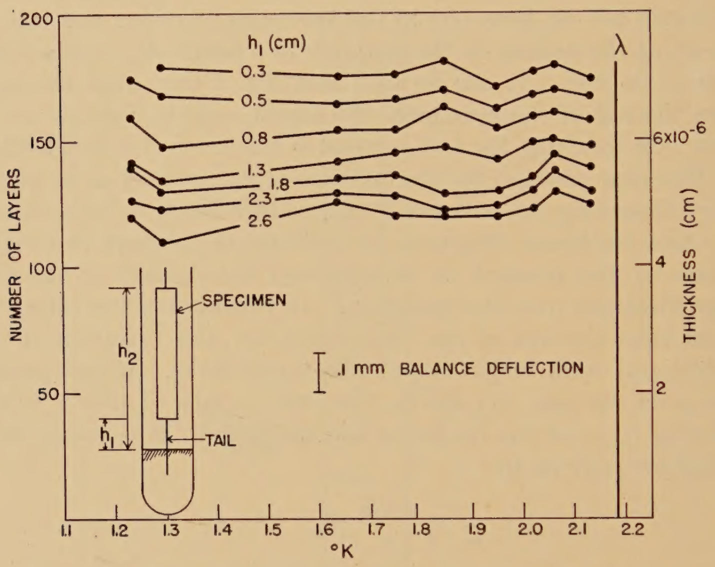

Variation of average thickness with temperature for various positions of the bulk liquid level.

We shall now describe our observations of average film thickness as the liquid level is raised further so that it is in contact with the wire tail. The variation of this thickness with temperature for various positions of the bulk liquid level in contact with the tail is shown in fig. 2. (Small corrections have been made for the effect of buoyancy and surface tension on the immersed part of the tail.) In this figure, h_1 is the distance of the bulk liquid level from the bottom of the foil. It can be seen that the values illustrated refer to distances of the liquid level from the bottom of the foil which vary between 2·6 cm and 0·3 cm. The experimental points have been connected by straight lines to distinguish corresponding data. We believe that the thickness, for a given height of the bulk liquid, is independent of temperature within our experimental error.

Fig. 3

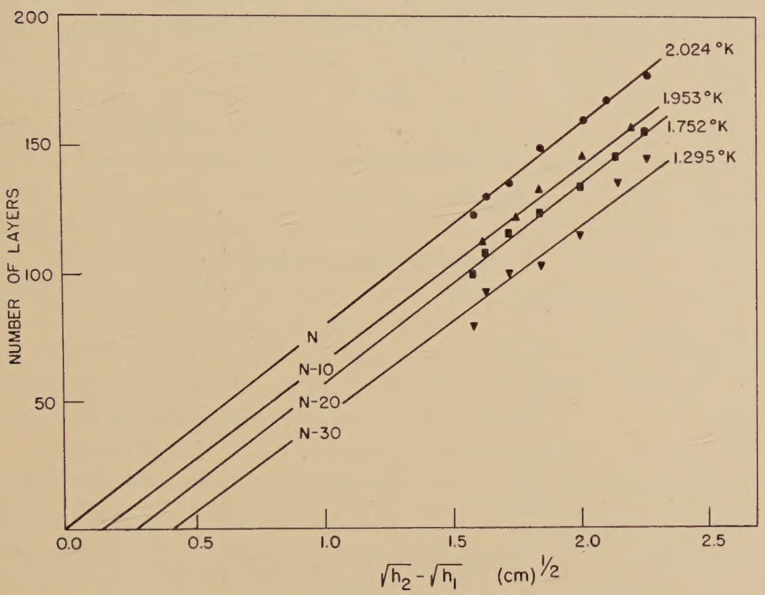

The variation of N with $\sqrt{h_2}-\sqrt{h_1}$. (To prevent overlap, the data for different temperatures have been displaced vertically by 10 atomic layers. The lines have been drawn to pass through the appropriate origin.)

With regard to the film profile, our data are best described by taking $n=2$ in eqn. (3) for all temperatures. In this case

$$N=\frac{2K}{at}\left(h_2^{1/2}-h_1^{1/2}\right). \quad . \quad . \quad . \quad . \quad . \quad . \quad . \quad . \quad (4)$$

Graphs of N against $h_2^{1/2}-h_1^{1/2}$ are shown in fig. 3 for a number of temperatures. The values of K calculated for different temperatures are shown in fig. 4. This graph, which is really a smoothed representation of all the data, shows the lack of dependence of film thickness on temperature (except very close to the lambda point).

Observations have also been made on the thickness of the saturated film above the lambda point. It is more difficult to measure the film thickness above the lambda point because the temperature cannot be held very steady. At 2·25°K we estimate the thickness of the saturated film to be between 10 and 15 atomic layers. This agrees with the work of Jackson and Henshaw (1953), but is smaller than the values due to Kistemaker (1947). We have also attempted to observe the precise temperature interval in which the thickness of the He II film falls from approximately 150 layers to the 10 layers observed above the lambda point. For this observation our specimen has certain disadvantages compared with that used by Burge and Jackson. The rate at which the film forms on our specimen is governed to some extent by the film creeping up the wire tail (diameter 0·002 in.). At the lowest temperatures, it is easily calculated that creep up the wire alone could furnish the complete film in about ten minutes. (Of course, equilibrium is reached in a shorter time.) However, very close to the lambda point, film creep up the wire becomes very small and above 2·17°K it is necessary to wait for more than a half hour for equilibrium. It is not easy to increase the diameter of the tail because buoyancy and surface tension corrections for the immersed part become large.

Fig. 4

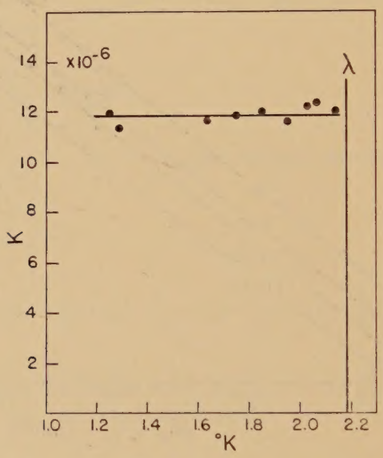

The variation of *K* with temperature.

Taking care to ensure that equilibrium had been reached, we found that the film maintained its full thickness to within 0·006 degrees of the lambda point. It was difficult to place more precise limits on the temperature interval than this because the experiments become very tedious nearer the lambda point. Our observation is essentially in agreement with that of Burge and Jackson who quote the interval as 0·004°K.

A series of observations have been made with the purpose of evaluating the influence of heat influx by radiation on the film thickness. It will be more convenient to discuss the results recorded so far before describing these observations.

§ 4. DISCUSSION

We shall first consider the case of the film which is isolated from the bulk liquid. This film was observed to be thinner than the film in contact with the liquid by a factor between 2·5 and 3·3. The heat contact due to the film creeping up the tail is not present in the case of the isolated film ; accordingly, we interpret the reduction in film thickness as being due to a lack of complete temperature equilibrium. An experiment by Daunt and Mendelssohn (Mendelssohn 1946) gave the result that an isolated film under conditions similar to these was only one-tenth as thick as when the specimen was in contact with the bulk liquid. The difference between their 10% and our 30% is attributed to fine differences in heat influx and the actual values obtained have little significance since they refer to a steady state but not to temperature equilibrium. Our interpretation of the smaller thickness of the isolated film is supported by the observation that for the film in contact with the liquid, the approach to equilibrium is slow very near the lambda point where the film creep is low. Nevertheless, it is surprising that heat and mass exchange between the film and the ambient vapour should be small enough for the creep rate to have this influence on equilibrium time. It is easily calculated that under the equilibrium conditions of our experiment, about $1{\cdot}5\times10^{23}$ molecules (1 g) hit 1 cm^2 of foil per second (Mayer and Mayer 1940). With such a large flux, only a small accommodation coefficient between vapour molecules and the film can explain our observations.*

The thickness of the film in contact with the liquid measured in this investigation is more in accord with the results of Daunt and Mendelssohn and also of Long and Meyer than with those of Atkins and of Burge and Jackson. Actually, if our result $d=11{\cdot}8\times10^{-6}/h^{1/2}$ is averaged over the heights involved in the Daunt and Mendelssohn experiment, close agreement is obtained with their data. The value of the constant K observed by us is about 6 times that given by Atkins and by Burge and Jackson. However, the value of K recorded by Burge and Jackson arises from measurements of film thickness at about 1 cm above the liquid. It would not be correct to assume that our value of K gives the actual thickness of the film at a height of 1 cm above the liquid, because this would involve an extrapolation of our data well into a region which is not measured in the experiments. We have not checked the validity of eqn. (1) at small heights ; the highest film thickness observed by us refers to a film extending from 0·3 cm to 7·9 cm above the liquid level.

In looking for a general scheme into which one could fit the variety of values recorded by different workers, it is well to observe that, with the exception of the value due to Long and Meyer, the film thickness appears to be greater on metal surfaces than it is on dielectrics, as suggested by Frenkel. The data of Long and Meyer were obtained from an adsorption measurement on finely divided rouge. It has already been pointed out (Bowers 1953 b) that one would expect very high values for the film thickness in this case, since the measurement corresponds to a film at an effective height of the order of the grain size and this is very small. However, as a method of measuring the saturated film thickness, as opposed to the adsorption isotherm, the method of Long and Meter is subject to doubt. It is difficult to be sure that capillary condensation was not occurring very close to saturation or even some hysteresis due to over-saturation in the powder. Of course there is still insufficient data available to decide whether a scheme based on Frenkel's suggestion is valid. Indeed, reasons were given in the introduction to this paper why one would not expect the chemical nature of substrate to affect the film thickness.

---

* We are indebted to Professor L. Meyer for drawing our attention to this point.

In comparing the results of previous investigations, we are hampered by the fact that no values are given for the surface roughness factor of the specimens used. It is well known that for some metal foils the effective surface area for adsorption may be many times the apparent geometrical area (Brunauer 1945, p. 284). This is important in evaluating the results of Daunt and Mendelssohn and also of Kikoin and Lasarew, although the direct optical determination of film thickness by Burge and Jackson does avoid this difficulty. A high roughness factor in the specimens used by the former could provide an explanation of why their recorded values for the film thickness are higher than those of Burge and Jackson. Such an explanation would not, however, cover the values recorded in the present investigation, in which the roughness factor has been taken into account.

The value of n in eqn. (1) was found to be 2 for our data. This is the value predicted by Bijl, de Boer, and Michels (1941) on the basis of a theory involving zero point energy. A value $n=3$ as suggested by Frenkel (1940) and by Schiff (1941) cannot be fitted to our data. This is of interest because the calculation of Bijl, de Boer, and Michels is not satisfactory since it involves unrealistic forms of the wave functions in the film (Mott 1949).

The calculations of Frenkel and of Schiff were essentially a consideration of the film which would result from the van der Waals attraction to the wall. The profile given by them resulted from the effect of gravity on the film system. They suggested that the essential difference between He II and He I, which would explain the difference in saturated film thickness, concerns the balance of supply of matter through the creeping film and evaporation. Above the lambda point, where no film creep occurs, a thick film would evaporate faster than it could be formed from the bulk liquid or vapour. A question also arises as to the extent to which such a balance could determine the thickness below the lambda point. Although the contact of the mobile film is present, giving the observed thick film, it is conceivable according to these ideas that different conditions of heat influx might lead to different values of the film thickness. If this were the case, the film would only be well defined in a dynamic sense in terms of its transport properties ; the static aspects such as thickness would have little significance.

In evaluating the heat influx in our experiment, it should be remembered that the specimen tube is surrounded by liquid helium and liquid nitrogen in silvered dewars with narrow slits. Black paper was placed over the slits of the outer dewar to prevent radiation in the visible region from entering. This exclusion of visible radiation is to be contrasted with the experiments of Burge and Jackson and also Atkins. Accordingly, we have investigated the effect of shining light on the specimen.

Experiments with Radiation Influx

For this experiment a 10 w bulb was placed 20 cm from the outer dewar in a galvanometer lamp housing. The lens was replaced by a shutter and a variable aperture. Filters could be placed in the light path.

Our intention was to use a source of radiation which approximated the sources used in visual observations on the film flow (Atkins 1949) and optical investigations such as those of Burge and Jackson. Of course we have not reproduced exactly the optical system used by them and it is quite certain that the amount of radiation absorbed between the source and specimen is somewhat different. For this reason we shall not describe our results in quantitative detail, but rather concern ourselves with the general magnitude of the effect.

In the first observations, a sheet of heat-absorbing glass and a heavy green filter were placed in the light path. With an aperture of 1·3 cm, the effect of the source was to evaporate the film to 40% of its original value ; the evaporation was complete in $1\frac{1}{2}$ minutes. It is important to demonstrate that the deflection of the balance which results from the light source is really due to an evaporation of the film and not to some movement of the gas around the specimen resulting from local heating. This we have demonstrated in three ways. The radiation has been directed on to the counterweight ; the latter has a very small surface area so that evaporation of the film would be unobservable but motion of the ambient gas could deflect the balance appreciably. No deflection was observed. It may be argued that the different geometrical form of specimen and counterweight reduces the validity of this test. Accordingly, we have made the following checks on the specimen. Having observed the evaporation of the saturated film at 1·80°K (vapour pressure=12·3 mm Hg), the temperature was altered to 2·02°K (vapour pressure=24·8 mm Hg) and observations made on the unsaturated film at 50% saturation. The pressure in the specimen chamber for 50% saturation at 2·02°K is the same as for complete saturation at 1·80°K, so that any deflection of the balance due to gas movement would be the same in both cases. However, the effect of film evaporation would be quite different because the saturated case involves 150 layers and the unsaturated 3 or 4. We indeed established that the deflection due to radiation in the unsaturated case corresponded to less than 5 layers evaporated, hence the effect of gas motion is negligible. The only objection that can be made against this observation is that the presence of liquid might be of importance. This is not valid since we have observed that the same radiation produces an evaporation of about 3 layers in 13 above the lambda point in the presence of bulk liquid.

The evaporation can be reduced by decreasing the aperture. Exchanging the green filter for a yellow filter resulted in little change, indicating that most of the energy is entering via the infra-red. The amount evaporated can be reduced by extra sheets of heat-absorbing glass. At an aperture of 1·3 cm, one sheet of glass resulted in 60% evaporation, two sheets 50%, and three sheets 37%.

In giving only the general magnitude of the effect, we hope to emphasize the fact that the *actual* values recorded by us have little significance except to the extent that the light source approximates that commonly used in liquid helium experiments.* A quantitative study of the effect would require some estimate of the energy impinging on the specimen itself and this we have not done. The evaporation from a specimen due to incident radiation would also depend on the nature of the contact between the specimen and the liquid. This contact may well be better in the case of Atkins' experiment and also in Burge and Jackson's than in ours. Accordingly, the effect of incident radiation would be less in their case.

Burge and Jackson have considered the effect of radiation in their earliest experiment. One observation made by them involved turning off their light source for some time and then turning it on again to see if the film was any thicker. No increase in film thickness was detected. Two remarks are necessary on this observation. In the first place, we have observed the evaporation to be very rapid, the bulk of the film being evaporated in the first 30 seconds. More important than this, the observation (and others in the paper) obviously concerns only heat input by the light source and has no bearing on the more general question of whether differences in the heat influx in the experiments of various workers lead to disparities in values of film thickness. Such a possibility is reduced to a conjecture ; the sensitivity to heat influx is evident from our radiation experiments, but they do not prove the point.

Burge and Jackson have drawn attention to the very rapid rise in the film thickness at the lambda point, particularly as a basis for discussing residual heat influx. They point out that if the thickness is governed by the balance of flow onto the specimen through the mobile film and reduction due to evaporation, then the slope of this thickness-temperature curve should change with heat influx. They observed no change as the result of turning off their light source. It is interesting that our observation on the slope of this line agrees with that of Burge and Jackson. Such an observation appears to contradict the idea that residual heat influx is responsible for the disparity between our results. We have found some difficulty in investigating the region close to the lambda point, but we hope to investigate this point further in future experiments, since Burge and Jackson's argument is an important one.

---

* The source used can have little effect on the transfer rate (Bowers and Mendelssohn 1950).

In our previous paper (Bowers 1953 b) we discussed the observed mobility of saturated and unsaturated films (Bowers, Brewer and Mendelssohn 1951, Long and Meyer 1952 a, 1952 b) in terms of the film thickness involved. A further discussion of this question will not be undertaken here because it must first be established that there is some definite saturated film thickness which is independent of experimental conditions.

In concluding this discussion, some remarks on the method used in this investigation are appropriate. This investigation has demonstrated that the gravimetric method may be applied to the problem of the saturated He II film. Much could be done to improve the sensitivity by providing space for a larger specimen. Furthermore, other surfaces may be investigated. Unfortunately, the substrate of greatest interest for comparison with other work, i.e., glass, is the most difficult. The problem is that of shaping glass sheet to provide a large enough surface area with a small total weight.

ACKNOWLEDGMENTS

Grateful acknowledgment is made of the encouragement and advice given by Professor E. A. Long. Thanks are also due to Professor L. Meyer and Professor J. W. Stout for helpful discussions.

REFERENCES

ATKINS, K. R., 1950, *Proc. Roy. Soc.* A, **203,** 119.
BIJL, A., DE BOER, J., and MICHELS, A., 1941, *Physica,* **9,** 655.
BOWDEN, F. P., and THROSSELL, W. R., 1951, *Proc. Roy. Soc.* A, **209,** 297.
BOWERS, R., 1953 a, *Phil. Mag.,* **44,** 465; 1953 b, *Ibid.,* **44,** 487; 1953 c, *Phys. Rev.* (in the press).
BOWERS, R., BREWER, D. F., and MENDELSSOHN, K., 1951, *Phil. Mag.,* **42,** 1445.
BOWERS, R., and LONG, E. A., 1953, *Rev. Sci. Instrum.* (in the press).
BOWERS, R., and MENDELSSOHN, K., 1950, *Proc. Phys. Soc.* A, **63,** 1318.
BRUNAUER, S., 1945, *Adsorption of Gases and Vapours* (Oxford: University Press).
BURGE, E. J., and JACKSON, L. C., 1949, *Proc. Roy. Soc.* A, **205,** 270.
CHANDRASEKHAR, B. S., and MENDELSSOHN, K., 1952, *Proc. Phys. Soc.* A, **65,** 226.
DAUNT, J. G., and MENDELSSOHN, K., 1939, *Proc. Roy. Soc.* A, **170,** 423.
DINGLE, R. B., 1952, *Advances in Physics,* **1,** 111.
FRENKEL, J., 1940, *J. Phys. U.S.S.R.,* **2,** 365.
JACKSON, L. C., and HENSHAW, D. G., 1953, *Phil. Mag.,* **44,** 14.
KIKOIN, A. K., and LASAREW, B. G., 1938, *Nature, Lond.,* **141,** 912; **142,** 289.
KISTEMAKER, J., 1947, *Physica,* **13,** 81.
LONG, E. A., and MEYER, L., 1949, *Phys. Rev.,* **76,** 440; 1952 a, *Ibid.,* **85,** 1030; 1952 b, *Ibid.,* **87,** 153.
MAYER, J. E., and MAYER, M. G., 1940, *Statistical Mechanics* (New York: John Wiley), p. 18.
MENDELSSOHN, K., 1946, *Proc. Int. Conf. on Low Temp., Cambridge,* p. 41.
MOTT, N. F., 1949, *Phil. Mag.,* **40,** 61.
SCHIFF, L. I., 1941, *Phys. Rev.,* **59,** 839.

CXXXIX. *Isotopic Spin Selection Rules—IV: Radiations from* ^{20}Ne

By D. H. Wilkinson and A. B. Clegg
Cavendish Laboratory, Cambridge*

[Received August 10, 1953]

Abstract

The possibility is considered that the 13·70 Mev (2−) state of ^{20}Ne is $T=0$ in which case the electric dipole transition to the 1·63 Mev (2+) state of ^{20}Ne is forbidden by the isotopic spin rule. This transition is sought and is shown to have a radiative width of less than 2 ev corresponding to a $(2J+1)\,|M|^2$ value of less than 0·007. From this we may deduce that the contamination of this state with $T=1$ is less than 3% in *intensity* if we neglect the possible diminution of the transition matrix element due to the high level density.

§ 1. Introduction

This paper continues the series (I—Wilkinson and Jones 1953, II—Wilkinson 1953 a, III—Clegg and Wilkinson 1953) in which an attempt is being made, by investigating the validity of the isotopic spin selection rules, to assess the purity of isotopic spin states in a variety of light nuclei with various degrees of excitation. As I, II and III the present paper concerns itself with the rule that electric dipole radiation is forbidden between states of the same isotopic spin in self-conjugate nuclei (Radicati 1952, Gell-Mann and Telegdi 1953).

§ 2. States of ^{20}Ne

Many states are known in ^{20}Ne above the excitation of 12·87 Mev produced by adding a proton to ^{19}F. Several of these states decay by emission of alpha-particles to states of ^{16}O at 6 or 7 Mev excitation; we concern ourselves principally with that of 13·70 Mev formed by protons of 874 kev; it is (2−) (Ajzenberg and Lauritsen 1952, Seed and French 1952). The total width of this level is 5·2 kev made up of a proton width of 1·1 kev and an alpha-particle width of 4·1 kev (Chao 1950) or vice versa. It matters little which width we take as which; we adopt the first of the alternatives since it is that usually chosen. This corresponds with a conventional interaction radius of $5{\cdot}7\times10^{-13}$ cm, to reduced alpha-particle widths of about 0·8, 0·8 and 2% of the Wigner limit (Teichmann and Wigner 1952) for the three alpha-particle groups involved. It therefore seems probable that this state is of $T=0$.† We cannot be certain of this assignment since the density of known states in ^{20}F at the excitation of 3–4 Mev that corresponds to the region

---

* Communicated by the Authors.

† Compare reduced widths of 0·52, 0·93, 0·03, 0·12 and 0·016% of the Wigner limit for the indubitable $T=0$ states of ^{20}Ne at 6·7 to 7·9 Mev (Cameron 1953).

of ^{20}Ne of present interest (the first $T=1$ state of ^{20}Ne is expected at about 10 MeV) is high (about 6 per MeV) and comparable with that observed for ^{20}Ne (about 12 per MeV). The possibility that we have guessed wrongly will be considered later. We may also consider the state in ^{20}Ne at 13·44 MeV formed by protons of 598 kev; according to unpublished work by J. Seed and G. Dearnaley this state is also probably (2−) and, by the same argument as that presented above, may well also be $T=0$. (The widths for this state are 0·04 and 37 kev.)

The first excited state in ^{20}Ne is at 1·63 MeV and is certainly of even parity from the *ft* value of the β-decay of ^{20}F (Alburger 1952 and Bromley, Bruner and Fulbright 1953) and is expected to be (2+) (Scharff-Goldhaber 1953); this expectation has been confirmed by Seed (1953). There is therefore the possibility of electric dipole radiation of about 12 MeV between the (2−) and (2+) states. But if we are correct in our assignment of $T=0$ to the (2−) states these transitions should be isotopic spin forbidden. They have indeed long been known to be feeble compared with the well-known capture radiation from the 13·51 MeV state formed by protons of 669 kev (Devons and Hereward 1948); J. E. Sanders (1952) has reported that the ratio of their intensity to that of alpha-particles leading to excited states of ^{16}O is less than 5% of the same ratio for the 13·51 MeV state.

§ 3. EXPERIMENTAL INVESTIGATION

We have carried out a survey of the capture radiation from several states of ^{20}Ne including those at present under consideration. We have used NaI(Tl) crystals for this work and have sought the expected 12 MeV radiation directly against the background of the much greater flux of 6 and 7 MeV radiation from the states of ^{16}O reached by alpha-particle emission. The crystal was at 90° to the proton beam; the expected angular distribution for the 12 MeV radiation is $1+\frac{7}{11}\cos^2\theta$. This work will be reported in detail elsewhere but we may say here that the well-known uncertainties associated with the interpretation of a high-energy 'tail' in the crystal pulse spectrum were reduced by irradiating the crystal under identical conditions with the 7·48 MeV gamma-rays from the reaction ^{9}Be (pγ)^{10}B and those of 8·06 MeV given by ^{13}C (pγ)^{14}N. The ^{10}B and ^{14}N distributions, which were similar in form, were used to construct the expected tail due to the 6·1 and 7·1 radiations from ^{19}F (pα)^{16}O; which tail, correctly normalized, was compared with the distribution due to the bombardment of fluorine by protons when any excess at high energy in the latter distribution would represent the contribution from gamma-rays of energy greater than 7 MeV. There is no significant excess and upper limits of 0·05 and 0·04% maybe placed on the intensity of the expected 12 MeV radiation relative to that of the 6 and 7 MeV gamma-rays for the 13·70 and 13·44 MeV states respectively (using the data of Devons and Hereward (1948), Rae, Rutherglen and Smith (1950), Carver and Wilkinson (1951), and our own work for the relative abundances from the 13·51 MeV state).

§ 4. INTERPRETATION

If we continue our assumption that $\Gamma_\alpha > \Gamma_p$ our result implies that $\Gamma_\gamma < 2$ and 15 ev for the electric dipole radiation of 12 MeV from the 13·70 and 13·44 MeV states respectively. This corresponds to values of $(2J+1)\,|\,M\,|^2 < 0{\cdot}007$ and 0·05 for these two transitions in terms of the estimate of the single particle model (Weisskopf 1951). Now for allowed electric dipole transitions in light elements $(2J+1)\,|\,M\,|^2 \sim 0{\cdot}2$ with a rather small spread (Wilkinson 1953 b) and so the first of the present transitions appears to be discouraged by a factor of about 30 or more, while little may be said about possible discouragement of the second.

It may be argued, however, that when the level spacing becomes small radiative widths should become smaller than those given by the single-particle model (see, for example, Blatt and Weisskopf (1952)); this effect has been noticed by Kinsey (1953) in a survey of experimental material throughout the periodic table. Kinsey suggests $|\,M\,|^2 \sim 0{\cdot}1\,D$ where D is the level spacing (in MeV) for states of the same spin and parity. Now at the present excitation in ^{20}Ne $D \sim 300$ kev so Kinsey's suggestion would yield for the (2−) state in question $(2J+1)\,|\,M\,|^2 \sim 0{\cdot}15$ in close accord with the earlier suggestion.* It is therefore doubtful whether the effect of level density is yet of great importance; $(2J+1)\,|\,M\,|^2$ values similar to those for levels of a few MeV excitation are found for transitions from states at 16·1 MeV in ^{12}C, 13·1 MeV in ^{16}O, 13·51 MeV in ^{20}Ne, 12·6, 13·0 and 13·0 MeV in ^{28}Si where the level spacings (irrespective of spin and parity) are respectively about 500, 200, 100, 30, 20 and 20 kev. Conversely no cases are established with certainty in light nuclei of high level density of dipole radiative widths that fall greatly below the single-particle figure (though two possibilities of *magnetic* dipole transitions with $(2J+1)\,|\,M\,|^2 < 0{\cdot}1$ occur in ^{20}Ne—from the 13·19 MeV state).

If, then, we may interpret the above 'discouragement factor' as due to the isotopic spin rule we would say that the contamination of the predominantly $T=0$ state at 13·70 MeV with $T=1$ is less than 0·03 in *intensity*; in the notation of Radicati (1953) $\alpha_0^2(1) < 0{\cdot}03$.† We must stress, however, that this conclusion is rather more tentative than those based on the behaviour of more widely-spaced levels at lower excitation owing to our uncertainty of the exact importance of the increase in level density for the uninhibited transition strengths. It is perhaps a little surprising that the contamination should be as low as 0·03 since, as we have noted above, $D \sim 300$ kev, which is of the same order as the probable matrix element of the Coulomb perturbation that is responsible for mixing states of different isotopic spin. We may compare the situation for the 13·09 MEV state in ^{16}O where, with a value of D of about two or three times greater than in ^{20}Ne, $\alpha_1^2(0) > 0{\cdot}03$ (Wilkinson 1953 c).

---

* It must be emphasized that there is little or no justification for the factor $(2J+1)$ used in these comparisons; its use is purely one of convenience in reducing and tabulating the experimental data, since it is usually $(2J+1)\,\Gamma_\gamma$ rather than Γ_γ that emerges from the experiments.

† If the choice $\Gamma_p > \Gamma_\alpha$ turns out to be the right one for this level, the values of Γ_γ, $|\,M\,|^2$ and $\alpha_0^2(1)$ must be diminished by a factor of four. This makes little difference to the argument. If, however, $\Gamma_p > \Gamma_\alpha$ for the 13·44 MeV state we find, for the forbidden electric dipole transition, $\Gamma_\gamma < 0{\cdot}02$ ev, $(2J+1)\,|\,M\,|^2 < 0{\cdot}0001$, $\alpha_0^2(1) < 0{\cdot}0005$; these values appear so low as to be inadmissible.

We may, as noted in § 1, have guessed wrongly that $T=0$ for the 13·70 MEV state. If in fact $T=1$ the electric dipole transition would be allowed by the isotopic spin rule and we must regard the low value of $(2J+1)\,|\,M\,|^2$ as due either to the effect of level density or to an unusually low value for the matrix element or to both, and this may appear unlikely, although it is certainly possible. For $T=1$ the emission of alpha-particles would be forbidden, and we would say, following the data presented in § 1, $\alpha_1^2(0) > 0{\cdot}04$* with the strong possibility that a more realistic estimate would be considerably larger since this figure is based on the Wigner limit and it is rather unlikely that a contaminating level at so high an excitation in ^{20}Ne should possess single-particle alpha-particle characteristics.†

REFERENCES

AJZENBERG, F., and LAURITSEN, T., 1952, *Rev. Mod. Phys.*, **24**, 321.
ALBURGER, D. E., 1952, *Phys. Rev.*, **88**, 1257.
BLATT, J. M., and WEISSKOPF, V. F., 1952, *Theoretical Nuclear Physics* (New York: Wiley).
BROMLEY, D. A., BRUNER, J. A., and FULBRIGHT, H. W., 1953, *Phys. Rev.*, **89**, 396.
CAMERON, J. R., 1953, *Phys. Rev.*, **90**, 839.
CARVER, J. H., and WILKINSON, D. H., 1951, *Proc. Phys. Soc.* A, **64**, 199.
CHAO, C. Y., 1950, *Phys. Rev.*, **80**, 1035.
CLEGG, A. B., and WILKINSON, D. H., 1953, *Phil. Mag.*, **44**, 1269 (III).
DEVONS, S., and HEREWARD, H. G., 1948, *Nature, Lond.*, **162**, 331.
GELL-MANN, M., and TELEGDI, V. L., 1953, *Phys. Rev.*, **91**, 169.
KINSEY, B. B., 1953, *Nuclear Physics Conference Report* (Birmingham).
RADICATI, L. A., 1952, *Phys. Rev.*, **87**, 521; 1953, *Proc. Phys. Soc.* A, **66**, 139.
RAE, E. R., RUTHERGLEN, J. G., and SMITH, R. D., 1950, *Proc. Phys. Soc.* A, **63**, 775.
SANDERS, J. E., 1952, *Thesis*, Cambridge.
SCHARFF-GOLDHABER, G., 1953, *Phys. Rev.*, **90**, 587.
SEED, J., 1953, *Phil. Mag.*, **44**, 921.
SEED, J., and FRENCH, A. P., 1952, *Phys. Rev.*, **88**, 1007.
TEICHMANN, T., and WIGNER, E. P., 1952, *Phys. Rev.*, **87**, 123.
WEISSKOPF, V. F., 1951, *Phys. Rev.*, **83**, 1073.
WILKINSON, D. H., 1953 a, *Phil. Mag.*, **44**, 1019 (II); 1953 b, *Phil. Mag.*, **44**, 450; 1953 c, *Phys. Rev.*, **90**, 721.
WILKINSON, D. H., and JONES, G. A., 1953, *Phil. Mag.*, **44**, 542 (I).

---

* Or $\alpha_1^2(0) > 0{\cdot}01$ if $\Gamma_p > \Gamma_\alpha$.

† If the 13·44 MEV state is $T=1$ with $\Gamma_\alpha > \Gamma_p$ then $\alpha_1^2(0) > 0{\cdot}3$ and the concept of isotopic spin has little meaning. The possibility $T=1$, $\Gamma_p > \Gamma_\alpha$ appears even less likely than $T=0$, $\Gamma_p > \Gamma_\alpha$ discussed earlier on account of the tiny value of $(2J+1)\,|\,M\,|^2$ ($<0{\cdot}0001$) that would have to be assumed for the then allowed electric dipole transition.

CXL. *The Nuclear Disintegrations Produced by High Energy Protons*

By G. C. Morrison, H. Muirhead and W. G. V. Rosser
Department of Natural Philosophy, University of Glasgow*

[Received July 10, 1953]

SUMMARY

A comparison is made between the nuclear disintegrations observed when 140 MeV protons pass through photographic emulsions and the nature of the disintegrations expected on the Goldberger model (1948). Satisfactory agreement is found for all the features of the disintegrations examined.

§ 1. INTRODUCTION

IN a previous paper from this laboratory (Lees *et al.* 1953), referred to as I, the cross sections for the production of nuclear disintegrations by 130 MeV protons in the heavy (silver and bromine) and light (carbon, nitrogen and oxygen) constituents of photographic emulsions were obtained. The results were shown to be in agreement with the 'optical model' of Fernbach, Serber and Taylor (1949).

The ' optical model ' assumes that at high energies a nuclear interaction can be produced by the collision of the incident nucleon with a single nucleon inside the nucleus, and merely predicts the probability for the occurrence of this collision. After the first collision, however, both nucleons may have sufficient energy to undergo further collisions inside the nucleus (i.e. initiate a nucleon cascade), and the knocked-on nucleons can reach the surface of the nucleus and escape, or lose sufficient energy to be absorbed in the nucleus leaving it in an excited state. Charged and uncharged particles are subsequently evaporated from the excited nucleus (Weisskopf 1937).

A detailed theoretical description of the cascade process has not so far proved feasible. Goldberger (1948) has, however, suggested that numerical results may be predicted by considering the passage of a sufficient number of nucleons through the nucleus and allowing the position and nature of the collisions to be determined by the laws of chance. This will be referred to as the ' Goldberger Method '.

Bernardini *et al.* (1952) have shown that the Goldberger model of successive single nucleon–nucleon collisions inside the nucleus is satisfactory for describing the stars produced by 400 MeV protons in photographic emulsions. It may not be as reliable for primary particles of

---

* Communicated by Professor P. I. Dee, F.R.S.

lower energy, since the cross sections for free nucleon–nucleon collisions increase as the energy of the primary particles becomes smaller, and at the same time their de Broglie wavelengths increase. It is, therefore, of interest to determine the range of validity of the single nucleon–nucleon picture. In this paper an account is given of a calculation carried out by the Goldberger method for the stars produced by 140 MeV protons in nuclear emulsions. The calculated data will be compared with the experimental results obtained using G5 emulsions which were exposed to 146 MeV protons accelerated by the Harwell cyclotron.

§ 2. METHOD OF CALCULATION

The calculations were carried out for a heavy nucleus ($Z=41$, $A=94$), and a light nucleus ($Z=7$, $A=14$). The nuclear radius was taken as $1{\cdot}42\times10^{-13}A^{1/3}$ cm. One hundred primary protons were followed in each case.

A Fermi gas model was used for the nucleons inside the nucleus ; their maximum energy was taken as 22 MeV. The binding energy of the nucleons was taken as 8 MeV, making the depth of the potential well equal to 30 MeV. It was assumed that the incident protons moving with a kinetic energy of 140 MeV gained 30 MeV on entering the nucleus.

In making the calculation it was assumed that the primary proton could initiate a nucleon cascade inside the nucleus, and that the cascade would develop through a series of single nucleon–nucleon collisions. Allowance was made for the following features in each encounter :—

(*a*) collision with either a neutron or proton,

(*b*) variation of the free n–p and p–p scattering cross sections with energy (Christian 1952, Pickavance and Cassels 1952),

(*c*) variation of the energy of struck particle and angle between the colliding particles inside the nucleus,

(*d*) variation of the angular distribution of n–p and p–p scattering in the centre of momentum system with energy (Christian *loc. cit.*, Randle *et al.* 1952).

The detailed procedure for carrying out the calculation will not be described, as it was essentially the same as that used by Bernardini *et al.* (*loc. cit.*).

The individual nucleons set in motion during the cascade were followed until they reached the nuclear surface, or were absorbed. Reflection at the nuclear surface was neglected. A value of 6 MeV, which is smaller than the accepted value of 8–9 MeV, was used for the Coulomb potential barrier for protons in the heavy nucleus. This figure was adopted so as to allow for some Gamow penetration of the barrier. Therefore, if after a collision the energy of a proton was less than 36 MeV (inside the heavy nucleus), or 30 MeV in the case of a neutron, it was assumed that the particle was absorbed leaving the nucleus in an excited state. Thirty MeV were subtracted from the energy of each particle as it left the nucleus.

The excitation energy of the nucleus following the cascade is given by

$$U=[140-\sum_{i=1}^{N} E_i-8(N-1)]\ \text{MeV}, \qquad (1)$$

where E_i is the energy of a knock-on nucleon (after escaping from the nucleus), and N is the total number of knock-on nucleons emerging from the nucleus.

The calculations were not extended to nucleons with energies below 60 MeV inside the light nucleus (see § 5).

Fig. 1

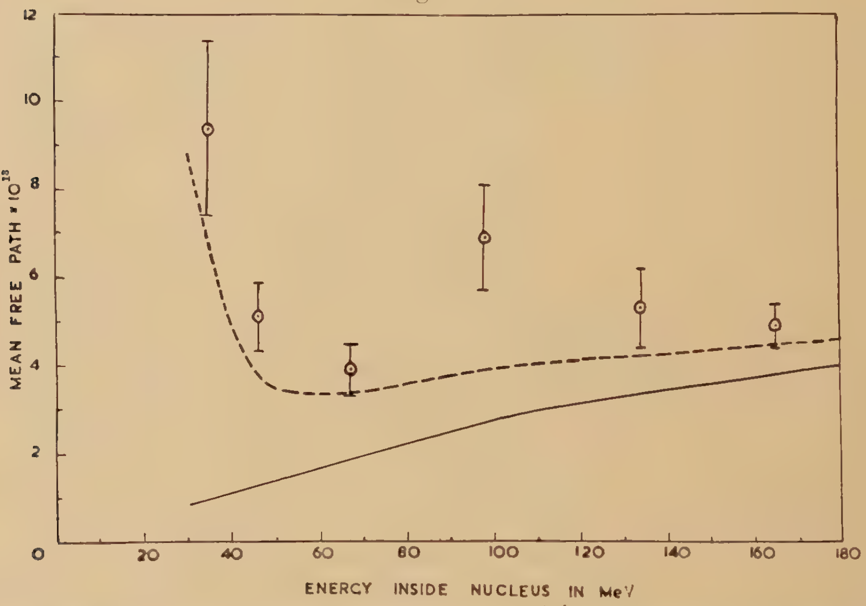

Mean free paths for nucleons in nuclear matter ; ϕ points derived from cascade calculation ; ——— value expected from free nucleon–nucleon scattering without application of Pauli exclusion principle ; – – – – value modified by Goldberger's formula to allow for the effect of the exclusion principle.

It was assumed that only single nucleon–nucleon collisions took place at all energies, and, therefore, at all energies the free particle cross sections were used. If in any encounter either particle was calculated to possess an energy less than 22 MeV after the collision, then it was assumed that the collision was forbidden by the Pauli Exclusion Principle. It is of interest to note the effect of the exclusion principle as a function of energy. In fig. 1 the mean free path for nucleons in nuclear matter resulting from the calculations is shown as a function of energy. For comparison the uncorrected mean free path of nucleons in nuclear matter and the same path length corrected using an analytical expression given by Goldberger (*loc. cit.* eqn. (14)) are shown. It can be seen that the mean free paths obtained using this expression are rather lower than those obtained by us. This difference is to be expected since Goldberger assumed isotropic scattering in the centre of momentum system when deriving this formula, whereas the rise observed experimentally near 0° and 180° in n–p scattering tends to increase the effect of the Pauli Exclusion Principle.

§ 3. THE CROSS SECTIONS FOR NUCLEAR INTERACTIONS

In table 1 the cross sections for nuclear interactions in light and heavy nuclei derived by the Goldberger method are compared with those obtained in Paper I. It can be seen that the overall agreement is satisfactory.

Table 1

	Heavy Nucleus	Light Nucleus	
No. of primary protons	100	100	Goldberger method
No. of nuclear interactions	81	59	
Cross section for nuclear interaction	$(104 \pm 15) \times 10^{-26}$ cm²	$(21 \pm 3) \times 10^{-26}$ cm²	
Cross section for nuclear interaction—Experimental	$(128 \pm 16) \times 10^{-26}$ cm²	$(16 \pm 7) \times 10^{-26}$ cm²	Paper I
Cross section for nuclear interaction—Perry's Method (1952)	$(110 \pm 5) \times 10^{-26}$ cm²	$(24 \pm 2) \times 10^{-26}$ cm²	

§ 4. COMPARISON OF THE CALCULATED AND EXPERIMENTAL DATA FOR PROTONS EMITTED WITH ENERGIES GREATER THAN 30 MEV

The model of successive single nucleon-nucleon collisions inside the nucleus is most likely to hold for high energy particles, whose mean free paths for such collisions are considerably greater than the average inter-nucleon distance. This is considered to be the case for nucleons of energy greater than 60 MEV inside the nucleus (Peaslee 1952). Furthermore some of the charged particles leaving the nucleus with energies less than 30 MEV are emitted during the evaporation process. The number of evaporation protons with energies above 30 MEV is negligible. Therefore in this section we will confine our comparison to protons emitted with energies greater than 30 MEV, and will extend our analysis to energies below 30 MEV in § 5.

The results obtained by the Goldberger method for heavy and light nuclei were combined in the proportion of the geometrical area presented by each to protons in Ilford G5 emulsions, that is approximately 3 to 1.

The experimental results were based on stars obtained by area scanning and were confined to those stars whose primary protons had energies greater than 130 MeV, their mean energy being close to 140 MeV. The energies of the primary and secondary protons were determined by grain counting. Some of the plates were underdeveloped so that energies as low as 30 MeV could be determined by this technique.

4.1. *Energy Distribution of the High Energy Protons*

In table 2 a comparison is made between the calculated and experimental distributions of protons emitted with energies greater than 30 MeV. The data has been normalized in each case to represent the number of protons emitted per star. In Paper I it was pointed out that 0p stars are difficult to detect in ' area ' scanning, and that primary protons which lose less than 25 MeV in a nuclear encounter and are scattered through small angles are difficult to distinguish from elastically scattered protons. The effective number of stars in the calculated data was therefore made to correspond to experimental conditions by rejecting from the calculated results all the 0p stars, and the 1p stars in the above category.

Table 2

Energy in MeV	30–50	50–70	70–90	90–110	>110
No. of protons per star—Experimental	0·23 ± 0·04	0·13 ± 0·02	0·07 ± 0·02	0·11 ± 0·03	0·05 ± 0·02
No. of protons per star—Calculated	0·22 ± 0·04	0·16 ± 0·04	0·21 ± 0·04	0·12 ± 0·03	0·08 ± 0·03

4.2. *Angular Distribution of the High Energy Protons*

In making the cascade calculations a two-dimensional geometry was used. Thus there is no exact correspondence between the calculated and the observed angular distributions. For a sufficiently large number of stars, however, the calculated angular distribution should approximate to the distribution of the actual angle in space between the primary proton and the secondary protons. The two distributions are compared in table 3, where the intervals given represent angles between the directions of the primary and secondary protons. The calculated results are normalized to the total measured number of protons with energies greater than 30 MeV.

4.3. *Discussion*

It can be seen from tables 2 and 3 that the measured energy and angular distributions of the high energy protons are in satisfactory agreement with the distributions calculated on the assumption that the primary proton initiates a nucleon cascade. The only point at which a large discrepancy appears between the experimental and calculated results is in the 70–90 MeV energy interval in table 2. This difference could possibly be accounted for by statistical fluctuations, since both values deviate from the general trend of figures as a function of energy, and the deviations are in opposite senses.

Table 3

Angle in degrees	0–20	20–40	40–60	60–80	80–100	100–120	>120
No. of protons—Experimental	22	46	27	11	3	5	3
No. of protons—Calculated	22	41	26	20	4	2	2

§ 5. COMPARISON OF THE CALCULATED AND EXPERIMENTAL DATA FOR THE CHARGED PARTICLES EMITTED WITH ENERGIES LESS THAN 30 MEV FROM STARS PRODUCED IN SILVER AND BROMINE

For nucleons of low energies ($\lesssim$60 MeV inside the nucleus) the compound nucleus picture is believed to hold (Peaslee *loc. cit.*). In this model the incident nucleon is assumed to share its energy quickly with the rest of the nucleons in the nucleus giving rise to a compound nucleus which subsequently decays. If this model were entirely correct one would expect very few knock-on protons of energies less than 30 MeV to emerge from the nucleus. The model of single nucleon–nucleon collisions is also more likely to break down at low energies where simultaneous collisions of more than two nucleons may take place. In making our calculations by the Goldberger method, however, the nucleons were followed through the nucleus assuming single nucleon–nucleon collisions, until the particles either left the nucleus or were absorbed. A large proportion of the protons with energies less than 30 MeV then come out of the nucleus as their apparent mean free path inside was increased due to the action of the Pauli Exclusion Principle (see fig. 1). It is therefore interesting to compare the results of the calculation made on the assumption of a nucleon cascade with the experimental data for protons emitted with energies below 30 MeV.

In this section the results of the calculations on the heavy nucleus will be compared with the experimental data. A fairly reliable evaporation theory is available for silver and bromine (Le Couteur 1950, 1952); such a theory would not be appropriate for light nuclei because of the limited number of nucleons, and the ease with which these nuclei disintegrate completely into α-particles and protons at comparatively low excitation energies.

In Paper I it was shown that 95% of the 1, 2, 3p stars and 70% of the 4p stars were produced in silver and bromine. Therefore, it is reasonable to compare the results of the calculations for the heavy nucleus with the sum of the experimental results for 1, 2, 3 and 4p stars. Protons from stars in this category having one or more α-particle of energy less than 9 MeV were not included in the experimental data in §§ 5.2 and 5.3 as these stars were probably produced in the light nuclei (Paper I).

All protons of energy less than 30 MeV will be called black.

5.1. *The Size-Frequency Distribution of Stars in Silver and Bromine*

For each interaction the Goldberger method gives the number of knock-on protons and the excitation energy of the residual nucleus. The calculated excitation energies varied from 2 to 148 MeV, the mean value being 44 MeV. Le Couteur (1950, 1952) has given a relation between the mean number of charged evaporation prongs and excitation energy. From this relationship the number of charged particles emitted during evaporation can be calculated for each star separately. The total number of charged prongs per interaction can thus be obtained. The resulting size-frequency distribution is given in table 4, where a comparison is made with the experimental results derived in Paper I.

Table 4

Type of Star	Calculated number of stars	Calculated cross section $\times 10^{26}$ cm^2	Experimental cross section $\times 10^{26}$ cm^2
0p	11	14	4 ± 3
1p	23	29·5	32 ± 12
2p	31	39	53 ± 7
3p	13	17	30 ± 5
4p	3	4·5	9 ± 3
5p	—	—	1 ± 2
6p	—	—	$-(1 \pm 1)$
Totals	81	104	128

5.2. *The Energy Distribution of Protons emitted in Silver and Bromine*

The experimental energy distribution of protons from 1, 2, 3 and 4p stars is shown in fig. 2; this was determined from the ranges of the protons ending in Ilford G5 emulsions. It is based on measurements on 388 stars; the total number of black protons emitted in these stars after applying a suitable geometrical correction for those leaving the emulsion was 420. For comparison the calculated data for the heavy nucleus was normalized to 388 stars; a correction was made for the 0p and 1p stars to allow for those that would not be found by area scanning as discussed in § 4.1.

On the basis of our calculations by the Goldberger method we would expect 180 protons to be emitted from 388 stars in evaporation processes. In obtaining this result, allowance was made for the variation of the excitation energy, U, as discussed in § 5.1. The number of evaporation protons expected using the above model is, therefore, not sufficient to account for the 420 tracks observed experimentally. However, the Goldberger model also predicts that an additional 190 protons of energy below 30 MeV would be emitted from the heavy nuclei in direct collision processes. The total calculated number emitted is, therefore, in satisfactory agreement with the experimental number.

Fig. 2

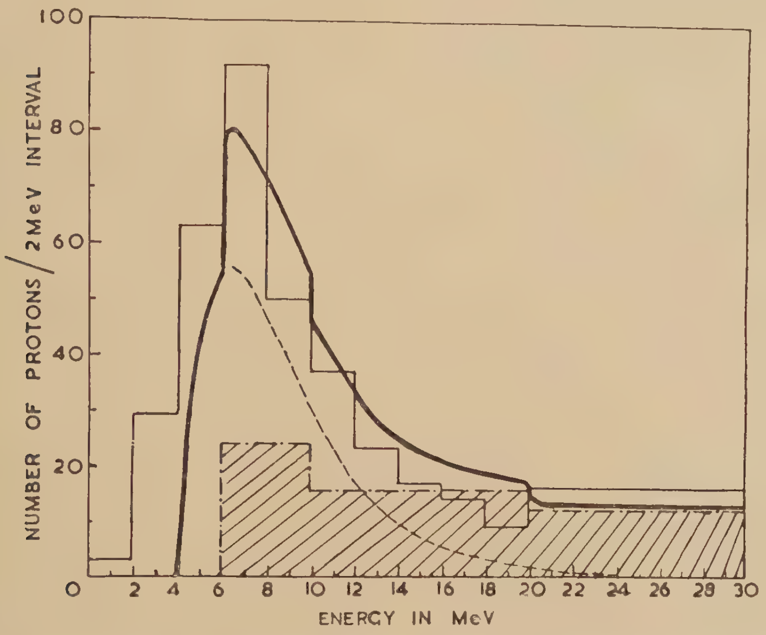

Energy distribution of protons below 30 MeV; ⊓ experimental results; –.–.–.–.– calculated spectrum for knock-on protons; – – – – calculated evaporation spectrum for average nuclear excitation of 44 MeV; ——— calculated knock-on plus evaporation spectrum.

In fig. 2 the shaded area represents the calculated number of knock-on protons emitted in the energy range 6 to 30 MeV. The agreement with the experimental energy distribution is reasonable for energies greater than 20 MeV. Below 20 MeV the effect of the knock-on protons is completely masked by the evaporation protons.

According to simple evaporation theory (Weisskopf *loc.cit.*) the probability for the emission of a particle of energy between E and $E+dE$ is

$$P(E)dE=\frac{E-V}{T^2}\exp\left[-\frac{(E-V)}{T}\right]dE \quad . \quad . \quad . \quad . \quad (2)$$

where V is the height of the Coulomb barrier and T is the nuclear temperature of the residual nucleus. Assuming a Fermi gas model we have

$$U=\beta T^2 \quad . \quad . \quad . \quad . \quad . \quad . \quad . \quad . \quad . \quad . \quad (3)$$

where, according to Le Couteur, β is $\sim$7·6 MeV^{-1} for a mean silver and bromine nucleus. In order to compare the calculated with the experimental results values must be assumed for V and T. In eqn. (2) T represents the temperature of the nucleus after emitting a proton. The excitation energy varied between 2 and 148 MeV, the mean value being 44 MeV. At low excitation energies neutron emission predominates so that most of the protons observed are emitted at an average excitation energy greater than 44 MeV. However, when the total number of evaporation protons was calculated, allowance was made for the variation of U as mentioned above. Therefore, the uncertainty in U affects the form of the evaporation spectrum only, but not the total number of evaporation particles emitted. Furthermore, T is proportional to $\sqrt{U}$ so that the uncertainty in the excitation energy of the residual nucleus does not seriously affect the shape of the energy spectrum of the protons resulting from evaporation. A value of 2·4 MeV was taken for T corresponding to an excitation energy of the residual nucleus of 44 MeV.

The experimental data presented in fig. 2 suggests that the effective Coulomb barrier is about 4 MeV. The potential barrier for a mean silver and bromine nucleus (unexcited) is 8–9 MeV for protons. However, the effects of barrier penetrability and thermal expansion of the excited nucleus could reduce the effective height of the barrier to $\sim$4 MeV. The resulting curve for 180 evaporation protons with $T=2{\cdot}4$ and $V=4$ MeV is shown in fig. 2 ; it is also shown added to the calculated knock-on spectrum. The agreement of the combined spectrum with the experimental spectrum is satisfactory, except that some protons of energies less than 4 MeV are found experimentally. Some of these may be from 1, 2, 3 and 4p stars produced in light nuclei, from which no α-particles of energy less than 9 MeV are emitted. Some of the particles may also be ‘ decay protons ’ from heavy nuclei (Le Couteur 1950, Fujimoto and Yamaguchi 1949).

The results obtained by the Goldberger method are, therefore, adequate to account for the numbers and energy distribution of protons below 30 MeV emitted from stars produced by 140 MeV protons.

It should be pointed out, however, that processes different from those assumed in our calculations could also account for the experimental energy spectrum below 20 MeV. If it were assumed that all nucleons with energies below 50 MeV (inside the nucleus) were absorbed, then the average nuclear excitation energy would be raised from 44 to 66 MeV. On using Le Couteur’s theory, as described in § 5.1, the total number of protons expected to be evaporated with energies between 0 and 20 MeV would be 310 compared with 340 protons observed experimentally. The energy spectrum calculated on this assumption is shown in fig. 3.

If it were assumed that all nucleons of energy less than 60 MeV inside the nucleus were absorbed, the average excitation energy would be increased still further but the form of the calculated evaporation spectrum would not be substantially different from that shown in fig. 3, and would not be in agreement with the number of protons in the energy range 20–30 MeV observed experimentally.* It therefore seems probable that some knock-on protons of energies between 20 and 30 MeV escape from the nucleus. Additional evidence for this view will be presented in the next section.

Fig. 3

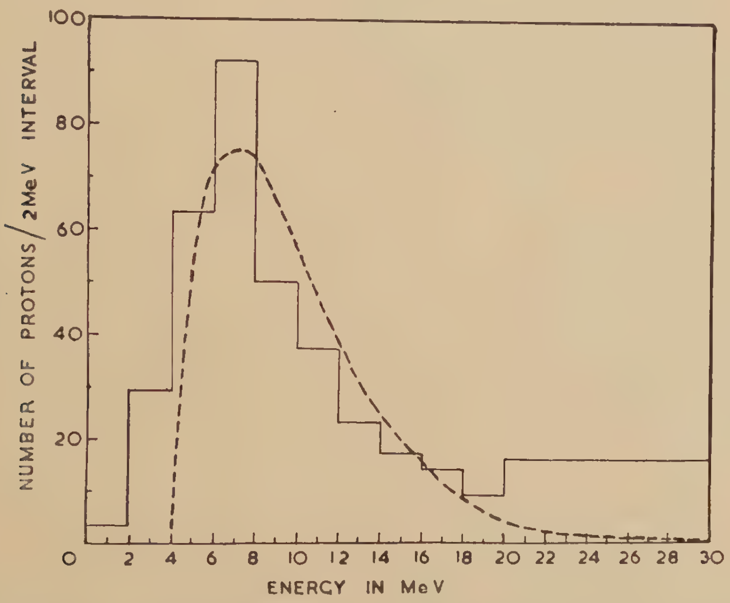

Energy spectrum of protons below 30 MeV ; ⊓ experimental results ; – – – – calculated evaporation spectrum for average nuclear excitation of 66 MeV.

5.3. *Angular Distribution of Protons of Energies less than* 30 MeV *emitted from Stars in Silver and Bromine*

The protons emitted during the evaporation of a heavy nucleus should be ejected isotropically relative to the recoiling nucleus. The velocity of the evaporation protons is $\sim 0{\cdot}1$ c whereas in our case the mean velocity of the recoiling nucleus is $\sim 0{\cdot}005$ c. Therefore the evaporation protons should have an approximately isotropic distribution in the laboratory system. The experimental angular distribution for protons of energy less than 30 MeV from 1, 2, 3, and 4p stars shows a marked anisotropic distribution, the ratio of the number of black protons in the forward direction to the number in the backward direction being 1·9±0·2. The calculated forward to backward ratio obtained by combining the calculated angular distribution for black knock-on protons with an isotropic angular distribution for the evaporation protons is 1·9±0·5. This value is in good agreement with the experimental figure and confirms that some knock-on protons of energy less than 30 MeV escape from the nucleus.

---

* Data from 900 stars was used to determine the mean number of protons in the energy range 20–30 MeV. The energies were determined from grain counts in the underdeveloped plates and from the ranges of the protons ending in the emulsion. The mean ordinate normalized to 388 stars in figs. 2 and 3 was 17 ± 4.

It was shown in the previous section that an evaporation process could not easily account for the production of protons with energies in the region from 20 to 30 MeV. The forward to backward ratio for the protons in this energy range offers confirmation for this conclusion; 20 protons were observed travelling in the forward direction, and 3 in the backward.

It is of interest to extend these observations to protons of energies less than 20 MeV. The Goldberger model gives a forward to backward ratio of 1·7±0·5 for protons of energies less than 20 MeV. The experimental forward to backward ratios for protons ending in the emulsion are 1·5±0·2 and 1·4±0·2 for protons in the energy ranges 0–20 MeV and 0–10 MeV respectively. However, some of the protons included in these figures could have come from stars produced in the light nuclei from which no α-particle of energy less than 9 MeV was emitted. Protons from identifiable stars produced in the light nuclei show a marked anisotropic distribution, so that it is not possible to conclude with certainty that knock-on protons of energies less than 20 MeV are emitted in the stars produced in silver and bromine.

5.4. *The Ratio of the Number of α-particles to the Total Number of Particles emitted in the Stars produced in Silver and Bromine*

The experimental ratios for the number of α-particles to the total number of prongs in a star as a function of star size were presented in Paper I (fig. 2), and the values for 1, 2 and 3p stars are reproduced in table 5. This ratio will be referred to as the α/total ratio.

Table 5

Type of star	α/Total	
	Calculated for Ag and Br	Experimental
1p	0·04±0·02	0·05±0·02
2p	0·08±0·02	0·07±0·01
3p	0·10±0·03	0·16±0·02

According to Le Couteur (1950), the ratio of the number of α-particles to the total number of charged evaporation particles emitted from silver and bromine should be 0·25. This figure was used in calculating the α/total ratios; the total number of charged particles in each star was obtained as discussed in § 5.1. The results are presented in table 5.

The agreement for 1p and 2p stars is very good, and the low α/total ratio found experimentally again shows that an appreciable number of knock-on protons are emitted in the stars. If it were assumed, as in § 5.2, that all nucleons of energy less than 50 MeV inside the nucleus might be absorbed, the increase in the excitation energy would approximately double the calculated number of charged evaporation prongs emitted, thereby doubling the calculated α/total ratios. It can be seen that the experimental α/total ratios for 1p and 2p stars are in better agreement with the theory that some knock-on nucleons of energies less than 50 MeV (inside the nucleus) escape from the nucleus. The calculated α/total ratios for 3p stars given in table 5 are significantly lower than the experimental value for 3p stars. This is probably due to the fact that some of the 3p stars found experimentally were produced in light nuclei for which the measured ratio is $\sim$0·5, rather than to the absorption of nucleons of energies less than 50 MeV inside the nucleus.

5.5. *Discussion*

From the number of protons occurring with energies greater than 20 MeV as shown in fig. 2, and the experimental forward to backward ratio for protons in the energy range 20–30 MeV, discussed in § 5.3, it is concluded that some nucleons with these energies escape during the nucleon cascade. There is no definite evidence for the existence of knock-on protons with energies below 20 MeV, but the forward to backward ratio for protons less than 20 MeV produced in 1, 2, 3 and 4p stars, and the α/total ratios found experimentally for 1p and 2p stars suggest that some nucleons of energies less than 20 MeV may also escape during the nucleon cascade.

This result suggests that nucleons of moderate energy may travel appreciable distances inside a nucleus before being absorbed. Evidence supporting this view has been recently presented by Feshbach, Porter and Weisskopf (1953). In making an analysis of the experimental data of Barschall and his co-workers (1952) on the total cross sections of heavy nuclei for the scattering of neutrons with energies between 0·1 and 3 MeV, Feshbach *et al.* have concluded that the incident neutrons penetrate a distance of about 2×10^{-12} cm into nuclear matter before they are incorporated into the compound nucleus. This distance may be compared with the figure of $\sim10^{-12}$ cm for the mean free path of low energy nucleons shown in fig. 1.

There is a possibility that sometimes a nucleon collides simultaneously with more than one nucleon inside the nucleus, leading to a sharing of energy between three or more particles. The simplifications and poor statistics inherent in the calculations do not allow us to exclude this possibility for nucleons of energies less than 60 MeV inside the nucleus. Though probably not entirely correct in detail, the model of a nucleonic cascade of single nucleon–nucleon collisions together with Le Couteur's theory of the evaporation process appears to be adequate to account for the main properties of stars produced in silver and bromine.

ACKNOWLEDGMENTS

The authors wish to express their gratitude to Professors P. I. Dee and J. C. Gunn for their interest in the course of this work. We are indebted to Drs. M. Grilli and B. Vitale of the University of Padua, and to Dr. K. Burton of this University for reading the paper prior to publication and for their constructive criticism.

We also wish to thank Dr. T. G. Pickavance and the members of the cyclotron group at Harwell for carrying out the exposure of the plates, and the Misses W. Green and M. Ross for assistance in the scanning of the plates.

REFERENCES

BARSHALL, 1952, *Phys. Rev.*, **86**, 431.
BERNARDINI, BOOTH and LINDENBAUM, 1952, *Phys. Rev.*, **88**, 1017.
CHRISTIAN, 1952, *Rep. Progr. Phys.*, **15** (London : Physical Society), p. 68.
FERNBACH, SERBER and TAYLOR, 1949, *Phys. Rev.*, **75**, 1352.
FESHBACH, PORTER and WEISSKOPF, 1953, *Phys. Rev.*, **90**, 166.
FUJIMOTO and YAMAGUCHI, 1949, *Phys. Rev.*, **75**, 1776.
GOLDBERGER, 1948, *Phys. Rev.*, **74**, 1269.
LE COUTEUR, 1950, *Proc. Phys. Soc.* A, **63**, 259 ; 1952, *Ibid.*, **65**, 718.
LEES, MORRISON, MUIRHEAD and ROSSER, 1953, *Phil. Mag.*, **44**, 304.
PEASLEE, 1952, *Phys. Rev.*, **86**, 269.
PERRY, 1952, *Phys. Rev.*, **85**, 497.
PICKAVANCE and CASSELS, 1952, *Nature, Lond.*, **169**, 520.
RANDLE, TAYLOR and WOOD, 1952, *Proc. Roy. Soc.* A, **213**, 392.
WEISSKOPF, 1937, *Phys. Rev.*, **52**, 295.

CXLI. *On the Annihilation of Positrons in Solids*

By A. T. G. Ferguson * and G. M. Lewis
Department of Natural Philosophy, The University, Glasgow†

[Received August 12, 1953]

Abstract

Using the method of delayed coincidences the lifetimes of positrons from ^{22}Na have been determined in various materials, the 1·28 Mev γ-ray of ^{22}Na announcing the emission of a positron.

A lifetime of ($1{\cdot}6 \pm 0{\cdot}6 \times 10^{-10}$ sec) has been deduced in aluminium, and comparative measurements show that it does not differ from this in other metals studied by us and by other writers. A second lifetime of ($2{\cdot}5 \pm 0{\cdot}3 \times 10^{-9}$ sec) involving ($0{\cdot}27 \pm 0{\cdot}03$) of the positrons has been found in distrene at room temperature. This lfetime has been found to increase by about 10% for 115°c rise in temperature. Three quantum emission from distrene has been found to be small. Experiments have also been carried out in plastic sulphur and magnetized iron.

§ 1. Introduction

The theory of positron annihilation in its early form (Heitler 1944) predicted a positron lifetime in lead of about 10^{-10} sec and lifetimes in other materials proportional to their electron density, assuming all Z electrons to be available. The experiments of De Benedetti and Richings (1951) showed that there might be little variation from metal to metal. It seemed therefore desirable to investigate both comparative and absolute positron lifetimes in a variety of materials. This would indicate how closely the theory is followed.

The effect of a magnetic field in iron on positron lifetimes was studied. This work arose from consideration of the effects of spin on the annihilation process.

The experiments of Deutsch (1951) on annihilation in gases in which positronium formation was established, suggested that complex time distributions might be found in the annihilation radiation from solids. Further it indicated the possibility that three-quantum annihilation might be more prevalent than the 1/370 of two-quantum processes calculated on the basis of free positron electron annihilation (cf. Ore and Powell 1949).

Bell and Graham (1952) had reported a complex time distribution in certain plastics and a difference in behaviour between crystalline and fused quartz. The latter difference pointed to considerable influence of the gross structure on annihilation. From these considerations it was decided to investigate the lifetimes of positrons in distrene and their variation with its expansion, melting and previous treatment. A search for three quantum annihilation was also carried out.

---

* Now at A.E.R.E., Harwell, Didcot, Berks.

† Communicated by Professor P. I. Dee.

Lifetimes in the allotropic modifications of sulphur seemed to be of interest in the light of the reported behaviour of quartz.

In the meanwhile De Benedetti and Richings (1952) and Bell and Graham (1953) have published further work in this field.

§ 2. Apparatus

The lifetimes were measured by the method of delayed coincidences using a coincidence unit of resolving time $\tau_0 = 2 \times 10^{-9}$ sec.

The principles of this unit are essentially the same as that of Bell, Graham and Petch (1952). A block diagram of the arrangement is shown in fig. 1 (cf. Lewis and Ferguson 1953). The scintillators were solutions of terphenyl in toluene contained in plane ended glass vessels 1 inch diameter by 1 inch long, surrounded by magnesium oxide. The photomultipliers were 14-stage E.M.I. type 6262 selected for large gain and high photosensitivity. They were run at voltages between 2000 and 2500. To obtain a linear response it was necessary to take the side channel pulse from the 11th dynode. Delay was introduced between the coincidence unit and counter by 95 Ω Uniradio 31 coaxial cable which gives a delay of 5×10^{-9} sec per metre.

Fig. 1

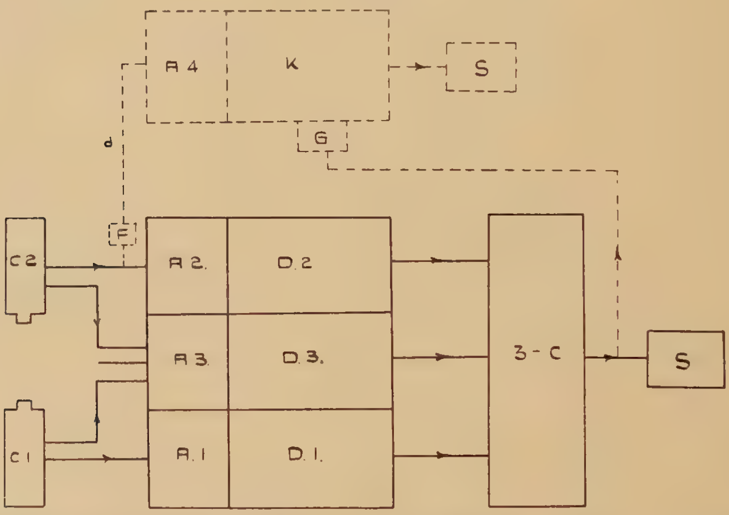

Block diagram of apparatus. Full line shows basic apparatus. Dashed line shows later additions. C.1, 2—counters; A.1, 2, 3, 4—amplifiers; D.1, 2, 3—discriminators; K—kicksorter; 3-C—triple coincidence unit; F—cathode follower; G—gate; d—1·25 μsec delay line.

The resolution curve, obtained by measuring the number of coincidences against delay introduced, shows a resolving time dependent particularly on the setting of the middle channel discriminator and times down to 1×10^{-9} sec are obtainable, though the efficiency at this resolving time is very poor. The actual position of the resolution curve is sensitive to the settings of the side channel discriminators D.1 and D.2 and to the photomultiplier voltage.

§ 3. EARLY COMPARISON EXPERIMENTS

Using the apparatus described, at an earlier stage of development, comparison measurements were made of positron lifetimes in various materials. The ^{22}Na source used was enclosed in 0·005 inch aluminium. It was placed between samples of the material under test and lead, the standard throughout these measurements. The geometrical arrangement of source and counters was the same as that of De Benedetti and Richings (1952).

The discriminator D.1 (see fig. 1) was set to exclude pulses from 511 kev γ-rays, and D.2 so as to minimize coincidences caused by scattered γ-rays. This ensured that the 1·28 MEV γ-ray of ^{22}Na was detected in counter 1, and an annihilation γ-ray in counter 2.

A resolution curve was obtained first with the sample then with lead, next the source. A typical set of data is shown graphically in fig. 2, comparing iron and lead.

The results were obtained by the analysis of Bay (1951). No difference was found between the positron lifetimes in lead and aluminium, magnesium and iron. The error is estimated to be $\pm 5 \times 10^{-11}$ sec. A centroid shift of about 2×10^{-10} sec was found for wax, mica and water, indicating a lifetime of not less than this in these materials. With the resolving time used, measurements on the non-metals were not continued to sufficiently long delays to detect the complex behaviour reported for these non-metals by Bell and Graham (1953).

§ 4. INVESTIGATION OF LONG PERIODS IN SOLIDS

In the search for a long period in solids, first, the tails of the resolution curves for metals were examined at long delays but no evidence of the existence of any second period was found.

The equality of the lifetimes in iron and the other metals indicates that the aligned spins of the d-shell electrons of the domain structure of the iron has little effect. To examine this matter further, the specimen, in the form of a hollow cylinder was magnetized. With a delay of 3×10^{-9} sec (see fig. 2) the number of coincidences was measured alternately with and without an induction of some 7000 gauss per cm^2. No delay greater than 3×10^{-11} sec at this point was introduced by magnetization.

The long period in distrene reported by Bell and Graham (1952) was investigated further by the comparison method using aluminium as standard.

At this stage, a new ^{22}Na source was prepared for these experiments, by boiling up turnings from a deuteron bombarded magnesium target, kindly supplied by Professor Burcham of Birmingham University. As the magnesium was oxidized the sodium went into solution as NaOH and was readily separated from the MgOH by virtue of its vastly greater solubility. The solution was deposited on 0·0002 inch aluminium foil, and covered with a foil of similar thickness. The total weight including backing was 4 mg/cm^2.

Fig. 2

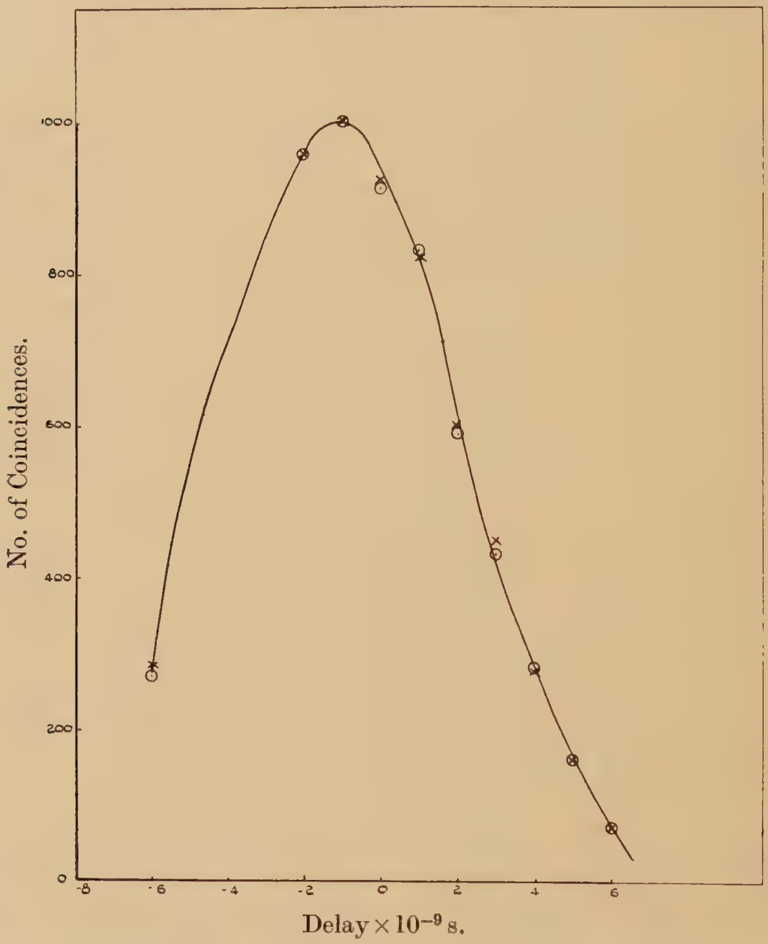

Coincidence resolution curve of coincidences between the 1·28 Mev γ-ray of ^{22}Na in C.1 and 511 kev annihilation γ-rays in C.2.

○ positrons annihilating in lead.
× positrons annihilating in iron.

The discriminator D.1 (see fig. 1) was set so as to exclude 511 kev γ-radiations and the discriminator D.2 was set so as to exclude the

^{203}Hg 280 kev γ-radiations. This helps to reduce spurious coincidences due to scattering. Care was taken with the geometry for this reason.

A resolution curve of positrons in distrene and a comparison curve using aluminium next the source were taken at room temperature (15°c). The curves obtained are shown in fig. 3. The detailed shape of the resolution

Fig. 3

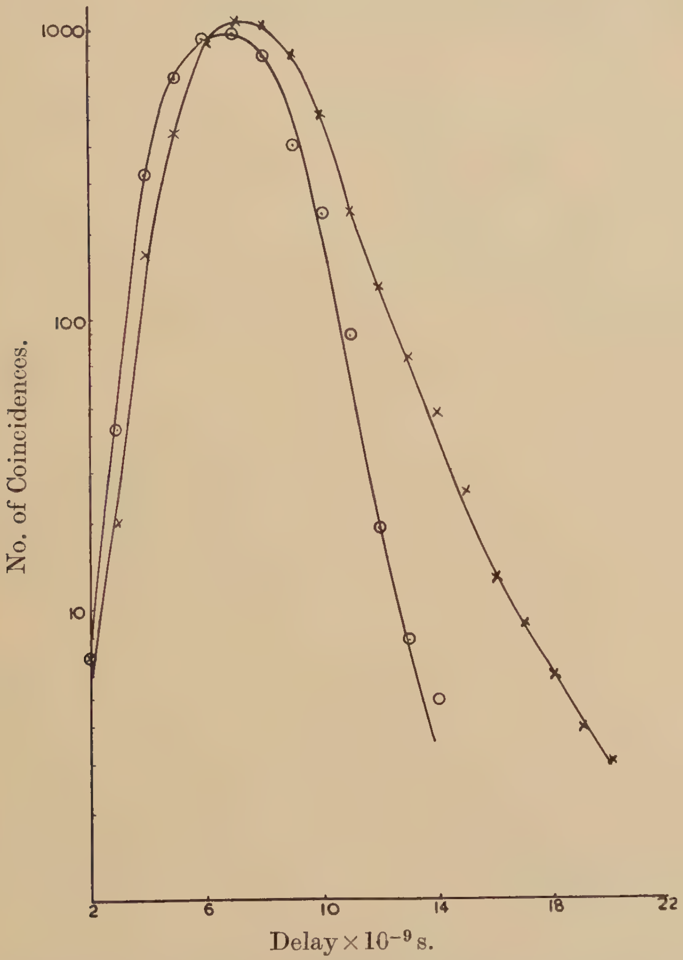

Coincidence resolution curves of coincidences between the 1·28 MeV γ-ray of ^{22}Na and 511 kev annihilation γ-rays in C.2.

× positrons annihilating in distrene.
○ positrons annihilating in aluminium.

curve for distrene, the large difference between the lifetime measured from the tail and from the centroid shift, showed that the long lifetime was associated with about one-third of the positrons. Assuming that the shorter period was comparable with that of aluminium the analysis of

Bay (1951) using second moments was applied. This gave the second mean life$=2{\cdot}5\pm0{\cdot}3\times10^{-9}$ sec for a fraction $0{\cdot}27\pm0{\cdot}03$ of the positrons. This is in good agreement with the period as found from the tail. These results agree with the recent work published by Bell and Graham (1953). The general features of the curves also correspond to those of the above authors.

To enable variation of lifetime with temperature to be studied without affecting the apparatus, the scintillators were surrounded by a jacket through which cold air was blown. The specimens were electrically heated.

The variation of lifetime with temperature was examined at a number of temperatures between room temperature (15°c) and 130°c when distrene begins to soften. An increase of about 10% was found for the 115°c increase in temperature.

The internal structural parameters of plastics are thought to vary with method of preparation and treatment. Samples machined from rod, cut from 0·1 inch sheet, made up from layers of 0·002 foil were examined. No difference was found between lifetimes in any of these.

No residual effects of heating, even to temperatures at which the distrene became soft, were found.

Plastic sulphur was examined in the same way as distrene. The samples, prepared by distillation on to the cold aluminium plates used in the experiment, were 0·1 inch thick and of a transparent straw colour. To avoid physical change the experiments were carried out immediately after preparation. With the resolution used no evidence indicating a second period exceeding 8×10^{-10} sec was found. Bell and Graham have reported some evidence for a partial period of about 4×10^{-10} sec.

§ 5. SEARCH FOR THREE-QUANTUM RADIATIONS FROM DISTRENE

On the hypothesis that the long period in certain materials is associated with three-quantum annihilation from the triplet state of positronium a search for this was made by two methods. In these, sodium iodide counters were used, with coincidence units of 0·5 μsec resolving time.

The first method used three counters at 120°, arranged to minimize scattering, and a ^{64}Cu source 0·0001 inch thick surrounded by distrene. The discriminators let pass only radiations above 280 kev. After subtracting randoms the number of coincidences was

Counters Coplanar 25 ± 5,
,, Non ,, $13\pm3{\cdot}5$.

A check experiment was made using aluminium in place of distrene. It is seen that little three-quantum annihilation occurs.

The second method measured the γ-ray coincidences at 180° using two counters 20 cm apart and the thin ^{22}Na source at the mid point of their axis. This geometry favours detection of two-quantum as against three-quantum annihilations by 100 : 1. The number of coincidences was measured with distrene and aluminium as absorbers and results indicated that less than 2% of the annihilations are three-quantum.

§ 6. LIFETIME OF POSITRONS IN ALUMINIUM

To measure the lifetime of positrons in metals it is necessary to produce a resolution curve for prompt events of similar energy. From the spins and parities of the two γ-emitting states in ^{60}Co (cf. for instance Metzger and Deutsch 1952) the delay in emission for the second γ-ray can be expected to be about 10^{-12} sec (cf. Moon 1949). In the case of ^{22}Na the 1·28 MEV γ-ray is thought to be prompt. An electric quadrupole transition would again give a lifetime of about 10^{-12} sec. A transition of higher order would have a lifetime readily detectable here. The experiments should

Fig. 4

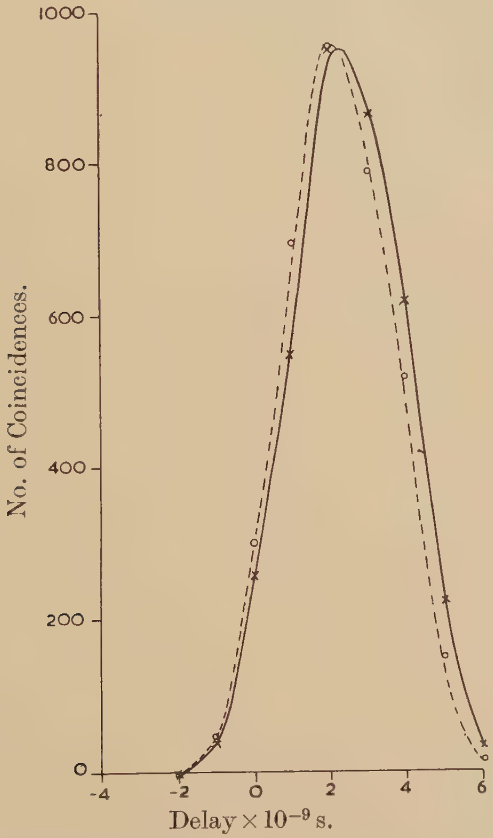

Coincidence resolution curves of coincidences between
× —— 1·28 MEV γ-ray of ^{22}Na and 511 kev annihilation radiation from aluminium.
○ – – – 1·17 MEV and 1·33 MEV γ-rays of ^{60}Co.

thus give an absolute measurement of the positron lifetime within the errors quoted below.

Those parts of the ^{60}Co γ-spectrum and the 1·28 MeV ^{22}Na γ-spectrum which lay above the bias of discriminator D.1 were examined with a kicksorter and found to lie close to one another.

Instead of counting all pulses from C.2 exceeding D.2 bias, only a band of pulses was accepted. The band was positioned at a region where the annihilation radiation spectrum and the ^{60}Co γ-ray spectrum were similar in shape. Thus in each counter the accepted spectrum of ^{22}Na and ^{60}Co was the same and hence their resolution curves could be compared.

In the first experiments the band was chosen by discriminator D.2 and another in parallel with it connected by an anticoincidence unit. Later the full apparatus shown in fig. 1 was used. The pulses fed to the kicksorter were about 10^{-7} sec wide. Delay of 1·25 μsec was inserted as shown using Z.14M delay cable so that these might coincide with the corresponding gateing pulses from 3–C.

Using the thin ^{22}Na source described above, surrounded by aluminium, a resolution curve was taken. The experiment was repeated using a ^{60}Co source of similar strength, giving a prompt resolution curve for comparison (see fig. 4). Several runs, sometimes in succession, were taken in this manner using both arrangements described above. Good agreement was obtained between their results. Each pair of curves was obtained in about two hours, with counting rates of a few hundred a minute at peak. Errors were mainly due to possible energy drifts of side channels. The result obtained was ($1{\cdot}6 \pm 0{\cdot}6 \times 10^{-10}$ sec). This is in good agreement with the value obtained by Bell and Graham (1953) using a different method.

A possible development of this technique may be mentioned, particularly useful for investigating delayed γ-cascades. By selecting only a suitable band of pulses from counter 1 also, prompt resolution curves from say the γ–γ coincidences of annihilation radiation could be obtained. These could be compared with a wide range of suspected delayed resolution curves.

§ 7. Discussion

The measured lifetime in aluminium, and by the comparison experiments, in all metals so far examined, is much shorter than that expected from simple annihilation of positrons. It would appear that the cross section for positron capture may be considerably greater than that for annihilation and that most annihilation comes from bound states. These considerations are strengthened by the results of De Benedetti *et al.* (1950) and Du Mond, Lind and Watson, which suggest that only the valence electrons take part in the annihilation process. Again, alignment of the d-shell electrons of iron does not seem important.

The experiments on distrene show that if the second period is due to triplet positronium, much of it is rapidly converted to the singlet state. If the long lived fraction were to find its way into sheltered states such as vacancies in the matrix, the interaction might be related to the spacing and so decrease with temperature.

ACKNOWLEDGMENTS

The authors wish to thank Professor P. I. Dee for his interest in this work, Dr. G. A. P. Wyllie for discussions and also the Department of Scientific and Industrial Research for a grant to one of us (A.T.G.F.).

REFERENCES

BAY, Z., 1950, *Phys. Rev.*, **77,** 419.
BELL, R. E., GRAHAM, R. L., PETCH, H. E., 1952, *Can. Journ. Phys.*, **30,** 35.
BELL, R. E., GRAHAM, R. L., 1952, *Phys. Rev.*, **87,** 236 ; 1953, *Ibid.*, **90,** 644.
DE BENEDETTI, S., COWAN, C. E., KONNEKER, W. R., PRIMAKOFF, H., 1950, *Phys. Rev.*, **77,** 205.
DE BENEDETTI, S., RICHINGS, H. J., 1951, *Phys. Rev.*, **81,** 310 ; 1952, *Ibid.*, **85,** 377.
DEUTSCH, M., 1951, *Phys. Rev.*, **83,** 866.
HEITLER, W., 1944, *The Quantum Theory of Radiation* (Oxford : University Press), p. 216.
LEWIS, G. M., FERGUSON, A. T. G., 1953, *Phil. Mag.*, **44, 1011.**
DU MOND, J. W., LIND, D. A., WATSON, B. B., 1949, *Phys. Rev.*, **75,** 1226.
METZGER, F., DEUTSCH, M., 1950, *Phys. Rev.*, **78,** 551.
MOON, P. B., 1949, *Artificial Radioactivity* (Cambridge : University Press), p. 80.
ORE, A., POWELL, J. L., 1949, *Phys. Rev.*, **75,** 1696.

CXLII. *Experiments on Magneto-Hydrodynamic Channel Flow*

By W. MURGATROYD
Department of Engineering, University of Cambridge*

[Received July 28, 1953]

SUMMARY

Experiments are described in which measurements of pressure gradient were taken during the flow of mercury in a rectangular channel of 15 : 1 aspect ratio, in the presence of a transverse magnetic field. It was possible to suppress turbulence even at the highest obtainable Reynolds Number ($R=10^5$).

For high values of R, the friction coefficient C_f appears to be a function of M/R and β. It is suggested that when R is large enough C_f might be a function of the single group $M/R\beta^{1/2}$. This is comparable with the simple relationship proposed by Hartmann and Lazarus (1937).

Lundquist (1952) has suggested that the transition from laminar to turbulent flow occurs at a fixed value of R/M, and that β does not enter into this criterion. The experiments suggest that the critical condition for the turbulent to laminar transition is $R/M \approx 900$, although since only one liquid was used, it was not possible to determine the influence of β.

§ 1. THE WORK OF HARTMANN AND LAZARUS

THE equations of motion for fully developed laminar flow between parallel plates, of a viscous, electrically conducting fluid, in the presence of a transverse magnetic field have been solved by Hartmann (1937). According to this theory the magnetic field flattens the velocity profile and increases the rate of shear at the walls, thus increasing the pressure gradient necessary to obtain the same rate of flow.

Hartmann and Lazarus (1937) carried out a series of experiments on the flow of mercury in rectangular and circular tubes with an imposed transverse magnetic field. They produced a series of curves showing pressure gradient as a function of field strength, each curve representing a constant volumetric flow rate. With flow which was laminar in the absence of a field, the effect of the field was to increase the pressure gradient in the manner predicted by Hartmann. When the flow was turbulent in the absence of a field, increase of field strength produced a decrease in pressure gradient up to a certain point, after which it increased again, finally obeying Hartmann's theory.

---

* Communicated by the Author.

The experimenters assumed that the phenomena observed in the turbulent regime were due to this ‘ Hartmann Effect ’ combined with the progressive damping of turbulence by the field. In order to separate these effects, they assumed that turbulent damping was proportional to H^2, where H is the field strength. On this basis, and after making other assumptions, they deduced that the decrease in pressure gradient due to damping of turbulence, $\Delta\dot{p}_r$, was proportional to H^2/d, where d is the tube diameter, and was independent of the mean velocity u. They sought to confirm this by a dimensionless analysis assuming that the decrease in pressure gradient was a function of H, d and u.

When conditions do not change with time, and when there are no free surfaces, magneto-hydrodynamic channel flow of a liquid metal depends upon the seven quantities $H, d, u, \rho, \eta, \sigma, \mu$, where d is a characteristic length (taken as the semi-width in the case of a high aspect ratio channel), ρ, η, σ, μ are respectively the density, viscosity, electrical conductivity and permeability of the fluid. The following dimensionless groups are particularly useful in channel flow experiments :

$$R=\frac{4\rho u d}{\eta}, \qquad M=\mu H d\sqrt{\left(\frac{\sigma}{\eta}\right)}, \qquad \beta=\frac{4\pi\mu\sigma\eta}{\rho};$$

R is the usual Reynolds Number, and β is a fluid property whose significance for the amplification of a small magnetic disturbance has been pointed out by Batchelor (1950). β is the ratio of two diffusivities, and in this sense is analogous to a Prandtl Number.

The dimensional analysis carried out by Hartmann and Lazarus tacitly assumes that $\Delta\dot{p}_r$ is independent of η and σ. When the flow is highly turbulent (their flow was not highly turbulent) it is plausible by analogy with ordinary hydrodynamic flow to assume independence of η, but they had no evidence to assume independence of σ.

§ 2. EXPERIMENTAL METHODS AND RESULTS

2.1. *Experimental Equipment*

The experiment to be described was designed to study the relationship between the pressure gradient, mean flow velocity and field strength, in the turbulent flow of mercury in a channel in the presence of a transverse magnetic field. The previous work of Hartmann and Lazarus was carried out with Reynolds Numbers below 5500, and so is hardly out of the transition range. The present apparatus was designed to give Reynolds Numbers up to 10^5, and at the same time a much higher value of M than was possible in the apparatus of Hartmann and Lazarus.

The channel was constructed from non-magnetic stainless steel plates, insulated internally with a coating of ‘ Araldite ’. Its length was 36 in. and the internal cross section measured 4 in. $\times$ 0·266 in. The width (0·266 in.) was checked at many points with an internal micrometer, the departure from the mean being less than 0·003 in. Over the test section the width was constant to within 0·001 in. Twenty-one static pressure holes were carefully drilled and broached in the top of the channel.

Pressures were measured on a multi-tube manometer. Since a gravity feed was used, the mean static pressure in the circuit varied during each test. For this reason the upper ends of the manometers were connected via a manifold to a small closed tank, the entire volume above the mercury being filled with air-free distilled water.

The volumetric flow rate was measured with a magnetic flowmeter, consisting of a section of insulated tube placed in a transverse magnetic field. Two electrodes were placed in the tube at opposite ends of a diameter, this diameter being perpendicular to the directions of flow and field. The flowmeter output was measured on a potentiometer, and the device was calibrated by measuring the throughput in a given time. The accuracy of calibration is believed to be ±1½%.

Fig. 1

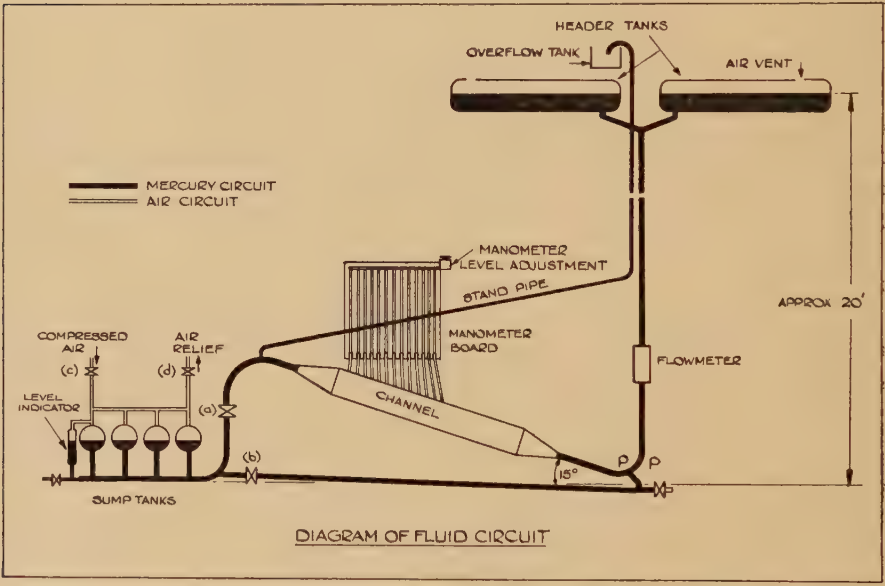

The fluid circuit is shown schematically in fig. 1. Freshly distilled mercury was contained in four oxygen cylinders placed horizontally about 20 ft. above ground level. On opening valve (*a*) flow was established through the flowmeter and channel into the sump tanks. At the end of each test, the sump was pressurized and mercury returned to the header tanks via the valve (*b*). The 15° inclination of the channel, in conjunction with the stand pipe, ensured that at the end of each test the channel and manometers remained full of mercury. The whole circuit was designed so as not to trap any air, since this would eventually displace mercury from one of the manometers. Great difficulty was experienced in removing all traces of air.

The transverse field was provided by a calibrated electromagnet having pole faces 12 in. × 5 in. and a gap of 1 in. The flux distribution in the gap was checked and found to be uniform within $\pm 1\frac{1}{2}\%$.

The last 12 in. of the channel were located in the magnetic gap, leaving a 24 in. entry length for the full development of turbulent flow.

2.2. *Experimental Results*

During the tests it was observed that the pressure gradient remained constant over the central six inches of the field, and increased rapidly at the edges. This was presumably due to the edge effect currents mentioned by Hartmann and Lazarus. Since only a limited time was available for each test, it was considered more profitable to concentrate on the central region of constant pressure gradient. Manometers 5 to 11 were read in semi-random order, care being taken to obtain repeated readings of at least numbers 5 and 11. Typical pressure gradients are plotted in fig. 2. Where only one point is given opposite manometers 5 and 11, the repeated readings coincided.

Fig. 2

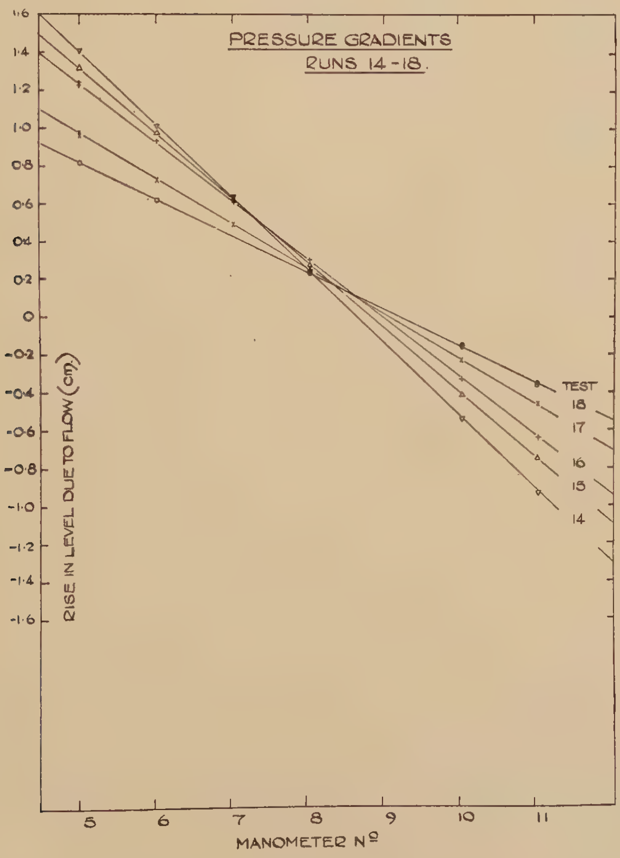

The table shows the complete results in dimensionless form. C_f is the usual friction coefficient, defined by $\tau_0 = C_f \rho u^2/2$, where τ_0 is the wall shear stress.

$10^{-5}R$	M	10^3C_f	$10^{-5}F$	M	10^3C_f
1·21	0	4·27	0·88	120·5	11·2
1·22	22·0	4·32	0·87	128·8	12·0
1·21	31·0	4·48	0·80	0	4·81
1·21	60·3	5·31	0·80	11·5	4·65
1·21	66·8	5·58	0·81	24·2	4·87
1·22	86·5	6·39	0·80	35·9	5·31
1·21	99·8	7·02	0·80	46·2	5·74
1·21	112·5	7·67	0·80	51·9	6·03
1·21	125·5	8·33	0·80	80·3	8·11
1·21	129·0	8·80	0·81	115·0	11·73
1·01	0	4·58	0·70	0	4·99
1·02	14·3	4·41	0·70	20·3	4·90
1·02	32·6	4·72	0·70	29·0	5·00
1·02	40·7	4·98	0·705	42·4	5·82
1·01	49·2	5·17	0·705	48·4	6·29
1·01	72·2	6·41	0·70	60·0	7·24
1·00	105·8	8·51	0·70	110·5	13·81
1·00	118·5	9·36	0·70	124·7	14·32
1·01	130·5	10·32	0·30	0	5·95
0·88	0	4·67	0·30	5·2	5·81
0·88	0	4·63	0·30	10·4	5·86
0·88	23·0	4·72	0·30	18·0	6·01
0·88	30·0	4·87	0·30	26·0	7·05
0·88	42·1	5·35	0·30	63·1	17·1
0·87	75·7	7·38	0·10	0	7·73
0·87	99·3	7·49	0·10	5·4	5·67
0·87	105·8	9·85	0·10	10·4	9·27
			0·10	46·0	37·0

§ 3. DISCUSSION

Figure 3 shows a graph of C_f against M/R and shows several interesting features. Apart from the two low Reynolds Number curves (which are of lower accuracy owing to the small pressure gradient) the experimental points lie quite well on a single curve, except at low values of M/R. This curve approaches the laminar ‘ Hartmann ’ line slowly, which seems to indicate that turbulence is not suddenly suppressed, or that if it is, it persists so long that its effect on C_f is swamped by the Hartmann effect. Within the experimental scatter, the flow appears to be laminar whenever $R < 900M$. It is interesting that laminar flow can be obtained in this manner even when $R = 10^5$.

Figure 3 shows that at the higher Reynolds Numbers, the trend is for C_f to be a function of M/R, and that the range of validity of this relationship widens with increasing R. One may speculate that at high enough values of R, C_f is a function of M/R and β only. Now if at high values of R, the effects of viscosity can be neglected by comparison with the other forces present, then dimensional reasoning shows that C_f must be a function of the two groups $(M/R\beta^{1/2})$ and $(R\beta)$. If this is to be a function of (M/R) and β then this function must be of the single group $(M/R\beta^{1/2})$. It is interesting to note that this quantity does not contain dissipative terms and is, in fact, equal to the square-root of the ratio of magnetic to kinetic energy per unit volume. This speculation is a generalization of the relationship intuitively assumed by Hartmann and Lazarus. They assumed a simple form for the function, and moreover did not restrict it

Fig. 3

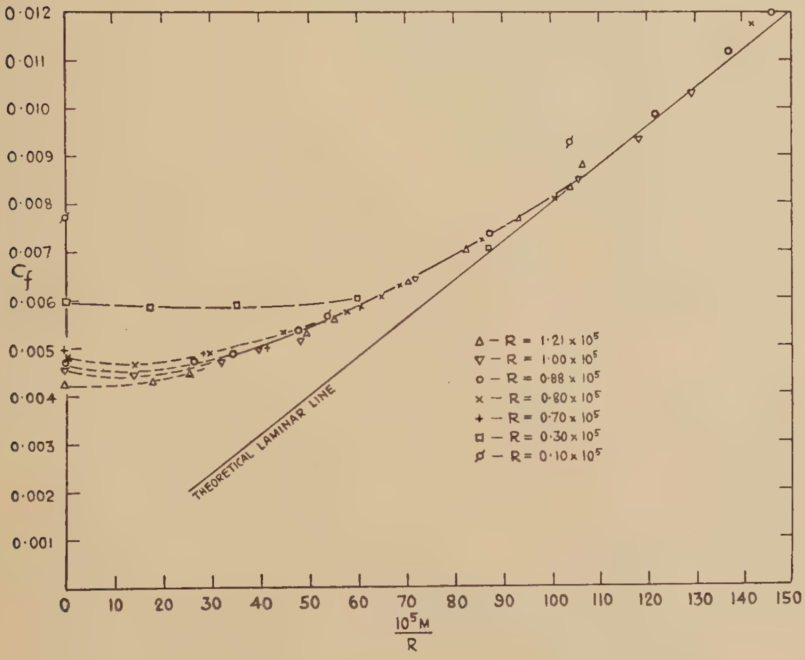

to high values of R, although their attempts to separate the Hartmann effect were equivalent to removing direct viscous action. They had no justification for omitting σ from their dimensional analysis.

At first sight there appears to be a paradox since $(M/R\beta^{1/2})$ does not contain σ, and so the speculations might equally apply to a non-conducting fluid. It must be remembered, however, that M and R can separately enter into the conditions under which the speculations apply. These conditions remain as yet undetermined.

In a recent paper (Lundquist 1952) it is suggested that transition from laminar flow occurs at a certain critical value of the boundary layer Reynolds Number R'_{crit} $(R'=4\rho uL'/\eta$, where L' is a dimension characterizing the boundary layer). In the present notation $L'=d/M$ and thus $R'_{\text{crit}}=(R/M)_{\text{crit}}$, and is independent of β. It appears from fig. 3 that transition the other way (i.e. from turbulent to laminar flow) takes place at approximately $R/M=900$, although since only one fluid was used, it is not possible to assert or deny independence of β.

The essence of Lundquist's argument is that magneto-hydrodynamic forces are important only insofar as they determine the thickness and velocity distribution in the boundary layer, and that apart from this, they do not enter into the stability criterion. The parameter β, therefore, does not affect stability. It is very desirable that similar experiments be carried out using other fluids, and so varying β.

The present writer has attempted to separate the Hartmann effect from the turbulent damping effect in a more refined way than that of Hartmann and Lazarus. The essence of the method is to apply Hartmann's equations to a 'magneto-hydrodynamic boundary layer', i.e. a layer near the wall in which only electro-magnetic and viscous forces are important. A relationship follows between the shear at the two boundaries of this layer in terms of M, R and the thickness of the layer. Thus knowing the velocity gradient at the wall, from the pressure gradient, the velocity gradient at the inner boundary of the layer can be estimated, and this can be used to measure the dissipation in the turbulent core. The results obtained, however, are very sensitive to the choice of boundary layer thickness, which at present is arbitrary. Until more experimental evidence is available it is not desirable to publish these results.

The writer is grateful to Dr. S. G. Bauer and Mr. C. D. Boadle of the Ministry of Supply for their valuable experimental assistance and continuous encouragement. He also wishes to thank the Director, Atomic Energy Research Establishment, for permission to publish the results.

REFERENCES

Batchelor, G. K., 1950, *Proc. Roy. Soc.* A, **201**, 405.
Hartmann, J., 1937, *Det. Kgl. Danske Vidensk. Selskab.*, XV. 6.
Hartmann, J., and Lazarus, F., 1937, *Det. Kgl. Danske Vidensk. Selskab.*, XV. 7.
Lundquist, S., 1952, *Arkiv för Fysik*, **5**, 297.

CXLIII. *On Conduction in Impurity Bands*

By Walter Baltensperger
The Physical Laboratories, University of Manchester, England*

[Received July 10, 1953]

Summary

The idea of conduction by electrons in the energy bands of an impurity system is examined. For a lattice of hydrogen-like impurities the edges of the 1s, 2s, and 2p bands are calculated. Effective masses for electrons in these bands are introduced. With their help measurements of the conductivity and the Hall constant are interpreted. Depending on the density of the impurities and on the temperature, conduction takes place predominantly either in the band of the medium, or in excited impurity states, or in the 1s impurity band. In this last case the activation energy vanishes.

This interpretation implies a description of the electronic state of the impurities with band wave functions and indicates the validity of such a description up to rather large values of the lattice constant. This can, however, be reconciled with the insulating properties of the oxides of transition metals.

§ 1. Introduction

In recent years various authors have indicated the importance of conduction by charges in impurity states. Busch and Labhart (1946) explained their measurements of the conductivity and the Hall constant of SiC with a model which attributes a mobility to the electrons in impurity levels. Similarly Hung (1950) postulated conduction in impurity bands in view of Hall effect measurements on Ge at low temperatures. Erginsoy (1950, 1952) suggested an investigation of impurity bands and calculated the lower edges of the s bands. Earlier the work of Pearson and Bardeen on Si (1949) had shown that the activation energy of the charges depends on the impurity content, and these authors had assumed that this results from an interaction between the free charges and the ionized impurities. However, this argument was criticized by Castellan and Seitz (1951), who investigated various alternative theories without finding a satisfactory explanation. In particular, for a density of impurities such that the samples show a metallic characteristic the interaction energy between the impurity centres in their ground state turned out to be small. Hence the Heitler–London scheme seemed to be the appropriate description of the impurity system, whereas the Bloch scheme which could describe a metallic

---

* Communicated by Prof. L. Rosenfeld.

behaviour was considered as representing an excited state. The possibility had to be faced that fundamental changes in the theory would be necessary.

We take up the idea of conduction in impurity bands without justifying the application of the band scheme. First we investigate the upper and lower edges of the 1s, 2s, and 2p bands, and then define an effective mass for an electron in each of these bands. A comparison with the effective mass for the conduction band of the medium suggests an interpretation of conductivity and Hall effect measurements, in particular the observed decrease of the activation energy. The agreement with experiment is significant for solid state theory, since it indicates the applicability of the band scheme up to rather large values of the lattice constant.

§ 2. THE ENERGY BANDS

As a model for a semiconductor we take a medium, characterized by the effective mass m^* of a conduction electron, and by the dielectric constant κ, sufficiently large, in order that the hydrogen-like picture of a single impurity is justified (Baltensperger 1951). We assume that the impurities are arranged in a regular close-packed lattice. Applying the Wigner–Seitz method atomic polyhedra are set up, which we approximate by spheres of equal volume. Their radius r_s is then related to the density of the impurities N by

$$(4\pi/3)\, r_s^3 = 1/N. \qquad \text{(1)}$$

On the average an electron in a sphere will be subject only to the ionic potential $V = -e/\kappa r$. The Schrödinger equation

$$\frac{\hbar^2}{2m^*}\Delta\psi + \left(\frac{e^2}{\kappa r} + \epsilon\right)\psi = 0 \qquad \text{(2)}$$

has the general regular solution

$$\psi = R_{n,\,l}(r) \times Y_{l,\,m}(\vartheta, \phi) \qquad \text{(3)}$$

$$R_{n,\,l}(r) = \exp\,(-r/n\kappa a) \times (2r/n\kappa a)^l \times F(l+1-n,\, 2l+2,\, 2r/n\kappa a)\,, \qquad \text{(4)}$$

where

$$F(\alpha, \gamma, x) = 1 + \frac{\alpha}{\gamma}\frac{x}{1\,!} + \frac{\alpha(\alpha+1)}{\gamma(\gamma+1)}\frac{x^2}{2\,!} + \dots \qquad \text{(5)}$$

is the confluent hypergeometric function, and

$$a = \hbar^2/m^* e^2\,. \qquad \text{(6)}$$

The energy is given by

$$\epsilon = -\frac{e^4 m^*}{2\hbar^2\kappa^2} \times \frac{1}{n^2}, \qquad \text{(7)}$$

where n is to be determined by an appropriate boundary condition.

This boundary condition is obtained from the requirement that the wave functions have Bloch's form (Slater 1934)

$$\begin{aligned}\psi &= \exp\,(2\pi i \mathbf{k}\mathbf{x}) \times u(\mathbf{x}) \\ u(\mathbf{x}+\boldsymbol{\tau}) &= u(\mathbf{x})\end{aligned} \qquad \text{(8)}$$

where $\boldsymbol{\tau}$ is a primitive translation of the lattice. We only consider special points of a reduced Brillouin zone, namely the centre, $\mathbf{k}=0$, to which corresponds a periodic wave function, and the corners, given by $2(\mathbf{k}\boldsymbol{\tau})=1$, the wave function thus being antiperiodic. With the spherical approximation for an atomic cell, l is a good quantum number. If a wave function is even about the nucleus (even l), the corresponding boundary condition is

$$\left.\frac{\partial\psi}{\partial r}\right|_{r=r_s}=0 \quad . \quad . \quad . \quad . \quad . \quad . \quad . \quad . \quad . \quad (9)$$

for $\mathbf{k}=0$ and

$$\psi(r_s)=0 \quad . \quad . \quad . \quad . \quad . \quad . \quad . \quad . \quad . \quad (10)$$

for $2(\mathbf{k}\boldsymbol{\tau})=1$. For odd wave functions $\mathbf{k}=0$ belongs to (10) and $2(\mathbf{k}\boldsymbol{\tau})=1$ to (9). We shall consider the eigenvalues belonging to (9) and (10) to be respectively the bottom and the top edges of the bands.

Fig. 1

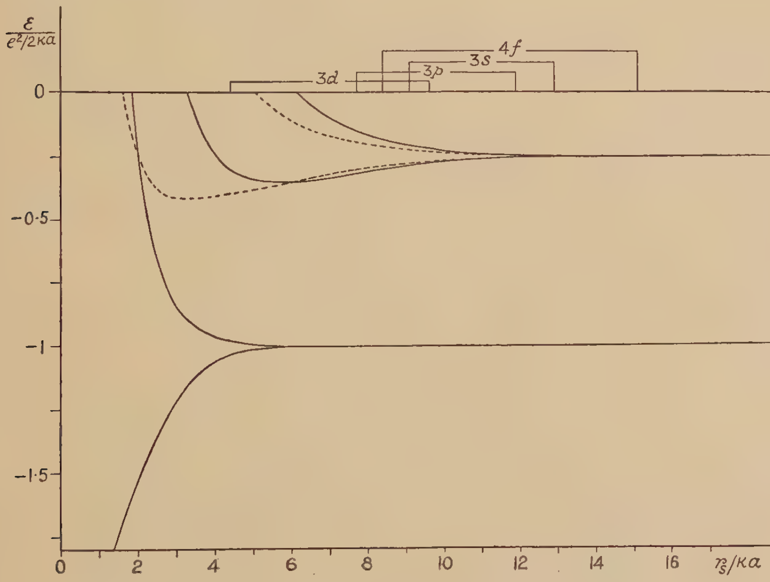

———————— edges of the 1s and 2s bands.
— — — — — — edges of the 2p band.
The radii of the atomic cell for which the edges of some further bands cross the value $\epsilon=0$ are indicated.

Using (3) and (4) the conditions read

$$\left(\frac{1}{n}-\frac{l\kappa a}{r_s}\right)F(l+1-n, 2l+2, 2r_s/n\kappa a)$$
$$=\frac{1}{n}\times\frac{l+1-n}{l+1}F(l+2-n, 2l+3, 2r_s/n\kappa a) \quad . \quad . \quad . \quad (9\,a)$$

$$F(l+1-n, 2l+2, 2r_s/n\kappa a)=0. \quad . \quad . \quad . \quad . \quad . \quad . \quad . \quad . \quad . \quad (10\,a)$$

Equation (10 *a*) has been used by Michels, De Boer and Bijl (1937), Sommerfeld and Welker (1938), and by De Groot and Ten Seidam (1946) to determine n, and therefore ϵ, as a function of $r_s/\kappa a$ and l. Further, eqn. (9 *a*) has been discussed by Erginsoy (1952) with $l=0$, and n approximately equal to an integer. Similar methods can be used for $l=1$ and some further values can be obtained from existing tables of $F(\alpha, \gamma, x)$ (Webb and Airey 1918, Jahnke and Emde 1945). For $n \rightarrow \infty$ the conditions

$$(2l+2)\times(8r_s/\kappa a)^{-1/2}\times J_{2l+1}([8r_s/\kappa a]^{1/2})=J_{2l}([8r_s/\kappa a]^{1/2}) \quad . \quad . \quad . \quad (9\,b)$$

$$J_{2l+1}([8r_s/\kappa a]^{1/2})=0 \quad . \quad . \quad . \quad . \quad . \quad . \quad . \quad (10\,b)$$

give the values of $r_s/\kappa a$ for $\epsilon=0$. The edges thus obtained are shown in fig. 1.

§ 3. Definition of Effective Masses

Instead of discussing the band widths $\Delta\epsilon$, we introduce quantities $m^\dagger$, defined by

$$\Delta\epsilon=h^2k^2/2m^\dagger, \quad . \quad . \quad . \quad . \quad . \quad . \quad . \quad . \quad (11)$$

Fig. 2

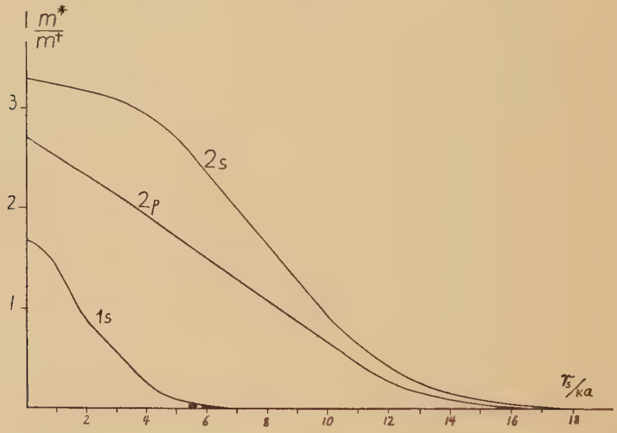

Ratio of effective masses versus radius of the atomic cell.

where k is the largest wave-number for a spherical Brillouin zone and satisfies

$$(4\pi/3)k^3=N. \quad . \quad . \quad . \quad . \quad . \quad . \quad . \quad . \quad (12)$$

From (11), (12), (1) and (6), we get

$$\frac{m^*}{m^\dagger}=\left(\frac{4}{81\pi^2}\right)^{1/3}\times\frac{2}{e^2\kappa a}r_s^{\,2}\Delta\epsilon=0{\cdot}1710\times\left(\frac{r_s}{\kappa a}\right)^2\times\frac{\Delta\epsilon}{e^2/2\kappa a}. \quad . \quad (13)$$

For $r_s\rightarrow 0$, $m^*/m^\dagger$ was found by solving (2) with (9) and (10), neglecting the potential energy. Introducing this as a perturbation, we obtain the slope of $m^*/m^\dagger$ for $r_s\rightarrow 0$. In fig. 2, $m^*/m^\dagger$ is plotted against $r_s/\kappa a$ for the 1s, 2s, and 2p bands.

While m^* characterizes the dynamical property of an electron moving through the medium, either free or bound to an impurity, $m^\dagger$ will be considered as the effective mass of an electron whose energy lies in an impurity band, for its movement through the impurity lattice. The definition (11), (12) of a constant $m^\dagger$ for a whole band is of course rough, since it implies a parabolic dependence of the energy on the wave-number for an entire Brillouin zone.

The mobility of an electron is finite because of deviations from a perfectly regular lattice. For an electron in the conduction band scattered by thermal vibrations, the mobility is proportional to $m^{*-5/2}$ (Seitz 1948), while scattering due to impurity ions according to the formula of Conwell and Weisskopf (1946, 1950) gives a dependence like $m^{*-1/2}$. The conduction mechanism of electrons in impurity states is obscured by the fact that the impurities in reality do not form a lattice. On the one hand irregularities in the arrangement of the impurities will lead to scattering. On the other hand the disorder will increase the average interaction between the impurities, which is a minimum for a regular arrangement, so that the present model overestimates the effective mass. This is confirmed by a calculation of Aigrin and Jancovici (private communication) who have calculated the energy levels for a disordered arrangement of the impurities. The exact relation between the mobility of an electron in an impurity state and the effective mass $m^\dagger$ is not known. For a qualitative interpretation of the measurements it is sufficient to assume that $m^*/m^\dagger$ (fig. 2) is of the order of magnitude of the ratio of the mobility belonging to the impurity band to the mobility of the band of the medium.

§ 4. INTERPRETATION OF MEASUREMENTS

The temperature determines the distribution of the charges amongst the bands. If there are N_i charges in the ith band having a mobility μ_i, the conductivity is

$$\sigma = e\sum_i N_i \mu_i , \quad . \quad . \quad . \quad . \quad . \quad . \quad . \quad . \quad . \quad . \quad (14)$$

and the Hall coefficient (in practical units)

$$R = F\Big(\sum_i e_i N_i \mu_i^2\Big) \times \Big(\sum_j e_j N_j \mu_j\Big)^{-2}, \quad . \quad . \quad . \quad . \quad . \quad (15)$$

where $e_i = +e$ if the charges are holes, and $e_i = -e$ if they are electrons, and where F is a constant of order 1. If only one band, the ith say, contributes to the conduction, the Hall coefficient determines the number of charge carriers:

$$R = F(e_i N_i)^{-1} \quad \text{if} \quad N_j \mu_j = 0 \text{ for } j \neq i. \quad . \quad . \quad . \quad . \quad (16)$$

We consider the measurements of Pearson and Bardeen (1949) (see table 1). For sample 1 the mobilities of the impurity bands are negligible, hence the measured activation energy is the energy required to raise a charge into the band of the medium. In samples 2, 3, 4, A, B, activation into an excited impurity band is sufficient to provide conduction. Sample 5 with $r_s/\kappa a = 5{\cdot}2$ is intermediate. The mobility in the 1s band is small but not negligible. Thus at high temperatures the resistivity of sample 5 behaves similarly to that of sample 4, while at low temperatures the conduction in the 1s band becomes predominant, and then the measured activation energy vanishes. Samples 6, 7, 8, C, D, have the metallic behaviour corresponding to conduction in the 1s band. The Hall coefficient shows that in these cases there is one charge carrier per impurity atom. The mobilities are largest for the samples 2, 3, 4, A, B, for which the excited impurity bands are important. However, it must be remembered that when different bands contribute to the conduction the determination of the numbers of charge carriers, the mobilities, or the mean free paths becomes ambiguous.

Bands belonging to large quantum numbers n have not been considered. Since the extension of hydrogenic wavefunctions is essentially proportional to n, we expect by extrapolation that for intermediate temperatures these bands are important in a range, $6n > r_s/\kappa a > 2n$. In fact, for low densities, $r_s/\kappa a > 6n$, the mobilities will be negligible, while for high densities, $r_s/\kappa a < 2n$, the bands are shifted to such high energies that only few electrons are activated into them.

Table 1. Interpretation of the Measurements of Pearson and Bardeen (1949) on Silicon Alloys

Sample	Solute	Carriers/cc. in saturation range	$r_s/\kappa a$	Conductivity mainly due to
1	Boron	$8{\cdot}0 \times 10^{15}$	45	Silicon band
2	Boron	$6{\cdot}0 \times 10^{17}$	10·7	Excited impurity bands (2s, 2p, 3s, 3p, 3d, . .)
3	Boron	$1{\cdot}3 \times 10^{18}$	8·3	
4	Boron	$2{\cdot}5 \times 10^{18}$	6·6	
5	Boron	$5{\cdot}3 \times 10^{18}$	5·2	1s band for low temperature
6	Boron	$1{\cdot}4 \times 10^{19}$	3·7	1s band
7	Boron	$1{\cdot}2 \times 10^{20}$	1·8	
8	Boron	$4{\cdot}8 \times 10^{20}$	1·15	
A	Phosphorus	$1{\cdot}05 \times 10^{17}$	13	Excited impurity bands
B	Phosphorus	$1{\cdot}25 \times 10^{18}$	5·6	
C	Phosphorus	$1{\cdot}7 \times 10^{19}$	2·4	1s band
D	Phosphorus	$2{\cdot}6 \times 10^{20}$	0·95	

$r_s/\kappa a$ according to (1) and (6) with $\kappa = 13$, and
$m^* = m$ for the silicon–boron alloys,
$m^* = 0{\cdot}67\, m$ for the silicon–phosphorus alloys.

§ 5. SIGNIFICANCE FOR SOLID STATE THEORY

Although the disordered arrangement of the impurities makes quantitative predictions difficult, experiments with semiconductors may indicate the qualitative behaviour of a system of atoms for a large range of densities. In the usual theoretical method the electron state is approximated by a determinant of one-electron functions. In the Heitler–London scheme these are localized, and, for a description of the ground state of a system with N ions and N electrons, N different spatial functions will be occupied. In the Bloch scheme the functions extend over the whole lattice, and in the ground state $N/2$ functions belonging to the lowest energies will be occupied twice.

In fig. 3, as an illustration, the total energy of the system according to the two schemes is plotted against $r_s/\kappa a$. For the Heitler–London scheme the curve corresponds to a formula which was derived by Slater (1930) disregarding the normalization difficulties that arise from non-orthogonal wavefunctions. However, for a system containing a large number of electrons, this invalidates the quantitative results of such a calculation (Slater 1930, 1953, Löwdin 1950). As to the Bloch scheme, for high densities the curve represents the results of the calculations on metallic hydrogen by Kronig, de Boer, and Korringa (1946), while for large interatomic distances it is based on the considerations by Seitz (1940). The occupation of the $N/2$ functions with lowest energies is a good approximation for wide bands only, as was pointed out by Slater (1953), whereas for narrow bands the wavefunctions should be chosen to be a sum of determinants corresponding to all different configurations. A calculation of this type may yield a much lower energy. At present no reliable quantitative treatment is available for a lattice of atoms with weak interaction.

Fig. 3

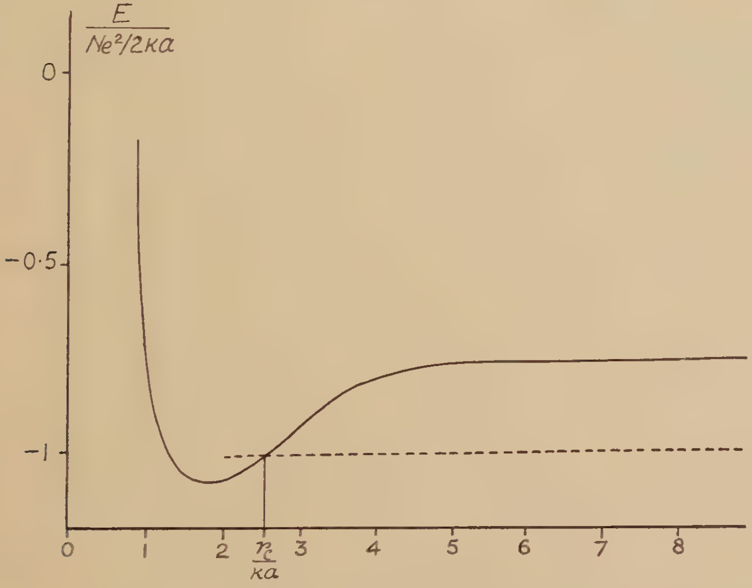

——————— total energy for the Bloch scheme.
— — — — — total energy for the Heitler-London scheme.

The two types of description are qualitatively different (Schubin and Wonsowski 1934). At low temperatures the Heitler–London scheme does not allow any conduction. This is true provided the numbers of electrons and atoms are exactly equal; otherwise the difference between these numbers gives the number of free charges. The Bloch scheme with incompletely filled bands describes a metallic conductor.

Mott (1949) has pointed out that the state of a substance will either correspond to one or the other scheme, and not to some intermediate description. Oxides of transition metals, such as NiO, are insulators in the pure state, although they have partially filled energy bands ; for these the Heitler–London scheme must apply. If the lattice constant of a metallic substance is increased, at a critical value a phase transition will occur, corresponding to a change from the Bloch to the Heitler–London description. For impurities in a disordered arrangement this transition may not be sharp (Mott 1951).

We have seen that the idea of conduction in impurity bands explains the dependence of the conductivity and the Hall coefficient on impurity content and temperature. It implies that the impurity states are described by band wave functions, whenever they are found to contribute to the conduction. It should be mentioned that a finite conductivity at low temperatures alone could arise from some secondary effect ; since a sample will contain both donors and acceptors, and since one impurity type will trap charges of the other, even the Heitler–London description permits conduction, though for this the number of free charges is given by the density of the secondary impurities. However, the measurements of Pearson and Bardeen (1949), and, more especially, those of Hung and Gliessmann (1950) show that at low temperatures, at which conduction in excited states becomes negligible, the Hall coefficient is constant and approximately equal to the Hall coefficient at saturation temperatures, at which all electrons are in the conduction band of the medium.

This observation demands a description of the ground state of the impurity system in which all electrons are free to move (Hung 1950). It excludes an explanation of the low temperature conductivity by a secondary effect. It also indicates, that if the phase transition to the Heitler–London scheme is not sharp, it is not yet noticeable in the samples, for which the constant Hall coefficient at low temperature was measured. Sample 5, table 1 then gives a lower limit for the critical radius of the atomic sphere for which the phase transition occurs

$$r_c/\kappa a > 5. \qquad (17)$$

The value $r_c/\kappa a = 2{\cdot}5$ of fig. 3 shows that the underlying theory is inadequate, even considering that the disordered arrangement of the impurities is a source of error.

The question arises, whether the condition (17) can be reconciled with the insulating properties of the oxides of transition metals, which demand a Heitler–London description for the 3d states of the metal ions (Mott 1949). The above discussion was based on the parameter $r_s/\kappa a$, i.e. the radius of an atomic sphere measured in units which are atomic units divided by the effective number of charges, $1/\kappa$. For a rough argument we define a similar parameter for metal oxides, such that for equal values of the parameters we may expect an interaction of comparable relative importance.

NiO, for example, has a simple cubic structure, in which the Ni^{++} ions alone form a cubic face-centred lattice. The atomic volume is $18{\cdot}2$ A^3, so that $r_s=1{\cdot}63$ A. We express r_s in units na_0/Z_{eff}, where $a_0=0{\cdot}529$ A is the Bohr radius, and $n=3$ accounts for the increase in size of the wavefunctions with higher quantum numbers. The effective number of charges Z_{eff} for one of the 8 electrons in the 3d shell of a Ni^{++} ion will be larger than 3, since each of the remaining 7 electrons in the shell screens the nucleus only for a fraction of the time. If this fraction is $\frac{1}{2}$, then $Z_{\text{eff}}=3+\frac{1}{2}\times 7=6{\cdot}5$ and

$$\frac{r_sZ_{\text{eff}}}{na_0}=\frac{1{\cdot}63\times 6{\cdot}5}{3\times 0{\cdot}529}=7. \qquad . \quad . \quad . \quad . \quad . \quad . \quad . \qquad (18)$$

The value of the parameter is larger than the minimum required by (17). It must be remembered, however, that this argument ignores the presence of the O^{--} ions, and also that for very large values of the parameter even the Bloch scheme leads to an unobservably small conductivity.

Thus the evidence from semiconductors and from the oxides of transition metals are consistent with the view that a description of a solid must be either of the Bloch or the Heitler–London type but the phase transition between the two seems to take place for larger values of the lattice constant than expected according to the present simple theory.

I am grateful to Professor L. Rosenfeld for his kind support and stimulating discussions.

References

Aigrin, P., and Jancovici, B., 1952, private communication.

Baltensperger, W., 1951, *Phys. Rev.*, **83,** 1055.

Busch, G., and Labhart, H., 1946, *Helv. Phys. Acta*, **19,** 463.

Castellan, G. W., and Seitz, F., 1951, *Semiconducting Materials* (London : Butterworths Scientific Publ.).

Conwell, E., and Weisskopf, V. F., 1946, *Phys. Rev.*, **69,** 258 ; 1950, *Phys. Rev.*, **77,** 388.

Erginsoy, C., 1950, *Phys. Rev.*, **80,** 1104 ; 1952, *Phys. Rev.*, **88,** 893.

De Groot, S. R., and ten Seldam, C. A., 1946, *Physica*, **12,** 669.

Hung, C. S., 1950, *Phys. Rev.*, **79,** 727.

Hung, C. S., and Gliessmann, J. R., 1950, *Phys. Rev.*, **79,** 726.

Jahnke, E., and Emde, F., 1945, *Tables of Functions* (New York : Dover Publications).

Kronig, R., De Boer, J., and Korringa, J., 1946, *Physica*, **12,** 245.

Löwdin, P. O., 1950, *J. Chem. Phys.*, **18,** 365.

Michels, A., De Boer, J., and Bijl, A., 1937, *Physica*, **4,** 981.

Mott, N. F., 1949, *Proc. Phys. Soc.* A, **62,** 416 ; 1951, *Semiconducting Materials* (London : Butterworths Scientific Publ.).

Pearson, G. L., and Bardeen, J., 1949, *Phys. Rev.*, **75,** 865.

Schubin, S., and Wonsowski, S., 1934, *Proc. Roy. Soc.* A, **145,** 159.

Seitz, F., 1948, *Phys. Rev.*, **73,** 549 ; 1940, *The Modern Theory of Solids* (New York : McGraw-Hill Book Company Inc.), Chap. IX, Sec. 75a.

Slater, J. C., 1930, *Phys. Rev.*, **35,** 509 ; 1934, *Ibid.*, **45,** 794 ; 1953, *Rev. Mod. Phys.*, **25,** 199.

Sommerfeld, A., and Welker, H., 1938, *Ann. Physik* (5), **32,** 56.

Webb, H. A., and Airey, J. R., 1918, *Phil. Mag.*, **36,** 129.

CXLIV. *Thermoelectric Power of Monovalent Metals at High Temperature*

By D. K. C. MacDonald and S. K. Roy*
National Research Council, Ottawa†

[Received May 4, 1953]

Abstract

The band theory of metals is applied to analyse the thermoelectric power of 'simple' metals at high temperatures. The conventional analysis is first carried through for entirely free electrons and then extended to include variation in number of free electrons per atom, departure from a quadratic dependence of energy on wave number, and non-spherical Fermi surface. Consideration of the data on the alkali and noble metals shows potassium to present a special problem in interpretation.

§ 1. Introduction

On the basis of the electron theory of metals, the variation with temperature of the electrical and thermal conductivity can be discussed, and the theory has been used to study particularly the alkali metals, which are often regarded as more or less ideal. In the case of electrical resistance, the features of the dependence on temperature are quite well predicted, but the agreement between theory and experiment is less satisfactory for thermal conductivity. The actual magnitude of the conductivities is more difficult to analyse without an explicit knowledge of the potential energy of an electron in the metallic lattice.

The phenomenon of thermoelectricity presents fresh problems. At low temperatures, such that impurity scattering becomes significant, a rather detailed knowledge of the mechanism of scattering of electrons by impurity atoms appears to be called for to explain the varied anomalies in thermoelectric behaviour in this region (e.g., Borelius 1935, MacDonald and Pearson 1953). Such theories of impurity scattering as are available at present are inadequate to account for the experimental results.

In this paper we shall confine our attention to the region of 'high' temperatures, that is, when T, the temperature of the metal, is at least of the order of the Debye characteristic temperature Θ, but is below the melting point.

This region of temperature is then *classical* in nature, a relaxation time always exists, and impurity scattering is in general negligible. Furthermore, the Einstein model to describe the heat motion of the lattice should be adequate. Rather definite theoretical conclusions may then be derived on the basis of this model, and compared with experimental results to throw further light on the basic assumptions of the theory.

---

* National Research Laboratories Postdoctorate Fellow.
† Communicated by the Authors.

§ 2. EXPRESSION FOR THERMOELECTRIC POWER

The absolute thermoelectric power S of a metal is given by (for a fuller account see Wilson 1936, Mott and Jones 1936)

$$S=\frac{1}{eT}\left(\frac{K_1}{K_0}-\zeta\right) \qquad \ldots \ldots \ldots \ldots (1)$$

where ζ is the Fermi energy at the temperature T, e is the charge on the electron, and K_n is given by

$$K_n=-\frac{1}{4\pi^3\hbar^2}\int\int\int E^n\left(\frac{\partial E}{dk_x}\right)^2\frac{\partial f_0}{\partial E}\tau(\mathbf{k})dk_x dk_y dk_z. \qquad \ldots \ldots (2)$$

The integration in (2) extends effectively throughout the volume enclosed by the Fermi surface, and f_0 is the equilibrium distribution function. E is the energy of the electron in the state defined by the wave number $\mathbf{k}$ of the electron, k_x is the component of $\mathbf{k}$ in the x-direction in which the external field and the temperature gradient exist, and $\tau(\mathbf{k})$ is the relaxation time. It is *not* assumed here that $\tau(\mathbf{k})$ is a function of $|\mathbf{k}|$ only as is done in the case of electrical and thermal conductivity. Equation (1) should, therefore, be valid for any relation between E and $\mathbf{k}$ (cf. Mott and Jones, p. 311).

Substitution of (2) in (1) leads to

$$S=\frac{\pi^2k^2T}{3e}\left\{\frac{\partial}{\partial E}\log\int\frac{\tau(\mathbf{k})}{|\operatorname{grad} E|}\left(\frac{\partial E}{\partial k_x}\right)^2 dS\right\}_{E=E_0}, \qquad \ldots \ldots (3)$$

which is the expression given by Wilson (p. 176). The integration is over the surface of constant energy E; E_0 is the Fermi energy corresponding to $T=0$.

Writing now

$$\sigma(E)=\int\left(\frac{\partial E}{\partial k_x}\right)^2\frac{\tau(\mathbf{k})}{|\operatorname{grad} E|}dS, \qquad \ldots \ldots \ldots (4)$$

in eqn. (3), we get finally

$$S=\frac{\pi^2k^2T}{3eE_0}\left\{\frac{\partial \log\sigma(E)}{\partial \log E}\right\}_{E=E_0}, \qquad \ldots \ldots \ldots (5)$$

which is the expression given by Mott and Jones (p. 310).

For perfectly free electrons, the surfaces of constant energy are spheres. If we then take $\tau(\mathbf{k})$ as a function of $\mathbf{k}$ only, eqn. (4) can be written in the form

$$\sigma(E)=\text{const.}\,|\mathbf{k}|^3\tau, \qquad \ldots \ldots \ldots (6)$$

hence

$$S=\frac{\pi^2k^2T}{3eE_0}\left\{\frac{3}{2}+\frac{d\log\tau}{d\log E}\right\}_{E=E_0}, \qquad \ldots \ldots \ldots (7)$$

a formula effectively given by Wilson (p. 177). Let us write, following Mott and Jones,

$$S=\left(\frac{\pi^2k^2T}{3eE_0}\right)x, \qquad \ldots \ldots \ldots (8)$$

where x stands for the expression in brackets on the right-hand side of eqns. (5) or (7), depending on which particular formula we use.

§ 3. DISCUSSION OF THE CASE IN WHICH THE ELECTRONS ARE COMPLETELY FREE

In the case of completely free electrons, eqn. (7) can be used to evaluate S. The only unknown quantity in (7) is τ which has to be known as a function of E.

According to Wilson (p. 208), $\tau(\mathbf{k})$ at high temperatures, is given by

$$\tau \propto |\mathbf{k}| . E/C^2,$$

where C is the 'interaction constant' of electrons with the lattice and is of the same order of magnitude as the energy of the state $\mathbf{k}$. Now Wilson has assumed (p. 201) that *C is independent of $\mathbf{k}$*. Therefore, in this case

$$\tau \propto E^{3/2}. \qquad (9)$$

Hence, according to Wilson, $x=3$ *for all simple metals*. The experimental values of x for alkali and noble metals are given in table 1 below, and x evidently varies rather widely from metal to metal.

Table 1

	Li	Na	K	Rb	Cs	Cu	Ag	Au
x	-6.7	2.2	3.8	2.2	0.3	-1.8	-1.1	-1.4

On the other hand, Mott and Jones base their discussion of electron scattering in general on the Wigner–Seitz model, assuming specifically one free electron per atom and an Einstein model for the lattice. Using *this* model, let us work out the expression for τ explicitly for *any* number of free electrons per atom—within the limitations of the Wigner–Seitz model—neglecting, in the first place, any distortion of the energy surfaces. It will be found that the variation of the number of free electrons per atom leads to a variation in the thermoelectric power; and hence one could partly explain in this way the differing values of x.

On this basis we have

$$\frac{1}{\tau}=A\,|\mathbf{k}|\,r_0\int_0^{\pi} f(2\,|\mathbf{k}|\,r_0 \sin \tfrac{1}{2}\theta)(1-\cos\theta)\sin\theta\, d\theta \qquad (10)$$

(cf. Mott and Jones, eqn. (24), p. 254) where A is a constant independent of $|\mathbf{k}|$ or E, r_0 is the atomic radius, and $f(x)$ is given by

$$f(x)=\frac{(\sin x - x\cos x)^2}{x^4}. \qquad (11)$$

The integral above can be simplified to give

$$\tau \propto |\mathbf{k}|^3/F(t), \qquad (12)$$

where $\quad t=2|\mathbf{k}|r_0,$

and
$$F(t)=\frac{1}{2}\int_0^{2t}\frac{1-\cos\alpha}{\alpha}\,d\alpha+\frac{5}{8}\cos 2t+\frac{t\sin 2t}{4}+\frac{t^2}{4}-\frac{5}{8}. \qquad (13)$$

The first integral in (13) has been fully tabulated for various values of t (Harvard Tables, 1949).

From (12) it follows that

$$\left[\frac{d\log\tau}{d\log|\mathbf{k}|}\right]_{|\mathbf{k}|=k_0}=3-\left[\frac{d\log F(t)}{d\log|\mathbf{k}|}\right]_{|\mathbf{k}|=k_0}$$
$$=3-\left[\frac{(\sin t-t\cos t)^2}{F(t)}\right]_{t=t_0} \qquad (14)$$

where
$$t_0=2k_0r_0=3{\cdot}84n_0^{1/3} \qquad (15)$$

and n_0 is the number of free electrons per atom.

The values of $(d\log\tau/d\log|\mathbf{k}|)_{|\mathbf{k}|=k_0}$ calculated from eqn. (14) for various values of n_0, and the corresponding values of x are given in table 2 (see also fig. 1).

Table 2

n_0	∞	1·2	1·1	1·0	0·9	0·8	0·7	0·6	0·5	0·4	0
$(d\log\tau/d\log|\mathbf{k}|)_{|\mathbf{k}|=k_0}=a$, say	3	2·6	2·4	1·9	1·7	1·5	0·9	0·4	0·3	−0·4	−3
$x=(3+a)/2$ (cf. eqn. (7))	3	2·8	2·7	2·5	2·4	2·3	2·0	1·7	1·6	1·3	0

Fig. 1

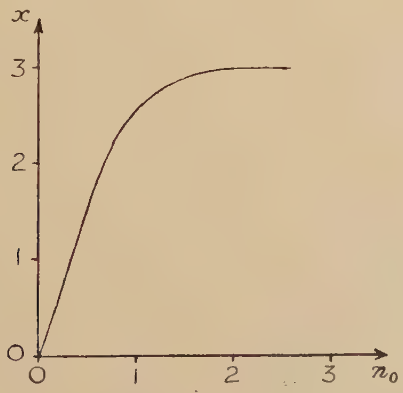

It appears that a range of values for x between ∼2·8 and ∼2·3 might be accounted for on the basis of an expected variation in the number of free electrons in these metals, although (cf. Mott and Jones, p. 98) on the extreme approximation of ‘ tight binding ’, one electron per atom would only correspond to as little as ∼0·26 free electron/atom. However, no value of n_0 which can be assumed on this model can make x greater than 3 or less than 0. Consequently, the case of potassium for which $x=3{\cdot}8$

and that of lithium for which x is negative cannot be explained on this basis.

§ 4. EXTENSION TO AN ENERGY-DEPENDENCE E=const. $\mathbf{k}^{2-\alpha}$, WHERE $0 \leqslant \alpha \leqslant 2$

In the foregoing, we have discussed completely free electrons where, therefore, $E=(\hbar^2/2m)\mathbf{k}^2$. In this section we shall consider a somewhat more general case where E is given by

$$E=\text{const. } \mathbf{k}^{2-\alpha} \quad . \quad . \quad . \quad . \quad . \quad . \quad . \quad . \quad (16)$$

and as α varies between 0 and 2, (16) will correspond to the transition from absolutely free electrons (or an almost empty band) to a completely full band.

Since we may always reasonably expect that the scattering due to lattice vibrations will only depend on the speed of the electrons,* and that the faster electrons will be less scattered than the slower ones (cf. Mott and Jones, p. 311), we may assume

$$\tau=\text{const.} \mid \text{grad } E \mid^{y} \quad . \quad . \quad . \quad . \quad . \quad . \quad . \quad . \quad (17)$$

where y is a positive numerical constant depending on the number of free electrons per atom in the metal (cf. previous section).

Hence from eqn. (4) we get

$$\sigma(E)=\text{const. } k^{y-\alpha(y+1)+3} \quad . \quad . \quad . \quad . \quad . \quad . \quad . \quad . \quad (18)$$

and hence

$$x=\frac{y-\alpha(y+1)+3}{2-\alpha} . \quad . \quad . \quad . \quad . \quad . \quad . \quad . \quad (19)$$

For convenience let us now give y its limiting value of 3 in what follows. This corresponds exactly to Wilson's model and sufficiently closely to the Wigner–Seitz model for $n_0 \gtrsim 1$.†

Then

$$x=\frac{2(3-2\alpha)}{2-\alpha} . \quad . \quad . \quad . \quad . \quad . \quad . \quad . \quad . \quad (20)$$

Figure 2 shows x as a function of α.

When the band is practically empty, i.e. when α is nearly zero, x is positive and takes practically its full value 3. It is obvious that x cannot be greater than +3, which is its limit towards the empty band side. On the other hand, when the band is nearly full, i.e. α is nearly equal to 2, x becomes negative and very large, tending towards infinity. This

---

[*] We are, of course, ignoring scattering due intrinsically to a possible *Bragg-reflection* of the electrons. Such scattering corresponds essentially to the Peierls' 'Umklapp-prozesse' of which there is no experimental evidence in the resistance of the alkali and noble metals.

[†] The inclusion of a more precise value for $y (0 \leqslant y \leqslant 3)$ throughout the filling of the band will not alter the limits for x deduced below.

implies that a very high positive thermoelectric power is possible when the band is almost full (cf. also Mott and Jones, p. 312). On the basis of such an argument, the case of lithium may be explained. It should, however, be noted that the band has to be markedly distorted by the time that x changes sign ($E \propto \mathbf{k}^{1/2}$) on this model; on the other hand, x then varies very rapidly with further distortion of the band.

§ 5. INFLUENCE OF A NON-SPHERICAL FERMI SURFACE ON THE VALUE OF x

So far we have evaluated x assuming a spherical Fermi surface. Let us now consider a Fermi surface which is not a sphere but can be divided up into segments whose surfaces are spherical or planar. These surfaces may be supposed oriented in k space in such a way that cubic symmetry of the Fermi surface is retained, since we only wish here to consider metals of cubic symmetry.

Fig. 2

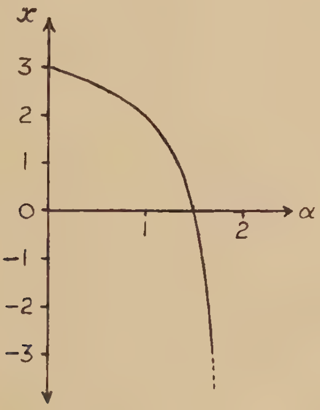

Considering then eqn. (4), it follows that $\sigma_i(E)$—the contribution from a particular ‘ segment ’ to the integral—can be written in the form

$$\sigma_i(E)=A_iE^{\alpha_i}. \qquad (21)$$

It can then be shown with analogous assumptions that $\alpha_i \leqslant 3$ for every segment of the type considered. The total contribution will therefore be given by

$$\sigma(E)=\sum_i \sigma_i(E)=\sum_i A_iE^{\alpha_i}. \qquad (22)$$

Hence

$$\frac{d\log\sigma(E)}{d\log E}=\frac{\Sigma A_i\alpha_iE^{\alpha_i}}{\Sigma A_iE^{\alpha_i}}. \qquad (23)$$

Since *each* $\alpha_i \leqslant 3$, it is trivial to show that

$$\frac{d\log\sigma(E)}{d\log E}\leqslant 3. \qquad (24)$$

In other words, it appears that x ought not to exceed $+3$ in a metal of cubic symmetry, even when the Fermi surface is not itself spherical.

Consequently one is still unable to explain the value of x for potassium, which is significantly greater than 3.

§ 6. CONCLUSION

While it appears possible on the band theory to account for the thermoelectric power at high temperatures of the noble and alkali metals, with the exception of potassium, this metal appears specifically anomalous. We might either suggest that in potassium the variation with energy of the thermal scattering is markedly different from that usually assumed or proposed. Alternatively, in view of earlier experiments by MacDonald (1952) on the electrical resistance, there may be additional band-to-band scattering, which would then depend on the density of states in the overlapping bands and their possible variation with temperature. One difficulty, however, in this hypothesis is that, while Rb and Cs also show an anomalous resistance variation at higher temperatures, both of these metals appear to fit sufficiently well into the theory already discussed.

In general, however, it should be noted that a considerable deviation from the idealized free-electron model is in any case called for in the theory to account for the range of thermoelectric power in alkali and noble metals.

ACKNOWLEDGMENT

We should like to thank Professor N. F. Mott, F.R.S., for his interest in this work, and Dr. W. B. Pearson for many useful discussions.

REFERENCES

BORELIUS, G., 1935, *Handb. d. Metalphysik,* 1.1, 385.

HARVARD TABLES, 1949, *Tables of Generalized Sine and Cosine Integrals,* Vol. 1 (Harvard : University Press), p. 3.

MACDONALD, D. K. C., and PEARSON, W. B., 1953, *Proc. Roy. Soc.* A (in press).

MOTT, N. F., and JONES, H., 1936, *Properties of Metals and Alloys* (Oxford : Clarendon Press).

WILSON, A. H., 1936, *Theory of Metals* (Cambridge : University Press).

CXLV. *Nucleation in a Dielectric*[*]

By VERA DANIEL and CLARA TURNER
British Electrical Research Association[†]

[Received August 13, 1953]

ABSTRACT

Nucleation from solid solution is investigated by means of dielectric measurements. The material investigated is a crystalline mixture of ' equivalent ' ketones, a system analogous to a mixture of isotopes which tends to segregate. During successive stages of nucleation within an unstable solid solution, dielectric constants and loss angles increase and pass through maxima. Early stages of nucleation represent short range ordering and are structure insensitive, while later stages represent long range ordering and are comparatively structure sensitive.

§ 1. INTRODUCTION

THE formation and development of nuclei of new phases out of a homogeneous solid solution (Smoluchowski 1951) has been studied extensively in alloys, but has so far not been investigated for dielectrics. However, certain types of polar organic materials offer exceptionally favourable conditions for the study of nucleation. Dielectric measurements during the break up of a mixture yield information not only with regard to the mechanism of nucleation, but also with regard to the dielectric properties of small aggregates.

§ 2. THE MATERIAL UNDER INVESTIGATION

The material investigated is a mixture of equal amounts of five equivalent ketones (Daniel 1950). Chemically, all these are derived from a saturated paraffin of given chainlength, by substitution of one oxygen atom for two hydrogen atoms, at a link not less than three carbon atoms from the end of the chain. The equivalent ketones used have a chainlength of eighteen carbon atoms, and can be described by the general formula $C_mH_{2m}\,.\,CO.C_{17-m}H_{35-2m}$. They have very closely similar physical and chemical properties, in consequence of their similar structure (Daniel 1950). The system used is a special case of a group of substituted long chain paraffins of equal chainlength, and other equivalent systems can be envisaged, with different chainlengths and different substituted sidegroups.

Although equivalent ketones are very similar to one another they have a tendency to unmix in the solid state, because in a crystal of a pure ketone all keto-groups are on one level, and their electrostatic interaction contributes a large term to the bonding energy of the structure. Mixtures of equal amounts of a sufficient number of such ketones are thermodynamically stable either as a single-phase solid solution or a multi-phase mixture of the constituents, depending on the number of components present. The single phase form occurs, however, not only when it is thermodynamically stable, but also as a metastable form. If this occurs, it changes in due course into the multi-phase form, but the course of precipitation may be very prolonged. The time taken depends on the number of equivalent ketones in the mixture, and is the longer the larger the number of ketones. For the five ketones used in this work, completion of the phase change takes some months.

---

[*] Based on Report L/T 291 of The Electrical Research Association.

[†] Communicated by the Authors.

The multi-phase form of the mixture of five ketones is thermodynamically stable up to its melting point at 27·5°c, and consists of five separate phases, each made up of one ketone with a small amount of the others in solid solution. The crystal structure of these phases is orthorhombic, as for the pure ketones.

The single-phase form of this mixture is not stable, but has the same melting point as the multi-phase form, within the limits of error. This metastable form undergoes a change of crystal structure at a temperature of 14·5±1°c. It is orthorhombic, like the multi-phase form, below the transition temperature and hexagonal above the transition.

§ 3. Theoretical Considerations

Nucleation from Solid Solution

The simplest case of nucleation in general is the formation of a solid or liquid phase out of vapour. This is reasonably well understood (Volmer 1939). The crucial point of the formation of a nucleus of a condensed phase is that the surface area of a solid or liquid has a higher free energy per molecule than its interior. In consequence small nuclei are comparatively less stable than large ones, and nuclei have to achieve a minimum size before they become thermodynamically stable. This has the effect that nucleation depends a great deal on circumstances which enable nuclei to reach the stable size, and makes nucleation, even in its simplest forms, erratic and difficult to control.

Nucleation within a solid matrix, as distinct from nucleation from the vapour or a liquid solution, is further complicated by size relationships. If a nucleus has not exactly the same specific volume and shape as the matrix, its formation involves stresses. These affect the stability of the nucleus, and if nucleus formation involves a great deal of stress, it may become practically impossible in the interior of the matrix. In this case, nucleation depends very much on the texture of the matrix; it is ‘ structure sensitive ’ because nuclei can usually arise much more easily on surfaces or other disturbances of the matrix than in the interior.

Theoretically, structure sensitive nucleation is exceedingly complex. and the existing theoretical work (Smoluchowski 1951, 1952) is restricted to ‘ structure insensitive ’ nucleation and the erection of nuclei within the solid matrix. Most of the existing theories use a particular model of a solid solution for which certain simplifying assumptions are made. This model is a binary mixture of two substances, A and B, of equal crystal structure, for which the tendency to form two phases can be expressed by a single quantity :

$$V=V_{ab}-\tfrac{1}{2}(V_{aa}+V_{bb}) \quad . \; . \; . \; . \; . \; . \; . \; . \quad (1)$$

where V_{aa}, V_{bb} and V_{ab} are respective energies of pairs of atoms (or molecules). With this assumption the free energy per gramme atom of mixture of concentration α can be written :

$$f(\alpha)=VZ\alpha(1-\alpha)+kT(\alpha \log \alpha+(1-\alpha) \log (1-\alpha)) \quad . \; . \; . \quad (2)$$

where Z is the number of nearest neighbours in the structure. Equation (2) implies that for negative V the material is single-phase at all temperatures, while for positive V it breaks up into two phases below a temperature which depends on the concentration.

In discussing nucleation from solid solution Smoluchowski (1951) takes as his starting point the concept of random fluctuations of concentration which exist in any mixture. He shows that where the mixture is single-phase in equilibrium, positive V, that is a tendency towards precipitation, increases the amplitude of random fluctuations. In other words, the single-phase material contains very loose and indefinite aggregates of the two constituents, which are the more distinct the closer the material is to two phase conditions, but which are continuously formed and redissolved. If the material is two phase in equilibrium, aggregates of this kind act as embryonic nuclei which may grow into stable nuclei if the free energy conditions permit it.

The experimental evidence on nucleation consists mainly of investigations of alloy systems (Geisler 1951). It confirms the theoretical ideas qualitatively, but is rarely suitable for quantitative tests of the theories, because each alloy system tends to introduce its own complications (Smoluchowski 1952). However, x-ray evidence of the earliest stages of nucleation (Guinier 1952) that are accessible shows that early nuclei have structures which are neither quite like that of the final precipitated phase, nor quite like that of the matrix. This confirms the ideas of embryonic nuclei arising from random fluctuations within the single-phase matrix.

The mixture of five equivalent ketones is closely related to the idealized model of a binary mixture with a solid solubility gap, the properties of which are represented in eqn. (2). In fact, a binary system of two equivalent ketones is closer to this model than any alloy system can be, because of the great similarity of equivalent ketones.

A mixture of five equivalent ketones is not much more complicated than a mixture of two ketones, because its free energy conditions can still be represented with the help of a single constant,

$$V=V_{ab}-\tfrac{1}{2}(V_{aa}+V_{bb}),$$

where A represents a particular equivalent ketone and B any other equivalent ketone. The quantity V can in principle be deduced from measured properties of equivalent ketones (Daniel 1950), but the available data are at present not quite sufficient.

The characteristics of nucleation in the mixture of five ketones are clearly a matter for experiment, but certain points can be made *a priori*, since the ketones are equivalent and present in equal proportion. Each nucleus must consist predominantly of one ketone, with a proportion of the other four in solid solution. If any ketone forms a nucleus, it thereby supersaturates the solid solution with regard to the others so that groups arise of five nuclei. Such groups may be separated by regions of undisturbed solid solution. However, once a stable group has been formed, the growth of its nuclei propagates the nucleation, since each growing nucleus supersaturates the solution out of which it grows.

Dielectric Properties during Nucleation

In the present investigation the process of nucleation is followed largely by means of dielectric measurements, and it will be necessary to consider the significance of the dielectric data.

In general, the static dielectric constant of a material can be expressed by an equation (Fröhlich 1949) :

$$\epsilon_s - n^2 = \frac{3\epsilon_s}{2\epsilon_s + n^2}\,\frac{4\pi N}{3}\,\frac{\overline{mm^*}}{kT} \qquad \ldots\ldots\ldots\ldots \quad (3)$$

where n^2 is the square of the refractive index and N the number of polarisable units (e.g. dipoles) per unit volume. The expression $\overline{mm^*}$ has the dimensions of a dipole moment, squared, and depends on the configuration of dipoles as well as on their moment when in isolation. Equation (3) is derived under the assumption that the structure of the dielectric is uniform within a spherical region small compared with the dimensions of the test capacitor, i.e. in the sense of this expression a material is homogeneous if its structure has inhomogeneities only within dimensions that are small, as compared to 10^{-3} or 10^{-4} cm (the thickness of dielectric used being 5×10^{-2} cm). This means that nucleating material can be considered as homogeneous in the sense of eqn. (3) if there are many nuclei within dimensions of the order 10^{-4}–10^{-3}, that is, if average nuclei are smaller than about 10^{-6}–10^{-5} cm. In that case the material is indeed no less homogeneous than a protein with large molecules. If aggregates are larger, the dielectric properties of the material as a whole would have to be treated according to the equations applying to mixtures of dielectrics with different permittivity (Rushman and Strivens 1947).

If nucleation is structure sensitive, and groups of nuclei occupy an unknown and more or less small fraction of the material, dielectric measurements can yield little significant information about the condition of nuclei. All that can be said in this case is that the results of measurements will vary greatly with the texture of the single-phase solid solution, so that they are likely to be badly reproducible.

If nucleation is structure insensitive, the material in the course of nucleation consists of a mass of nuclei with boundary regions between them. The size of nuclei may obviously vary in space and time, but they may be expected to contain initially no more than some tens to thousands of molecules each. This follows from the metallurgical evidence on early nuclei (Guinier 1952) as well as from first principles, since diffusion over large distances is unlikely in the early stages of nucleation. This means that early nuclei are likely to be smaller than 10^{-6}–10^{-5} cm, so that the material as a whole is homogeneous in the sense of eqn. (3). In this case, the dielectric constant measures $\overline{mm^*}$ for an average nucleus, where a nucleus is taken to include an appropriate part of the boundary region dividing it from the neighbouring nuclei. For larger nuclei it may be necessary to consider nuclei and boundaries separately as regions of different dielectric constant (Rushman and Strivens 1947).

The quantity $\overline{mm^*}$, which can be deduced from measurements on a homogeneous material, is a measure of the tendency of dipoles to be parallel to each other (Fröhlich 1949). This quantity is large if dipoles tend to be parallel, small if they tend to be antiparallel. As a rule the tendency towards parallelism or otherwise is determined by the force fields of neighbouring molecules, i.e. short range forces. However, in the case of ketones dipolar interaction, which has a long range, plays an important role in bonding, and so both long and short range forces come into play.

The loss angle gives information, as it were, from the viewpoint of the individual dipole. According to Debye, the loss angle is given by an equation :

$$\tan\delta=\frac{(\epsilon_s-n^2)\omega\tau}{\epsilon_s+n^2\omega^2\tau^2} \quad . \quad . \quad . \quad . \quad . \quad . \quad . \quad (4)$$

while the simultaneously measured real dielectric constant ϵ_1 is given by

$$\epsilon_1-n^2=\frac{\epsilon_s-n^2}{1+\omega^2\tau^2} \quad . \quad . \quad . \quad . \quad . \quad . \quad . \quad . \quad (5)$$

where n^2 is the square of the refractive index, $\omega/2\pi$ is the frequency in cycles/second and τ the relaxation time. τ is given by :

$$\tau=A\exp(-E/kT) \quad . \quad . \quad . \quad . \quad . \quad . \quad . \quad . \quad . \quad (6)$$

where A is approximately constant, and E represents an energy barrier between two positions of a dipole. For the purposes of eqn. (6) it is assumed that E is the same for all dipoles in the material. This in in general not true, in that a large number of values of E may exist if all dipoles are not surrounded by identical force fields. In the case of precipitating aggregates we may expect a distribution of values of E and thus a distribution of relaxation times, with correspondingly modified eqns. (4) and (5). The values of E in the distribution of relaxation times give information about the various force fields surrounding individual dipoles.

§ 4. EXPERIMENTAL PROCEDURE

Nucleation in the mixture of five ketones was investigated using two experimental methods: dielectric measurements, and x-ray powder photographs.

Dielectric measurements were carried out using the cooling capacitor and metal desiccator described elsewhere (Daniel and Stark 1952). With this apparatus the specimen is kept free from contamination and may be heated and cooled during the measurements. The arrangement also permits quenching by passing cold fluid through the hollow bottom electrode of the capacitor. An accurate Schering bridge was used (Daniel and Stark 1952), at frequencies of 50 c/s, 800 c/s and 50 kc/s.

The process under investigation is a change of dielectric properties with time and temperature, and it was found impracticable to follow it simultaneously at all three frequencies. For this reason, heat treatments had to be repeated three times to obtain results at all frequencies used. This procedure is justified by the reproducibility of the results. However, it makes important a certain source of error which has been already mentioned (Daniel and Stark 1952). When a long-chain material is solidified in a temperature gradient it becomes preferentially orientated.

Preferential orientation markedly affects the dipolar part of the permittivity of a ketone, since dipoles reverse by rotation or twisting of the long-chain molecules. With the present material quenching produces very marked preferential orientation, and even slow cooling of the desiccator box does not quite eliminate it. Fortunately, the dielectric constant of the material in its hexagonal form can be used as a measure of preferential orientation: the higher its value, the more the material is oriented. If the dielectric constant of the hexagonal form is measured prior to a heat treatment leading to nucleation, the effects of preferential orientation can be eliminated, or allowed for by a numerical correction. Since this correction is mostly not large and is somewhat tedious, it is applied only where necessary for purposes of the argument. In general, uncorrected results are given. The details of the corrections applied are described in E.R.A. report L/T 291, but are omitted here for the sake of brevity.

Crystallographic work on the mixture was carried out using an apparatus (Daniel and Stark 1952) which allows photographs to be taken at temperatures above or below room temperature, and where six successive powder photographs can be recorded on the same film.

§ 5. Experimental Results

Dielectric Evidence

The type of result obtained by the dielectric measurements is shown in fig. 1, which shows the dielectric constants and loss angles obtained when the material is cooled and subsequently heated again, after varying periods at a low temperature. The measurements recorded were carried out at 800 c/s. The figure illustrates clearly the complicated effects of heat treatment. On cooling from the melt, the dielectric constant is first constant, then rises to a maximum, and finally decreases, when the specimen is kept at a low temperature. On subsequent heating, it rises again and passes through a maximum, which is the less pronounced, and occurs at the higher temperature, the longer the specimen had been kept at a low temperature.

Fig. 1

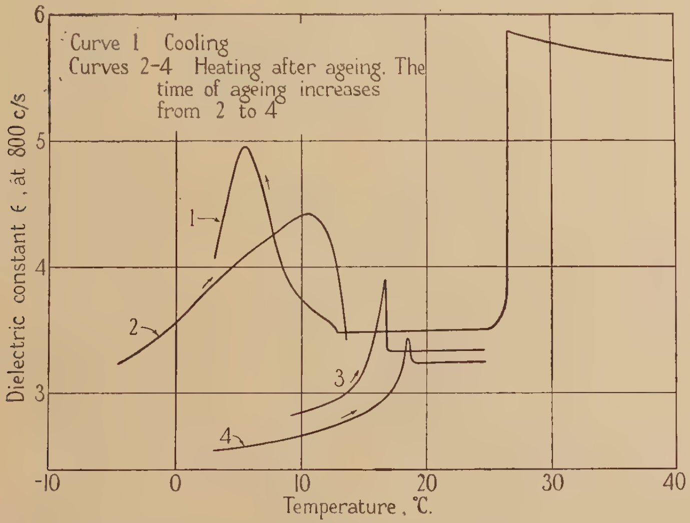

The dielectric constant of mixed ketones on cooling, and heating after ageing below 4°c.

The phenomena observed depend in a complicated way on time and temperature. In order to study them in more detail, heat treatments had to be devised which could be repeated conveniently. The most useful of these was obtained when the specimen was cooled very slowly, in a refrigerator set finally to about 6°c. Figure 2 shows the results of this heat treatment, at all three frequencies used, for both dielectric constant and loss angle. The results are given as a function of the time of cooling, the temperatures reached at a given time being marked on the time scale.

The phenomena observed are best considered in several stages. However, before doing this it will be necessary to record the x-ray evidence.

Fig. 2

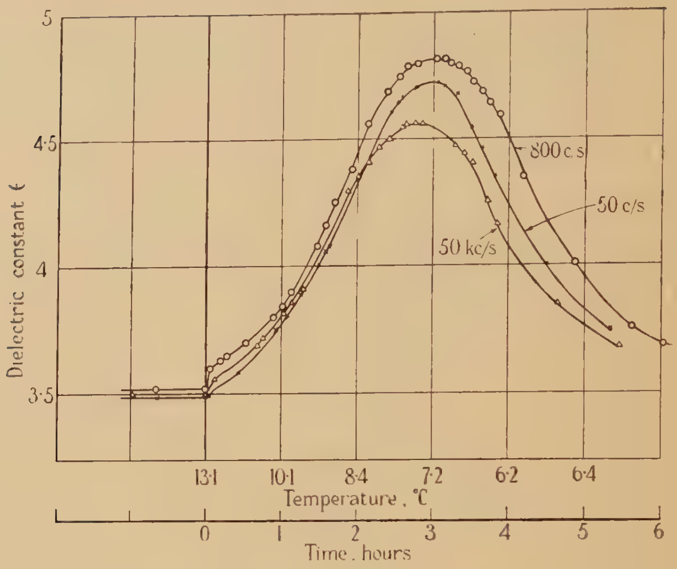

(*a*)

The dielectric constant during slow cooling.

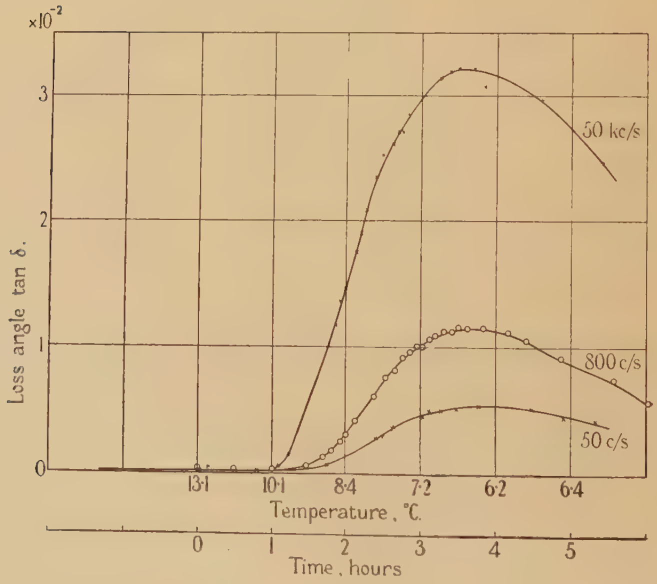

(*b*)

The loss angle during slow cooling.

Crystallographic Evidence

The heat treatments which give large dielectric effects as recorded in figs. 1 and 2, have only very small effects on the crystal structure, even though there are appreciable differences between the structures of the single-phase solid solution and the stable multi-phase form.

For the mixture of five ketones changes of crystal structure consist in an expansion or distortion of the (*ab*) plane, at right angles to the *c* axis (Daniel 1950). The area $a \times b$ of the basal plane (*ab*) of the unit cell can be taken as a measure of the specific volume, while the shape of the unit cell may be characterized by the angle $\frac{1}{2}\theta$, which measures the deviation of the basal plane from hexagonal shape. For a hexagonal structure $\theta = 60°$.

Figure 3 shows the cross sectional area *ab* and the angle $\frac{1}{2}\theta$ for the mixture in its various forms and for a pure equivalent ketone. The single-phase form is hexagonal above 14·5±1°C and orthorhombic below this temperature (as shown by the angle $\frac{1}{2}\theta$). The area $a \times b$ is continuous through this transition, which seems curious. However, a small volume change at the transition cannot be excluded on the basis of the available evidence. Between about −5°C and the melting point the single-phase form has a very high thermal expansion, as compared with that of the pure ketone.

Fig. 3

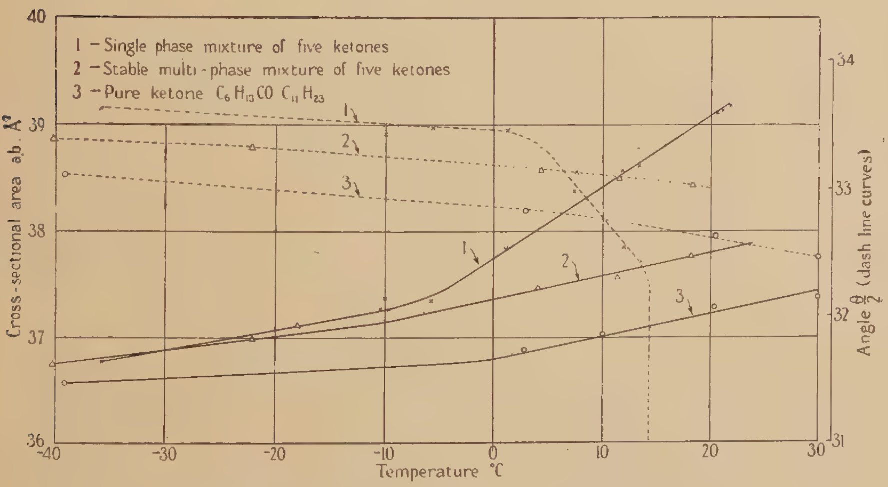

Thermal expansion in pure and mixed ketones.

The mixture approaches stability only very gradually, so that it is difficult to decide when stability has been reached. However, the specimen whose volume is recorded in fig. 4 was aged for five months at a temperature of approximately 5°C, and may be taken to be near to stability. The stable mixture shown has the same thermal expansion as the pure ketone, but a somewhat larger volume. This implies that its bonding is similar to that of the pure ketone, but that the material contains some of the other ketones in solid solution as is to be expected.

The early stages of nucleation, though exhibiting large dielectric effects, give x-ray powder photographs very similar to those of the single-phase form. Figure 4 shows the changes of structure corresponding to a heat treatment very similar to that which gave the dielectric effects recorded in fig. 2. For both heat treatments recorded the specimen had been cooled more or less gradually to 7·5°c, kept at that temperature until 3–3½ hours and then heated again. The ageing at 7·5°c produces a slight contraction which is undone on reheating.

Fig. 4

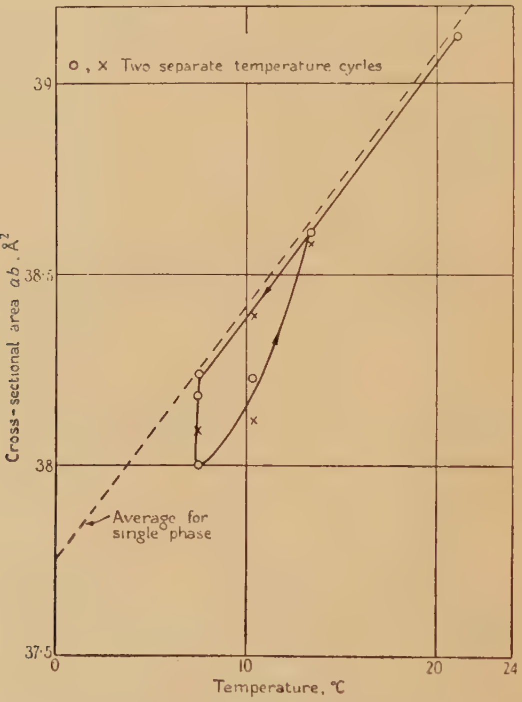

Volume conditions during two temperature cycles.

Structure Insensitive Nucleation

The x-ray record may be used to decide whether or not the changes on ageing occur uniformly throughout the material, i.e. whether the observed nucleation is structure insensitive. To this end, the x-ray lines 110 and 200 were photometred, to ascertain whether they broaden as they shift; a Hilger microphotometer was used. Details of the microphotometer record, as well as a reproduction of a typical set of photographs, are shown in E.R.A. report L/T 291. The maximum line shift observed (for 200) is only 0·05 cm, about half the width of the line, so that the data cannot be evaluated very accurately. However, the fact that no change of line width is observed while the lines shift may be taken to mean that changes occur simultaneously in at least two thirds of the bulk of each of the specimens examined. This implies that the changes observed are not restricted to surfaces or other anomalous parts of the specimen. Nucleation is essentially structure insensitive.

The crystallographic evidence is confirmed by a result of the dielectric measurements which will be discussed in more detail later. The highest value of the dielectric constant obtained on cooling during heat treatments as shown in figs. 1 and 2 was found to be reproducible to better than $\pm 6\%$, once allowance is made for preferential orientation. This result, confirmed for eleven separate heat treatments, would be very unlikely if nucleation were structure sensitive. The small scatter of the results suggests that nucleation occurs simultaneously in the larger part of the specimen, with a few exceptions in some of the crystals of the matrix.

The Successive Stages of Nucleation

The fact that nucleation proceeds uniformly within the bulk of the material makes it possible to interpret the observed changes of dielectric properties. These changes correspond to a process in the material, and the dielectric properties at each stage represent average properties of nuclei.

The process of nucleation appears to be divisible into a sequence of more or less separate stages which succeed one another as the temperature gradually decreases. These stages will be discussed in turn.

The Hexagonal Form

When the specimen is single-phase in the hexagonal form, no nucleation occurs within times of weeks or months. This is not surprising, since the multi-phase form has an orthorhombic crystal structure and nucleation within the hexagonal form would presumably produce large stresses.

The dielectric constant of the hexagonal form is almost independent of temperature. It is lower than that of the liquid mixture, but higher than that of the pure ketone, for which the dipolar contribution is zero. This means that the dielectric constant of the hexagonal form contains a comparatively small dipolar contribution. It is curious that this contribution is not larger and that it does not cause the dielectric constant to rise with falling temperature, as it should according to eqn. (3), if $\overline{mm^*}$ is constant. No convincing explanation is available of this fact, but it seems that in the hexagonal form dipoles of neighbouring different ketones tend to oppose each other, so giving a comparatively small $\overline{mm^*}$ which decreases with temperature.

The Earliest Stage of Nucleation

On cooling the single-phase specimen through the transition from hexagonal to orthorhombic, the dielectric constant rises suddenly. The sudden rise at 13°c in figs. 1 and 2 is reproducible, and corresponds to the sudden onset of the structural transition when the material is cooled to the lower limit of its temperature hysteresis. When the change is complete the dielectric constant rises slowly with falling temperature, while the loss angle at all three frequencies remains as low as for the hexagonal form until the temperature falls to about 10°c. On further cooling the loss angle also begins to rise.

Between the temperature of the transition and about 10–11°c the dielectric constant is almost independent of time. This is demonstrated by a temperature cycle (fig. 5) when the specimen was cooled to 11°c

Fig. 5

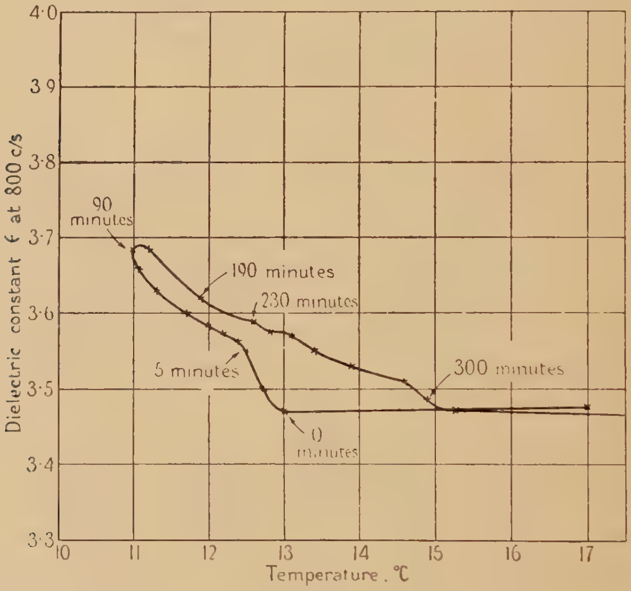

Cooling and heating sequence above 11°c.

and subsequently heated, the cycle taking 5 hours to complete. A small permanent change occurs at the lower end of the temperature range, and this is connected with a very slight contraction of the material. However, in first approximation the dielectric constant and volume are functions of temperature, but not of time.

The time independent rise of the dielectric constant just below the transition temperature may in principle be explained in two ways: it may be a property of the unchanged single-phase form or it may be due to a rearrangement of molecules which depends on temperature but is so rapid as to appear time independent. Two arguments speak for the latter alternative. Firstly, the slope of the $\epsilon(T)$ curve indicates an increase of $\overline{mm^*}$ with falling temperature; for constant $\overline{mm^*}$ we should expect a slope $d\epsilon/dT = 5 \times 10^{-3}$, while the measured value is always larger than $d\epsilon/dT = 4 \times 10^{-2}$. This indicates a tendency of the dipoles to become parallel to one another with decrease in temperature, as is to be expected if clusters of the individual ketones are formed. Secondly, the phenomena occurring between the transition temperature and 11°c appear to be a necessary preliminary of the more striking nucleation processes occurring at lower temperatures. If a specimen is quenched through this range in a matter of seconds, the (corrected) maximum value of the dielectric constant is low, $\epsilon = 4{\cdot}1$ at 800 c/s on the average of two occasions, as against $\epsilon = 4{\cdot}6 \pm 0{\cdot}2$ when the specimen is cooled more slowly, spending some 5–10 minutes between 13°c and 11°c.

The observed features of the first stage of nucleation suggest that it consists in an increase of short range order, in that the individual ketones form embryonic nuclei. The distinctness or number of these nuclei increases with falling temperature, and it appears that the character of nuclei is in a metastable equilibrium with temperature. This observation is in agreement with recent theoretical work by Dehlinger (1951), who considers structure insensitive nucleation in a material where the formation of aggregates creates stresses. He postulates that the stresses increase with increasing aggregate size, thus creating a limiting size beyond which aggregates cannot grow. The average size of nuclei should be in a metastable equilibrium with temperature.

In the mixed ketones the metastable equilibrium is restricted to a temperature range of only some 2°c. This is in good agreement with Dehlinger's ideas, because in the temperature region in question the volume difference between the stable multi-phase and the single-phase form decreases rapidly with falling temperature (fig. 3). Stresses may be expected to be the larger the larger this volume difference, so that the limiting size should increase rapidly as the temperature decreases.

The metastable equilibrium observed implies that the embryonic nuclei in question are formed and destroyed rapidly. This has the consequence that after a short time—say a few minutes—at a given temperature the material should be saturated with embryonic nuclei of the number and size appropriate for the temperature.

The Stage of Maximum Dielectric Constant

On cooling below about 11°c the character of nucleation changes, as shown in fig. 2. The dielectric constant rises more rapidly, and the loss angle begins to increase also. The increase in loss angle occurs the sooner the higher the frequency, and this, according to eqn. (4), indicates a gradual increase of the average relaxation time. The process observed is no longer independent of time, as shown by fig. 6, which gives the dielectric properties at 800 c/s for a rapid and a slow cooling sequence. For both heat treatments the dielectric constant reaches a maximum followed by a decline, but for rapid cooling the maximum is reached sooner, and at a lower temperature, than for slow cooling.

The experimental data indicate that the embryonic nuclei formed above 11°C become able to develop at lower temperatures and that their development needs time. The behaviour of the loss angle as a function of frequency indicates that this development consists, at least to some extent, in a growth of nuclei, in that molecules within them become more firmly bonded.

The development of nuclei always proceeds in the same way even if its speed varies with temperature. This is shown by the fact that the maximum dielectric constant observed during a heat treatment is, for a given frequency, independent of the speed of the treatment, once allowance is made for preferential orientation. Table 1 gives the characteristics of the condition of peak dielectric constant for eleven separate heat treatments. Preferential orientation is eliminated by calculating $\overline{mm}^*$ peak/$\overline{mm}^*$ hexagonal. The loss angle, which is also corrected for preferential orientation, refers to the condition of peak dielectric constant. The characteristics of the heat treatments are given by the temperature at which the peak occurred and the time between the beginning of nucleation at about 13°C and the occurrence of the peak.

Fig. 6

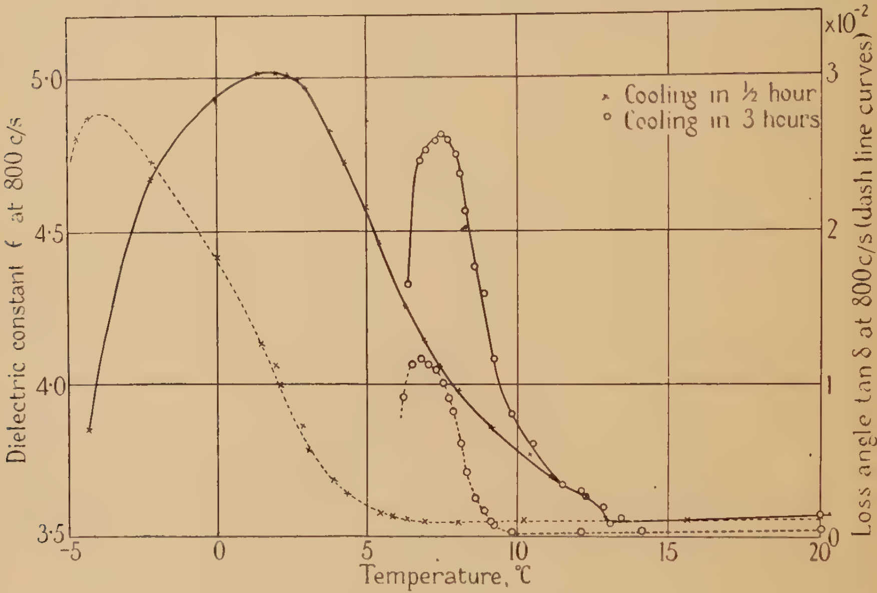

Fast and slow cooling sequence.

Table 1 shows that $\overline{mm}^*{}_{p}/\overline{mm}^*{}_{H}$ is constant independent of the length of the heat treatment, the temperature at which the peak occurs, and of preferential orientation. This indicates that the condition of maximum dielectric constant represents a certain texture through which the material passes in the course of nucleation. It appears to correspond to a certain stage in the development of the nuclei.

Table 1. Particulars of the Condition of Peak Dielectric Constant, Measured at 800 c/s

ϵ_p†	ϵ_H‡	$\overline{mm^*}_p/\overline{mm^*}_H$	tan $\delta\times10^2$		T_p (°c)	Time (minutes)	Remarks
			Uncorrected	Corrected			
5·02	3·54	1·91	1·2	1·03	1·4	30	
5·81	3·84	1·98	1·4	1·02	2·0	50	
4·56	3·33	1·86	0·8	0·77	2·8	50	
7·5	4·9	1·80	1·4	0·81	3·5	60	Quenched from melt
5·28	3·56	2·02	1·3	1·05	3·2	70	
4·44	3·34	1·79	0·7	0·72	6·1	70	
5·88	3·82	2·02	1·7	1·22	2·3	80	
4·94	3·50	1·89	1·0	0·88	4·5	100	
5·04	3·52	1·92	1·2	1·03	4·8	110	
4·81	3·52	1·79	1·0	0·91	7·2	180	See fig. 2
4·37	3·22	1·91	0·8	0·83	4·8	300	
		1·90		$0{\cdot}98\times10^{-2}$			Averages

† ϵ_p = the maximum dielectric constant reached during the heat treatment.
‡ ϵ_H = the dielectric constant of the hexagonal form, measured prior to the heat treatment.

Table 2. Particulars of the Condition of Peak Dielectric Constant, Measured at 50 c/s and 50 kc/s

$\overline{mm^*}_p/\overline{mm^*}_H$	tan δ (corrected)	T_p (°c)	Time (minutes)	Remarks
50 *c/s* :				
1·81	$4{\cdot}1\times10^{-3}$	7·2	180	See fig. 2
1·94	$3{\cdot}1\times10^{-3}$	4·8	75	
1·88	$3{\cdot}6\times10^{-3}$			Averages
50 *kc/s* :				
1·65	$2{\cdot}4\times10^{-2}$	7·5	160	See fig. 2
1·69	$1{\cdot}9\times10^{-2}$	3·7	55	
1·67	$2{\cdot}2\times10^{-2}$			Averages

Although the value of $\overline{mm}^*{}_{\mathrm{p}}/\overline{mm}^*{}_{\mathrm{H}}$ does not significantly depend on any of the recorded variables, there still exists a scatter of about ±6% about the average, indicating an influence of chance on the progress of nucleation. This is to be expected for a nucleation phenomenon, even if it is essentially structure insensitive.

The loss angle associated with the peak dielectric constant is also constant when corrected for preferential orientation. The scatter of values is higher than for the dielectric constant, being ±20%. However, the accuracy of measurement is lower in this case, because the loss angle usually rises rapidly while the dielectric constant is at its peak.

The peak values of the permittivity, and the corresponding loss angles were measured also at 50 c/s and 50 kc/s, giving results similar to those at 800 c/s, as shown in table 2.

Considerations of fig. 3 and of the two tables shows that the maximum permittivity at 50 c/s and 800 c/s corresponds to a distinct texture, and the crystallographic evidence (fig. 5) shows that this condition is not far removed from the single phase state. For 50 kc/s, the maximum is lower and reached earlier, indicating that some dipoles contributing to the dielectric constants at the lower frequencies are unable to do so at the higher one ; this is understandable on the basis of eqn. (5) and implies a ‘ freezing in ’ of dipoles with comparatively long relaxation times.

The occurrence of a maximum of the dielectric constant at some stage of nucleation is not difficult to understand. In a pure ketone, and therefore also in a stable nucleus of the multi-phase form, dipoles are arranged in ‘ dipolar planes ’, within which they are parallel to one another. Fröhlich (1946) shows that this configuration may, in certain critical conditions, lead to high values of $\overline{mm}^*$ and the dielectric constant. However, experiment (Daniel and Stark 1951) shows that pure ketones have a negligible dipolar contribution to the dielectric constant, presumably because the critical conditions are never reached, dipoles being too firmly bound. The dielectric constant of the stable multi-phase form, consisting of more or less pure ketones is similarly low (fig. 1). On the other hand, the single-phase form also has a permittivity low compared with that of the liquid, due presumably to a tendency of neighbouring dipoles of different ketones to be antiparallel. It seems plausible that at some stage between the extremes of mobile but more or less antiparallel, and largely parallel but immobile dipoles there exists a condition when dipoles are mobile and tend to be parallel, thus leading to a comparatively high value of the dielectric constant.

While the existence of a maximum of the dielectric constant at some stage of nucleation can be explained without difficulty, its observed magnitude can so far not be interpreted theoretically ; the comparatively low value observed may be due to a number of causes. Further progress would demand a knowledge of the structure of nuclei and the disordered regions between them, as well as a more detailed knowledge of the distribution of relaxation times. It is possible that dipoles in the interior of nuclei have very long relaxation times, and do not contribute to the dielectric constant even at low frequencies.

Information on the structure of nuclei might be obtained with the aid of x-ray methods analogous to those employed for alloys (Geisler 1951, Guinier 1952), but such work would demand single crystals and its chances of success are difficult to assess. However, the determination of a distribution of relaxation times as a function of aggregate size would be of considerable general interest with regard to the theory of viscous liquids and of plastics, which often show wide distribution of relaxation times and are often supposed to contain semi-crystalline aggregates.

The mixed ketones investigated in the present report may not constitute the most interesting system of equivalent substances for the investigation of dielectric properties of small aggregates. Long-chain secondary alcohols might be more interesting in this respect, for two reasons: because they exhibit comparatively high dielectric constants (Meakins and Welsh 1951), and because a theory (Sack 1952) exists for the dielectric constant and loss angle of chains of linked hydrogen bonds, such as would be formed in small aggregates of secondary alcohols. If such alcohols show nucleation similar to that in mixed ketones they may prove a fruitful system for investigation.

Later Stages of Nucleation

The stage of maximum permittivity is well at the beginning of the process of nucleation, and is followed by a long sequence of later stages. The dielectric constant and loss angle fall monotonously as these stages are traversed at constant temperature, and give little information on their nature. However, information can be obtained by reheating the specimen. As fig. 1 shows, heating after ageing at low temperatures reverses the development of nucleation, and the specimen appears to traverse again the condition of maximum dielectric constant. The conditions in which the peak occurs on reheating give information on the stage of precipitation that had been reached.

Figure 7 shows that if a specimen has been aged only for a short time after passing the peak of the permittivity, it develops a peak on reheating which is somewhat lower than the peak on cooling. This peak occurs at a temperature which is not very much higher than the temperature of the original peak. Figure 1 shows that the peak on reheating occurs at higher temperatures and becomes reduced in magnitude as longer ageing precedes reheating.

X-ray evidence on reheating after short ageing, shown in fig. 4, confirms the results of dielectric measurements in that the changes on cooling are undone by heating. For longer times, the changes are reversed at a higher temperature, again in accordance with dielectric evidence. The x-ray data also show that the specimen is no longer uniform when it has been aged for a matter of days or weeks: some parts of it retain their low temperature form up to a higher temperature than do others.

The experimental evidence on later stages of nucleation can be interpreted from the viewpoint of thermodynamics and from the viewpoint of kinetics.

The thermodynamics of the different stages of nucleation can be represented very simply for a mixture of equivalent ketones, because all constituents have identical thermodynamic properties. In any stage of nucleation, which occurs uniformly in the material, it is possible to define an average free energy G per mole of one (any one) of the ketones, and this quantity describes the stability of the material as a whole.

Fig. 7

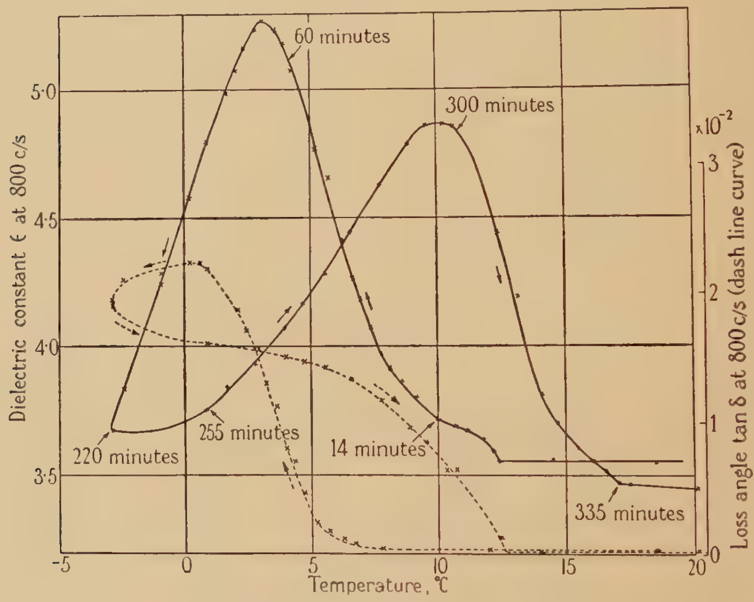

Cooling followed by heating.

Figure 8 shows a schematic diagram of the free energy conditions as revealed by the experiment. Graph 1 represents the liquid, graph 2 the single-phase form, graph 5 the stable multi-phase form, while graphs 3 and 4 are characteristic of two successive stages of nucleation. The figure implies that the intermediate stages of nucleation are more stable than the single-phase form at low temperatures, but that above some temperatures T_3 and T_4 the intermediate stages revert to the single-phase form.

The free energy equals $G=H-TS$, where H is the total energy and S the entropy. Hence the slope of the graphs is (roughly) indicative of S and their height of H. The explanation of the observed data demands a comparatively large increase of the total energy of the intermediate forms as compared with the stable form. This may be attributed to the energy of boundary regions.

As for the kinetics of the later stages of precipitation, the most salient fact is that the development of nuclei becomes less uniform the further it proceeds. The later stages of precipitation are increasingly structure sensitive. This is probably due to the breaking up of the coherence of the single-phase matrix by the formation of compact nuclei of the new phases. Boundaries between them are probably no longer regions of gradual transition, but clear cut interfaces across which diffusion can no longer proceed as simply as before, so that further growth depends on the configuration of the interfaces and so on chance. The formation of new interfaces is suggested by the appearance of the mixture in the later stages: while the material is transparent up to the stage of maximum permittivity, or a little beyond, it becomes opaque as nucleation proceeds further.

Fig. 8

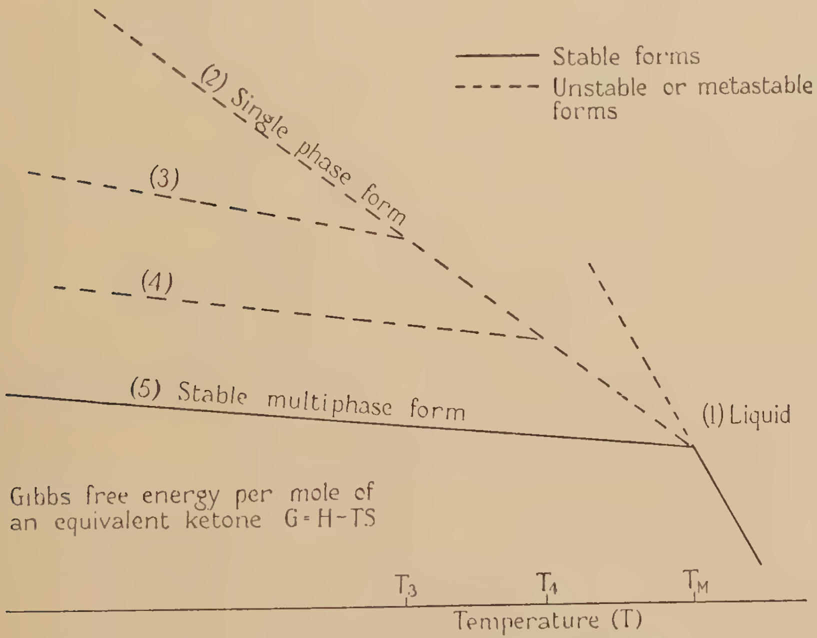
Stable forms
Unstable or metastable forms
(2) Single phase form
(3)
(4)
(5) Stable multiphase form
(1) Liquid
Gibbs free energy per mole of an equivalent ketone G=H−TS
T3
T4
TM
Temperature (T)

Schematic representation of the free energy conditions.

Once stable nuclei are formed, their further development is a process of grain growth and of uphill diffusion, i.e. diffusion against the concentration gradient. Uphill diffusion in the mixed ketones might perhaps be studied by methods analogous to those employed in a two-phase alloy (Daniel 1948), namely by comparing the speed with which corresponding stages are reached at different temperatures. In favourable circumstances such work would allow the measurement of coefficients of diffusion, or at least of their activation energy. This would be of particular interest in mixed equivalent ketones which may be assumed to have equal coefficients of diffusion, so that one would measure effectively coefficients of self diffusion for different conditions of texture.

§ 6. CONCLUSIONS

As regards nucleation, the chief result of the present work is that the early stages of nucleation in the mixed ketones represent short range ordering and are structure insensitive, while the later stages represent long range ordering and are comparatively structure sensitive.

The earliest stages of nucleation are of particular interest. In the temperature range above about 11°C the material appears to contain large fluctuations of the concentration which are in a condition of metastable equilibrium : their magnitude (or number) depends on temperature, but not significantly on time. Cooling below 11°C brings about a change in the character of nucleation, in that nuclei are now able to grow in time. This gradual, but fairly sharp change seems to mark a transition from embryonic to stable nuclei.

Once stable nuclei are formed, they soon make up the bulk of the material and later stages consist of a gradual development of the nuclei from loose aggregates to crystals of the fairly pure ketones. This development is reproducible in its early stages, in that the material always traverses the same sequence of textures.

The dielectric properties of the different stages of texture can so far not be interpreted in detail. Further experiments are needed to determine the size and structure of nuclei, and the distribution of relaxation times. The results of such work may be of general interest for the theory of viscous liquids and plastics, where long relaxation times may be due to the presence of semi-crystalline aggregates.

The methods used in the present investigation need not be restricted to the mixture of five ketones used, since this system is only one of several systems of equivalent substituted paraffins that can be envisaged. Of these, equivalent secondary alcohols would be of particular interest, in view of results which indicate high dielectric constants.

Systems of equivalent substances constitute rather cumbersome research tools because of the chemical work involved in their preparation. However, they offer the advantage that conditions are thermodynamically simple, and that they can be altered in small steps, by altering the chain-length, the nature of the side groups, or the number of equivalent substances. The use of such systems may be worthwhile for the systematic investigation of nucleation, diffusion, and of the physical properties of small aggregates.

REFERENCES

DANIEL, V., 1948, *Proc. Roy. Soc.* A, **192,** 575 ; 1950, *Phil. Mag.*, **41,** 631.

DANIEL, V., and STARK, K. H., 1951, *Trans. Faraday Soc.*, **47,** 149 ; 1952, *Ibid.*, **48,** 685.

DEHLINGER, U., 1951, *Z. Naturforschung*, **6a,** 718.

FRÖHLICH, H., 1946, *Proc. Roy. Soc.* A, **185,** 399 ; 1949, *Theory of Dielectrics* (Oxford : Clarendon Press).

GEISLER, A. H., 1951, *Phase Transformation in Solids* (New York : John Wiley ; London : Chapman and Hall), pp. 387–544.

GUINIER, A., 1952, *Acta Crystallogr.*, **5,** 121.

MEAKINS, R. J., and WELSH, H. K., 1951, *Aust. J. Sci. Res.*, **4a,** 359.

RUSHMAN, D. F., and STRIVENS, M. A., 1947, *Proc. Phys. Soc.*, **59,** 1011.

SACK, R. A., 1952, *Aust. J. Sci. Res.*, **5a,** 135.

SMOLUCHOWSKI, R., 1951, *Phase Transformation in Solids* (New York : John Wiley ; London : Chapman and Hall), pp. 149–182 ; 1952, *Ind. Eng. Chem.*, **44,** 1321.

VOLMER, M., 1939, *Kinetik der Phasenbildung* (Dresden : Steinkopff).

CXLVI. *An X-Ray Examination of an* α(Al–Fe–Si) *Ternary Compound*

By Keith Robinson* and P. J. Black
Crystallographic Laboratory, Cavendish Laboratory, Cambridge†

[Received August 14, 1953]

Summary

The unit cell of an α-phase in the Al–Fe–Si system is found to be hexagonal with $a_0=12{\cdot}3$ Å and $c_0=26{\cdot}2$ Å, and differs from the cells previously reported for other phases of closely similar composition. The most prominent Brillouin Zone associated with the structure of this compound is compared with that of one of these other phases with special reference to the possible ‘ effective valency ’ of transitional metal atoms in electron-rich environments.

§ 1. Introduction

This paper presents the results of an x-ray examination of single crystals of the α-phase in the Al–Fe–Si system prepared by Pratt and Raynor (1951 a). A number of other workers have also examined the aluminium-rich region of this system. All are agreed on the occurrence of at least two ternary phases, usually denoted α(AlFeSi) and β(AlFeSi), although Phragmén (1950) has called them *c*- and *m*- respectively, and Armand (1952) has suggested that the α-region contains three distinct phases denoted α_1, α_2 and α_3 in order of increasing silicon content ; α_3 may be outside the range of alloys examined by other workers.

The results of analyses of extracted crystals of these compounds are summarized below :

		Fe (wgt.%)	Si (wgt.%)
Dix and Heath (1928)	α	30	8
Phragmén (1950)	c	31·9	5·6
Pratt and Raynor (1951 a)	α	32·1–32·7	8·4–10·3
Armand (1952)	α_1	27·3	7·0
	α_2	29·2	11·3
	α_3	35·3	12·8

The unit cell of *c*-(AlFeSi) has been reported by Phragmén (1950) to be cubic with $a_0=12{\cdot}523$ kx, and the structure is considered to be isomorphous with that of *c*-(AlMnSi), for which $a_0=12{\cdot}625$ kx. Phillips and Varley (1943) have reported that in the quaternary Al–Fe–Mn–Si system these two phases are the end members of a continuous series of solid solutions. Armand's x-ray examination (1952) confirmed that his α_1-phase corresponds to the cubic *c*-(AlFeSi). His α_2-phase, on the other hand, has a hexagonal unit cell whose *a*- and *c*-parameters are multiples of 4·95 kx and 7·07 kx respectively.

---

* Now at Physics Department, The University, Reading.
† Communicated by Dr. W. H. Taylor.

§ 2. RESULTS OF THE X-RAY EXAMINATION

We have been able to make an x-ray examination of single crystals of all the samples of α(AlFeSi) described by Pratt and Raynor (1951 a) and find none of them to be cubic. They are, in fact, hexagonal, and the cell dimensions, as measured by layer line measurements on oscillation photographs, are

$$a_0=12{\cdot}3\pm0{\cdot}1\ \text{Å},\qquad c_0=26{\cdot}2\pm0{\cdot}2\ \text{Å}.$$

The Laue symmetry and systematic absences are consistent with space group D^4_{6h}–$P6_3/mmc$, although no test has been made for the presence or absence of a centre of symmetry. Additional evidence for the hexagonal symmetry of α(AlFeSi) may be seen in the external form of the crystals shown in fig. 18 in the paper by Pratt and Raynor (1951 a). There appears to be no simple relationship between the hexagonal unit cell found for Pratt and Raynor's crystals and that given by Armand for his α_2-phase.

Rotation and oscillation photographs of single crystals of α(AlFeSi) of composition 32·5 wgt.% Fe and 8·7 wgt.% Si, taken with Mo *K*α radiation, show a marked grouping of very intense reflections at Bragg angles, 2θ, close to 20° and no other intense reflections with 2θ less than 33°. The planes (*hkil*), listed below, which give rise to these reflections may therefore be considered to define a very prominent Brillouin Zone in wave number (*k*) space, with faces parallel to the planes (*hkil*) at a distance $p=1/2d(hkil)$ Å^{-1} from the origin of the zone, $d(hkil)$ being the interplanar spacing.

(*hkil*)	multiplicity of face	*p*(recip. Å)
(000·12)	2	0·229
$(20\bar{2}{\cdot}11)$	12	0·230
$(30\bar{3}{\cdot}10)$	12	0·238
$(32\bar{5}7)$	24	0·244
$(33\bar{6}0)$	6	0·244

This is the only prominent zone with faces closer than 0·40 Å^{-1} to the origin; it is shown in fig. 1.

§ 3. DISCUSSION

It is clear that there are at least two ternary compounds in the α-region of the Al–Fe–Si system, that having the lower silicon content being cubic (*c*- of Phragmén, α_1 of Armand) and that having the higher silicon content having a hexagonal structure (α of Pratt and Raynor). If the latter is really different from the hexagonal structure of Armand's α_2-phase, and if his α_3-phase is also included in this region, there must be four different ternary compounds in the 'α' region of the system, and further careful metallurgical work will be required to determine their precise relationship.

Fig. 1

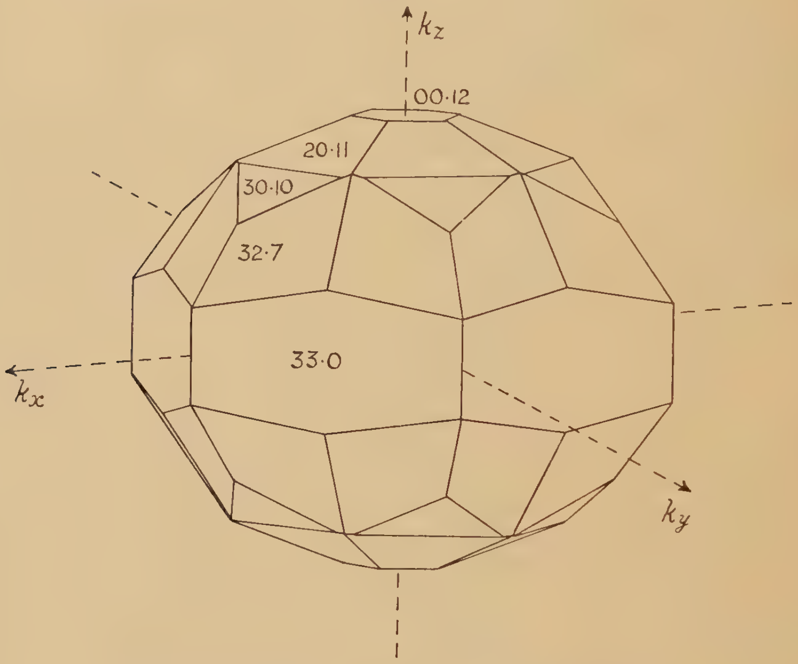

The first prominent Brillouin Zone of α(AlFeSi).

It would be interesting to consider the influence of their structures on the stability of these compounds, but sufficient data are not available. By considering the composition ranges of α(AlMnSi) and α(AlFeSi) Pratt and Raynor (1951 b) have suggested that both phases are stabilized by an electron/atom ratio of about two electrons per atom. If, as seems very likely, these compounds may be regarded as electron compounds, we can at least compare the stability of two of them (c- and α) on the basis of the x-ray measurements already made.

For α(AlFeSi), the very prominent Brillouin Zone described in the previous section has a volume (V) 0·0644 Å^{-3}. We might expect this hexagonal phase to be stabilized at a composition having a 'free' electron/atom ratio slightly less than $2Vv$, where v is the mean atomic volume. The value of v may be readily calculated from the composition, cell size and density ($3{\cdot}61 \pm 0{\cdot}02$ g cm^{-3}, determined by flotation) of the sample, and is found to be 15·0 Å^3. The stabilizing ratio would therefore be expected to be slightly less than 1·93 electrons/atom.

We have not been able to make the corresponding x-ray measurements on a sample of *c*-(AlFeSi), but can nevertheless calculate the form and volume of the Brillouin Zones associated with this compound from the lattice parameter (a_0=12·523 kx), density (3·61 g cm^{-3}) and composition given by Phragmén (1950), together with the knowledge that the phase is isomorphous with α(AlMnSi). For if the two phases are structurally identical or very closely similar, as indeed they must be to account for the observed range of solid solutions reported by Phillips and Varley (1943), then their very intense x-ray reflections, and hence the forms of their Brillouin Zones, must be identical. We have examined crystals of the sample (3/5) of α(AlMnSi) (see Pratt and Raynor 1951 a), and find them to be cubic (a_0=12·670±0·000$_5$ Å, based on Cu $K\alpha_1$ radiation, λ= 1·54050 Å) with 138 atoms per unit cell; the atomic arrangement has been determined at least to a first approximation, and will be described elsewhere. The x-ray reflections from the {530}, {600} and {352} planes are six times stronger than those from any other plane with $1/2d(hkl)<0{\cdot}39$ Å^{-1}.

Fig. 2

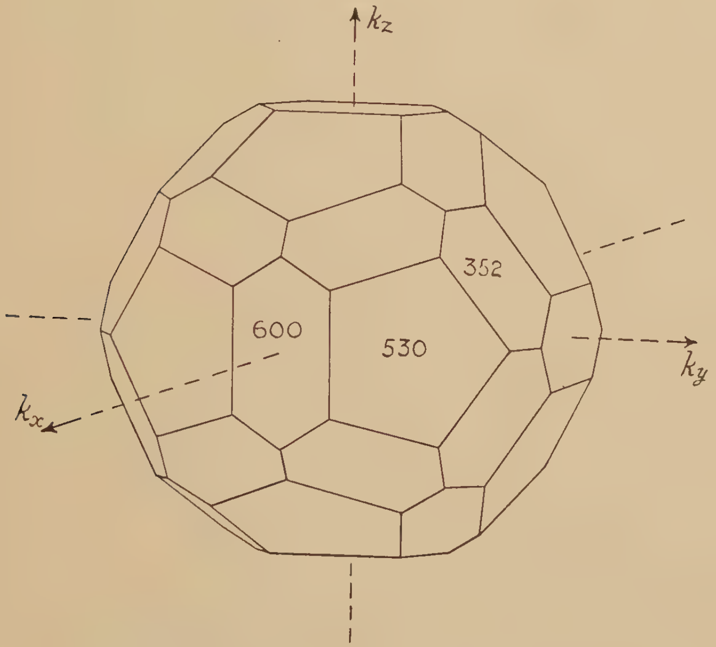

The first prominent Brillouin Zone of α(AlMnSi).

The only Brillouin Zone likely to affect the stability of these phases is therefore that shown in fig. 2, which is formed by the forty-two {530}, {600} and {352} faces. For *c*-(AlFeSi) these faces lie at p=0·231, 0·237 and 0·244 Å^{-1} respectively, from the origin of the zone. The volume of the zone (V) is then 0·0612 Å^{-3} and the mean atomic volume (v) is 14·9 Å^3.

The structure of c-(AlFeSi) would thus be expected to be stabilized at a composition corresponding to slightly less than 1·83 electrons/atom, i.e. a slightly lower electron/atom ratio than for the hexagonal α(AlFeSi) phase. It is clear that electronically the cubic and hexagonal structures do not differ greatly, but other things being equal we should expect the cubic phase to have the lower silicon content, since Si has the highest ' valency ' of the constituents.

We may now consider Pratt and Raynor's suggestion (1951 b) that the phases are characterized by a ratio of about two electrons per atom. In computing electron/atom ratios from chemical compositions they have used the model of Raynor (1944) for the behaviour of transitional metals in an electron-rich environment, i.e., ' effective valencies ' Al$=+3$, Si$=+4$, Fe$=-2·66$, Mn$=-3·66$. We might also consider other possible transitional metal atom valencies, e.g.,

(i) Fe$=-2·0$, Mn$=-3·0$, based on the theory of Mott and Jones (1936) ;

(ii) Fe$=$Mn$=0$, as in the β brass structures (e.g. FeAl, Ekman 1931) ;

(iii) Fe$=$Mn$=+5·78$, as suggested by Pauling (1938).

Electron/atom ratios calculated from the compositions already given would be as follows :

Fe ' valency '	c-(AlFeSi)	α(AlFeSi)
$-2·66$	2·02	2·03
$-2·0$	2·14	2·15
0	2·51	2·53
$+5·78$	3·58	3·63
Estimated from the Brillouin Zone	$<1·83$	$<1·93$

These phases may therefore be regarded as electron compounds governed by the form of the most prominent Brillouin Zone if each iron atom in some way prevents about three otherwise ' free ' electrons from behaving as if free. The Raynor model (Fe valency$=-2·66$) might be satisfactory if the faces closest to the origin of the zones are overlapped. Thus a c-(AlFeSi) zone formed solely by the twenty-four $\{352\}$ faces has a volume, $V=0·0721$ Å^{-3}, corresponding to 2·15 electrons/atom. For α(AlFeSi), however, the zone formed by $\{30\bar{3}·10\}$, $\{32\bar{5}7\}$ and $\{33\bar{6}0\}$ only raises the possible ratio to 2·01 electrons/atom.

It is worth noting that the zone calculated from our sample of α(AlMnSi) corresponds to an electron/atom ratio about 3% lower than that of the corresponding c-(AlFeSi), whilst the ratio computed from the composition of the sample on the Raynor model is 1·97 electrons/atom, also about 3% lower than that for c-(AlFeSi). This means that as far as the cubic phases are concerned the known compositions and structure are in accord with the view that the compounds are electron compounds in which the ‘ effective valency ’ of Mn is algebraically less than that of Fe by one unit.

Moreover, the forms of the most prominent Brillouin Zones of the compounds discussed in this paper are consistent with their chemical composition only if the transitional metals are given ‘ effective valencies ’, if anything, slightly more negative than those suggested by Raynor. However, this interpretation assumes that the zones are more full than has been necessary in other corresponding cases, e.g. β(AlMnSi) and α(AlCrSi) (Robinson 1952, 1953). If the zones were less full, as in the other cases, then the ‘ effective valency ’ of the transitional metal atoms would have to be regarded as being even more negative.

We should like to thank Dr. J. N. Pratt and Professor G. V. Raynor for the provision of the specimens examined, and Professor Sir Lawrence Bragg, F.R.S., and Dr. W. H. Taylor for their interest in the progress of the work. For financial assistance one of us (P. J. B.) wishes to thank the Dept. of Scientific and Industrial Research for a Maintenance Grant and the other (K. R.) thanks the Ministry of Supply (Basic Properties of Metals Committee) and the Royal Commissioners for the Exhibition of 1851.

REFERENCES

ARMAND, M., 1952, *Comptes Rendus*, **235,** 1506.
EKMAN, W., 1931, *Z. Phys. Chem.* B, **12,** 57.
DIX, E. H., Jr., and HEATH, A. C., Jr., 1928, *Trans. Amer. Inst. Min. Met. Eng., Inst. Met. Div.*, 164.
MOTT, N. F., and JONES, H., 1936, *The Theory of the Properties of Metals and Alloys* (Oxford : University Press).
PAULING, L., 1938, *Phys. Rev.*, **54,** 899.
PHILLIPS, H. W. L., and VARLEY, P. C., 1943, *J. Inst. Met.*, **69,** 317.
PHRAGMÉN, G., 1950, *J. Inst. Met.*, **77,** 489.
PRATT, J. N., and RAYNOR, G. V., 1951 a, *J. Inst. Met.*, **79,** 211 ; 1951 b, *Proc. Roy. Soc.* A, **205,** 103.
RAYNOR, G. V., 1944, *J. Inst. Met.*, **70,** 531.
ROBINSON, K., 1952, *Acta Cryst.*, **5,** 397 ; 1953, *Ibid.* (in the press).

CXLVII. *The Inelastic Scattering of Neutrons: II*

By M. J. Poole
Atomic Energy Research Establishment, Harwell, Berks.*

[Received August 17, 1953]

Abstract

Measurements of the spectrum of 2·5 mev neutrons scattered through 97° from Al, Ni, Bi, W, and Au are presented, together with the differential cross section for the processes.

§ 1. Introduction

This paper is an account of further measurements on the inelastic scattering of fast neutrons, using the method already described by the author (Poole 1952). The spectrum of scattered neutrons from nickel, tungsten, bismuth and gold has been observed, and the measurements on aluminium repeated and a more trustworthy result obtained than that previously published.

§ 2. Experimental Method

For a description of the apparatus, the reader is referred to the earlier paper (*loc. cit.*). 2·5 mev neutrons emitted at 90° from the D–D reaction are scattered by a ring of material placed round the target of the machine, and neutrons scattered through (usually) 97° are detected by a scintillation counter using an anthracene crystal. A ‘ background ’ run is made to determine the effect produced by γ rays and by neutrons scattered from the walls of the room. From the spectrum of pulses produced by this counter, the proton recoil spectrum, and so the neutron spectrum, may be deduced. The energy resolution is about ±200 kev at 2·5 mev.

Kinematics

To interpret the curves of scattered intensity the effect of the recoiling nucleus must be considered. For scattering through 90° it can be shown that the energy of the scattered neutron is

$$E_1=E_0(M-m)/(M+m)-E\{M/(M+m)\}$$

where E_0 and E are the initial neutron energy and energy of excitation of the residual nucleus respectively, while M and m are the masses of scattering nucleus and neutron.

Thus if an excitation energy is measured relative to the elastically-scattered group ($E=0$) the energy actually observed will be $E\{M/(M+m)\}$. It is apparent that this correction to E is important only in the case of the lightest nuclei. For scattering angles less than 90° the effect is less.

---

* Communicated by the Author.

§ 3. RESULTS

1. *Aluminium* (fig. 1)

Groups of scattered neutrons appear at 2·3 ± 0·15 MeV and 1·4 ± 0·15 MeV. The former is ascribed to elastic scattering of 2·5 MeV neutrons (E_1=2·32 MeV) and the latter to an inelastic group with mean excitation of the residual nucleus of 0·9 MeV (E_1=1·44 MeV). This is consistent with the inelastic proton scattering results (Reilley *et al.* 1952) giving levels in ^{27}Al at 0·81 and 0·99 MeV, and with the γ-spectrum work (Hedgran, Hole and Benes 1948, Itoh 1941) giving levels at 0·84 MeV and 1·05 MeV.

Fig. 1

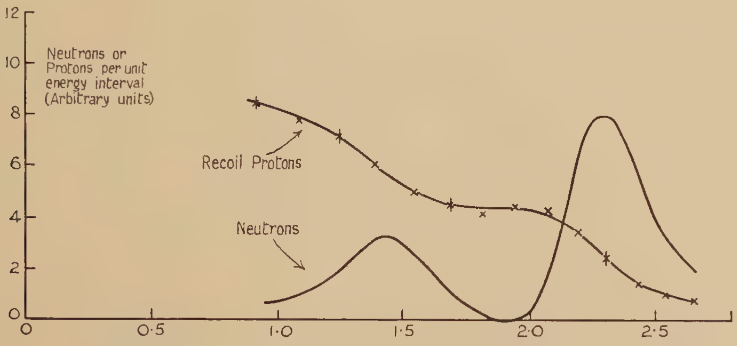

Spectrum of neutrons scattered from aluminium.

Fig. 2

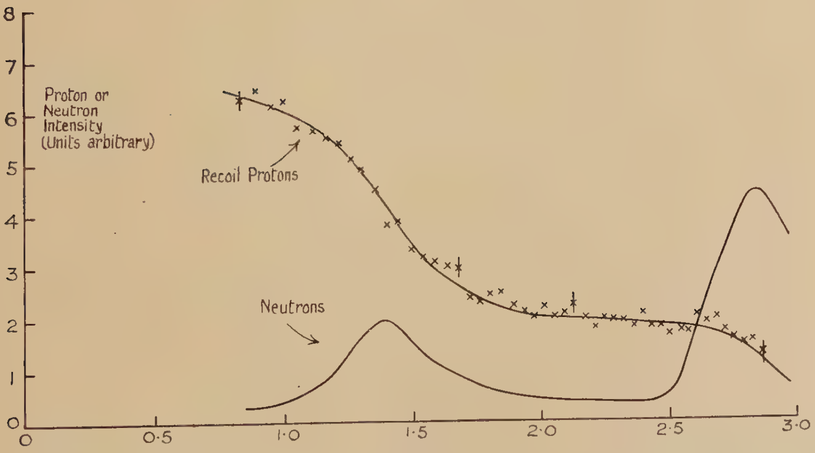

Spectrum of neutrons scattered from nickel.

2. *Nickel* (fig. 2)

Two runs were made with a nickel scatterer. The first showed a group with 1·4 MeV energy loss, and to make this more clear the experiment was repeated with the scatterer placed to receive neutrons emitted at

72° to the deuteron beam ($E_0=2\cdot8$ MeV). Although these neutrons are no longer strictly monokinetic this shows scattered groups at 2·8 MeV and 1·4 MeV, corresponding to elastic scattering, and inelastic scattering with 1·4 MeV energy loss. This may be compared with inelastic proton scattering results of Reilley *et al.* (1952) giving levels at 1·344 MeV and 1·48 MeV, and Cowie *et al.* (1952) who find a level at 1·44 MeV.

Fig. 3

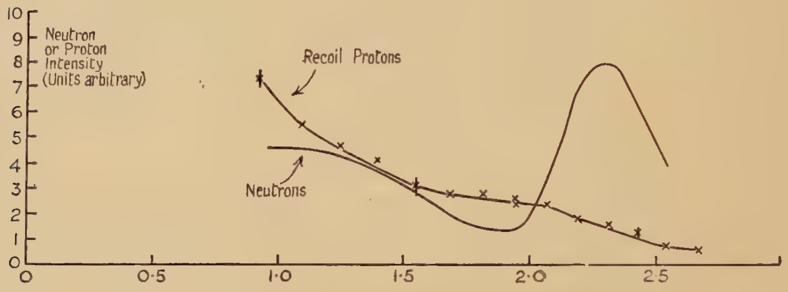

Spectrum of neutrons scattered from tungsten.

Fig. 4

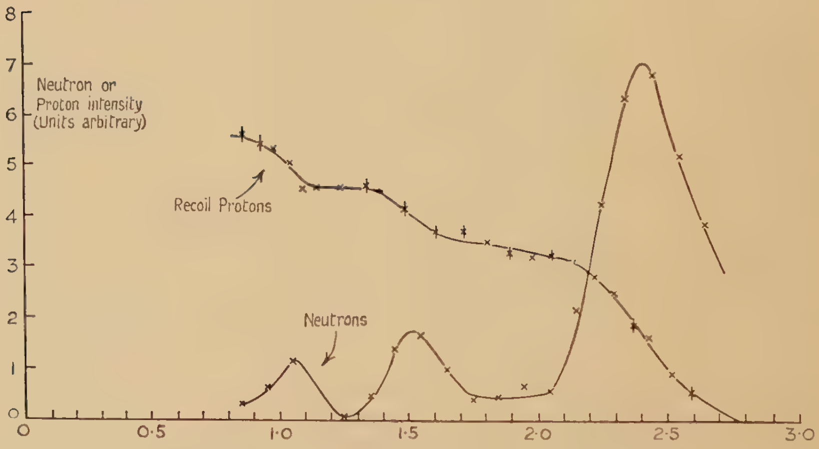

Spectrum of neutrons scattered from bismuth.

3. *Tungsten* (fig. 3)

Here apart from the elastically-scattered group at 2·5 MeV, the scattered spectrum is continuous, showing a steady rise at low energies. Due to poor resolution it is not possible to say exactly what inelastic scattering occurs in the region 2·0 MeV to 2·5 MeV scattered neutron energy, and therefore the elastic scattering cross section quoted below may include a contribution from inelastic scattering with small energy loss. This type of spectrum is not unexpected with heavy nuclei, due to the probability of a large number of closely-spaced levels.

Fig. 5

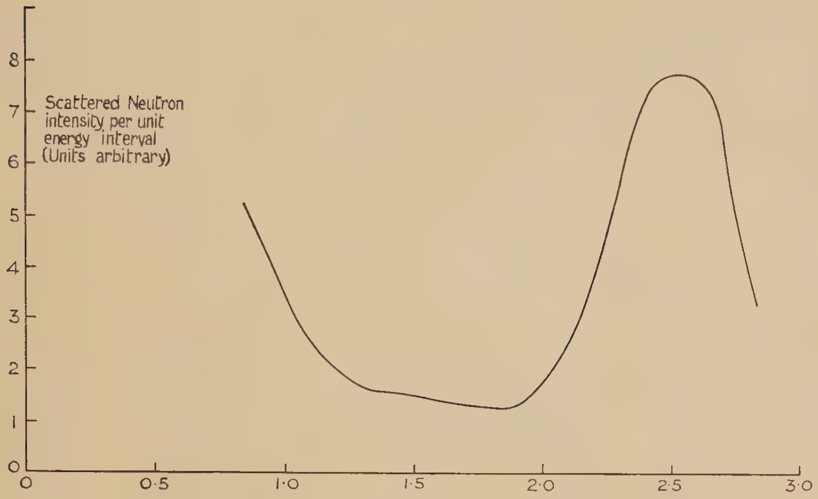

Spectrum of neutrons scattered from gold.

Table 1. Inelastic and Elastic Neutron Scattering Cross Sections

Nucleus	E_0 (MEV)	Scattering angle	E_1 (MEV)	Diff. cross section (barns/sterad.)	$4\pi \times$ diff. cross section (barns)	Total abs. cross section (barns)	Remarks
^{27}Al	2·5	97°	2·3	0·08 ±0·02		3·0	Elastic peak
			1·4	0·04 ±0·02	0·5 ±0·25		Probably two close levels
Ni	2·8	70°	2·8	0·07 ±0·02		6·0	Elastic peak
			1·4	0·05 ±0·02	0·6 ±0·25		Probably two close levels
W	2·5	97°	2·5	0·13 ±0·04		7·2	Elastic peak (plus low lying levels)
			1·0 to 2·0	0·10 ±0·04	1·3 ±0·5		Integrated continuous distribution
^{209}Bi	2·4	97°	2·4	0·23 ±0·04		6·4	Elastic peak
			1·5	0·06 ±0·02	0·75±0·3		First excited state
			1·1	0·025±0·01	0·3 ±0·15		Second excited state
Au	2·5	97°	2·5	0·2 ±0·05		7·0	Elastic peak (plus low lying levels)
			1·0 to 2·0	0·07 ±0·03	0·9 ±0·4		Integrated continuous distribution

4. *Bismuth* (fig. 4)

Groups appear at 2·4±0·1 MeV, 1·5±0·1 MeV and 1·1±0·1 MeV, the minima between these being quite low. These may be interpreted as elastic scattering together with inelastic scattering from excited states at 0·9±0·2 MeV and 1·3±0·2 MeV. The level spacing is unusually high for a heavy nucleus, as would be expected from the nearness of ^{209}Bi to the 'magic' numbers for both neutrons and protons.

5. *Gold* (fig. 5)

Shows elastic peak at 2·5 MeV plus a continuous distribution of neutrons, rising at low energies, consistent with many closely-spaced levels.

6. *Cross section values*

Values for 'light' elements (discrete levels) are differential cross sections for scattering through the stated angle, leaving the nucleus in the level concerned. Values for 'heavy' elements (continuous spectrum) are split into above 2·0 MeV ('elastic' scattering) and 1·0 MeV to 2·0 MeV ('inelastic' scattering). Additionally for comparison the integrated cross section assuming a spherically symmetrical angular distribution, and the total absorption cross section (taken from the literature) have been tabulated. Spherical symmetry is probably only justifiable in the case of inelastic scattering from many levels ('heavy' nuclei).

ACKNOWLEDGMENTS

The author wishes to thank the Director, A.E.R.E., for permission to publish this work, Dr. E. Bretscher for his continuous interest, and Mr. W. Howe who carried out the many hours of counting involved.

REFERENCES

COWIE, D. B., HEYDENBURG, N. P., and PHILLIPS, G. C., 1952, *Phys. Rev.*, **87,** 2.
HEDGRAN, A. G., HOLE, N., and BENES, J., 1947, *Ark. Mat. Astr. Fys.*, **34B**, 19.
ITOH, Z., 1941, *Proc. Phys. Math. Soc. Japan*, **23,** 405.
POOLE, M. J., 1952, *Phil. Mag.*, **43,** 1060.
REILLEY, E. M., ALLEN, A. J., ARTHUR, J. S., BONDER, R. S., ELY, R. L., and HAUSMANN, H. J., 1952, *Phys. Rev.*, **85,** 4.

CXLVIII. *A Method for the Determination of the Rate of Extension of the Helium II Film*

By A. C. Ham and L. C. Jackson
H. H. Wills Physical Laboratory, University of Bristol*

[Received October 5, 1953]

Abstract

The optical method of Burge and Jackson (1951) is employed to determine the rate of extension of the helium II film over a previously bare solid surface. The passage of the front of the film over two regions of the surface a known distance apart is observed, and a provisional apparatus has shown that the method is feasible and has indicated what changes should be made to obtain significant results.

§ 1. Introduction

Frenkel (1940) has derived a formula for the rate of the initial spread of a film of a normal liquid over a vertical solid surface partly immersed in the liquid. For the case of water the velocity of the outer layer of the film at a height of 1 cm above the liquid surface is calculated to be about 2 mm/s. In the case of liquid helium just above the λ-point, the corresponding value will be about 80 cm/s. The formula cannot, of course, be applied to the case of helium II because of the superfluid properties of the latter. No attempt has yet been made to derive a formula appropriate to the latter case. It therefore seems of interest to make a direct experimental determination of the rate of extension of the helium II film over a previously bare solid surface.

It seemed probable, from the observations of Burge and Jackson (1951) of the helium II film by an optical method, that it should be possible to observe the passage of the front of the film over two regions of the solid surface a known distance apart and so derive the velocity of extension of the film. Accordingly a provisional apparatus was devized, which involved the least possible alteration to the present optical system, and constructed from available material. This apparatus has shown that the method is feasible and has indicated what changes should be made in a future version to obtain accurate and reproducible results. As we do not anticipate being able to carry out observations with the new version of the apparatus in the immediate future, it is thought to be of interest to publish this preliminary account of the work.

---

* Communicated by the Authors.

§ 2. Apparatus and Method

The apparatus is shown in fig. 1. It consists essentially of two small stainless steel mirrors, M_1 and M_2, each 1 cm long, one above the other in the same vertical plane and connected by a wire of diameter 1 mm and about 30 cm long coiled into a spiral. As actually constructed the two halves of the coil were wound in opposite directions to avoid the mirrors being displaced from the same plane as the apparatus cools from room temperature. The arrangement is supported by a bent nickel rod N, the upper end of which is connected to a thin-walled glass tube T terminating in the pin-chuck shown above and the lower end is attached below the lower mirror at B. As in the experiments of Burge and Jackson, half of each mirror is coated with a layer of barium stearate one molecule thick and the other half with a layer three molecules thick. Sodium light linearly polarized at 45° to the plane of incidence is reflected from both mirrors and is observed through a $\lambda/4$ plate and a nicol prism. If the two latter are so adjusted that the intensity of the light reflected from the two halves of the mirrors is the same in the absence of the helium II film, then the passage of the film over a mirror can be observed by the lack of matching

Fig. 1

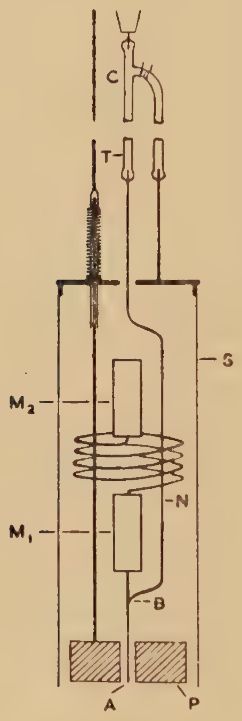

of the '1' and '3' areas of the mirror. The experiment consisted in principle in dipping the tip A into liquid helium II and measuring the time interval between the appearance of the film on M_1 and M_2.

Dipping the apparatus directly would have disturbed the optical settings and so a cylindrical spring-loaded plunger P was arranged with a central hole in it, operated externally, so that having set A 1 mm or so above the liquid level, contact could be made by lowering the plunger until it was immersed and so raising the level of the liquid above the tip A. The whole apparatus was surrounded by a cylindrical copper radiation shield S, which had appropriate windows cut in it and was supported by another glass tube which joined T at C just below the pin-chuck and about 20 cm above the mirrors. Since the chuck was in good thermal contact with a metal vessel containing liquid hydrogen at 20°K, the temperature of C would always be above the λ-point, and so the mirrors would not be covered with the film by the latter creeping over the surface of S, up the glass support and down T and N.

To obtain significant results it was essential that there should be no appreciable temperature gradient in the mirror system. Enclosing the latter inside the well-conducting copper shield, which was always in contact with the liquid helium and was covered by the helium II film, largely satisfied this requirement, but the method of supporting the mirror system was found to result in too large a heat influx (see later), and this must be improved in a future form of the apparatus.

§ 3. RESULTS

It was essential for the purpose of the experiment that a film should not form from the vapour phase to a thickness comparable with that from the liquid phase during the time of observation. This was first checked in a preliminary experiment.

Observations were first made immediately below the λ-point but no films were detected on M_1 or M_2 until the temperature was reduced to 2·09°K when A was in contact with the liquid. It then appeared that the heat influx down the wire support was sufficient to evaporate the film on A before it reached the junction at B for any temperature between 2·09°K and 2·19°K. For any temperature below 2·09°K the creep rate was sufficiently great for a film to pass B in spite of the heat influx, which was estimated to be about 100 erg/sec. A reduction of this figure by a change in the method of supporting the mirror system is clearly desirable in any future apparatus.

Observations were next made at 1·90°K and the passage of a film over M_1 and M_2 could be observed. It was, however, found necessary to fix the attention on one mirror for some 10–15 sec before it was possible to detect the subsequent lack of matching due to the passage of a film over the mirror. It was therefore not possible to observe the movement of the film past M_1, transfer the attention of the observer to M_2 and detect the movement of the film over the latter if the interval was less than

15 sec. However, by concentrating attention on M_2 the following intervals were observed between the time of contact of the liquid with A and the arrival of the film on M_2: 4·5, 4·2, 4·5, 4·5, 4·5, 4·0, 4·7 sec, with an average of 4·4 sec.

The film did not appear as a sharp edge passing over the mirror, but as a gradual change in the relative intensities on the two sides of the 1–3 boundary lasting for less than 1 sec which is included in the figures given. This was to be expected since the film was flowing on to the mirror from the much smaller periphery of the wire and having to ‘ build up ’ to its equilibrium thickness.

A repetition of the observations at 1·44°K gave the following times: 3·5, 4·3, 4·3, 3·5, 4·3, 4·5, 5·3, 3·5, 4·3, 5·5, 4·4, 4·0, 4·4 sec; average 4·3 sec. Each time contact with the liquid was broken the film evaporated from M_2 in about 5 sec, or rather a considerable reduction in thickness of the film took place as no attempt was made to measure the actual thickness in these experiments.

It would therefore appear that when further developed the apparatus will be capable of giving an accurate figure for the rate of extension of the helium II film over a solid surface. No actual velocity will be calculated from these preliminary observations because of the uncertainties due to (1) the finite time of spread of the film from the wire to the larger periphery of the mirrors, and (2) the fact that the film divides at B. It is not known whether the film preserves the same thickness on the mirror system and the corresponding point on the wire support N and so travels at a slower rate than on the wire at A, or whether the velocity remains constant and the film thickness decreases.

In the new apparatus now being constructed the method of support is being changed so that the heat influx is reduced and the division of the film at B is avoided. By making the mirror system of a continuous flat polished strip the change of periphery at the mirrors is avoided, and the latter are arranged side by side in the same vertical plane so that the two 1–3 boundaries are co-linear and no movement of the observer's eye from one mirror to the other will be required.

Acknowledgments

We are indebted to the Department of Scientific and Industrial Research, both for a grant in support of a programme of investigation of the helium II film of which the observations described above form a part, and also for a maintenance allowance to one of us (A. C. H.).

References

Frenkel, J., 1940, *J. Phys., U.S.S.R.*, **2**, 365.
Burge, E. J., and Jackson, L. C., 1951, *Proc. Roy. Soc.* A, **205**, 270.

CXLIX. CORRESPONDENCE

Estimation of Mean Lifetimes from Multiplate Cloud Chamber Tracks

By M. S. Bartlett
University of Manchester*

[Received October 14, 1953]

In a recent discussion (Bartlett 1953) of the statistical estimation of the mean lifetimes of unstable particles, the methods proposed were illustrated with reference to some data of Fretter *et al.* (1953) on neutral V particles. This may prove confusing to the reader, as I had overlooked the fact that these authors were making use of data from a *multiplate* cloud chamber, and the estimation equations are not strictly applicable in this case without modification. My attention was kindly drawn to this point by J. A. Newth (cf. Page and Newth 1954), and while the appropriate modification of the estimation equation has already been indicated and used by Bridge *et al.* (1953, § IX), it may be helpful to record it here, together with the further modified formulae if the accuracy of the estimate is to be precisely evaluated.

In relation to the track of the rth of n particles observed to decay in the chamber, there will now be, in addition to the time of decay t_r measured from an appropriate zero and the total possible time T_r, a number of further times T_{rs} ($s=1, 2, \ldots$) when the track or its continuation enters and leaves the intermediate plates (if any). It is convenient to write as before $t_r/\theta=u_r$, $T_r/\theta=U_r$, where θ is the unknown mean lifetime ; we now have also $T_{rs}/\theta=U_{rs}$. I shall use the further notation

$$\begin{aligned}
A_r&=1-e^{-U_r}+\Sigma_s(-1)^s\,e^{-U_{rs}},\\
B_r&=U_r\,e^{-U_r}-\Sigma_s(-1)^s U_{rs}\,e^{-U_{rs}},\\
C_r&=U_r^2\,e^{-U_r}-\Sigma_s(-1)^s U_{rs}^2\,e^{-U_{rs}}\,;\\
b_r&=T_r-\Sigma_s(-1)^s T_{rs},\\
c_r&=T_r^2-\Sigma_s(-1)^s T_{rs}^2,\\
d_r&=T_r^3-\Sigma^s(-1)^s T_{rs}^3.
\end{aligned}$$

Then the probability distribution of the decay times t_r is

$$\prod_{r=1}^{n} e^{L_r}\,dt_r \equiv \prod_{r=1}^{n} \frac{e^{-U_r}\,du_r}{A_r}, \qquad (1)$$

and the estimation equation (Σ_r denoting summation over the n different tracks) is

$$\theta\Sigma_r\frac{\partial L_r}{\partial\theta}=\Sigma_r(u_r-1+B_r/A_r)=0. \qquad (2)$$

---

* Communicated by the Author.

Moreover,

$$\theta^2 E\left\{\Sigma_r\left(-\frac{\partial^2 L_r}{\partial\theta^2}\right)\right\}=\Sigma_r(I_1)_r=\Sigma_r\left(1-\frac{C_r}{A_r}-\frac{B_r^{\,2}}{A_r^{\,2}}\right), \quad . \quad . \quad . \quad (3)$$

the approximate standard error of the estimate of θ obtained from (2) being $\theta/\sqrt{\Sigma_r(I_1)_r}$, or equivalently that of $1/\theta$ being $1/[\theta\sqrt{\Sigma_r(I_1)_r}]$.

The standardized quantity $S(\theta)$ with zero mean and unit standard deviation, most suitable for plotting (against, say, convenient values of $1/\theta$) if eqn. (2) is to be solved by interpolation or confidence limits for θ are required, is

$$S(\theta)=\Sigma_r(u_r-1+B_r/A_r)/\sqrt{\Sigma(I_1)_r}. \quad . \quad . \quad . \quad . \quad . \quad (4)$$

The higher moments of $S(\theta)$ could be worked out if required, though they will now be rather complicated. Even for the evaluation of $\Sigma_r(I_1)_r$ and $S(\theta)$ we cannot unfortunately make much use of the table provided in my paper; direct evaluation for one or two simple values of $1/\theta$, while tedious, is, however, still quite practicable.

In the particular region $1/\theta \sim 0$, the expression for $S(\theta)$ becomes

$$S(\theta)\sim\frac{\Sigma_r(t_r-\frac{1}{2}c_r/b_r)}{\sqrt{\Sigma_r X_r}}+\frac{1}{\theta}\sqrt{\Sigma_r X_r}, \quad . \quad . \quad . \quad . \quad . \quad (5)$$

where

$$X_r=\frac{d_r}{3b_r}-\left(\frac{c_r}{2b_r}\right)^2.$$

Thus for $1/\theta \sim 0$, the estimate becomes

$$\frac{1}{\theta}\sim-\frac{\Sigma_r(t_r-\frac{1}{2}c_r/b_r)}{\Sigma_r X_r}, \text{ with standard error } 1/\sqrt{\Sigma_r X_r}, \quad . \quad . \quad (6)$$

(the negative sign outside the expression on the right was inadvertently left out of the corresponding eqn. (6) of my paper). This rough solution must be used with caution, for it depends on T_r/θ being small; it is not recommended if $S(\infty)$ is significantly negative, say less than -2.

REFERENCES

BARTLETT, M. S., 1953, *Phil. Mag.*, **44**, 249.
BRIDGE, H. S., PEYROV, C., ROSSI, B., and SAFFORD, R., 1953, *Phys. Rev.*, **91**, 362.
FRETTER, W. B., MAY, M. M., and NAKADA, M. P., 1953, *Phys. Rev.*, **89**, 168.
PAGE, D. I., and NEWTH, J. A., 1954, *Phil. Mag.*, **45** (in the press).

Crystallographic Slip in Diamond

By M. SEAL and J. W. MENTER
Research Laboratory for the Physics and Chemistry of Surfaces, Department of Physical Chemistry, University of Cambridge

[Received October 1, 1953]

THE technique of reflection electron microscopy developed by von Borries (1940) and more recently by Menter (1952, 1953) and others has been applied to an investigation of surface features on polished diamonds.

In this method the surface is illuminated with electrons incident at a glancing angle of 1–2° and viewed at an angle of 6–12°. Contrast arises primarily from shadows cast by asperities standing out from the surface. Thus the most prominent features seen on polished diamonds examined in this way are parallel grooves formed by the abrasive. (All the diamond surfaces examined had been polished in one direction only.) The visibility of the grooves is greatest when they are oriented at right angles to the plane of incidence but surface features within the grooves are not seen on account of the shadows cast by their edges. However, the grooves may be rendered almost invisible by arranging to have them parallel to the plane of incidence. Detail within the grooves then becomes more readily visible and it has been found that there are a number of roughly parallel lines on the surface, different in character and direction from the polishing marks. These lines can be seen more easily by optical examination of the carbonaceous contamination layer which is formed on the surface by the action of the electron beam. The nature and origin of this contamination has been investigated by Ennos (1953). He showed that it is formed only where the electrons strike the surface. If, therefore, a specimen is irradiated in the electron beam and subsequently examined in the optical microscope, it has the appearance of having been shadowed at a very oblique angle.

Figure 1 (Pl. 52, figs. 1 and 2) shows an optical micrograph of a polished diamond surface which has been contaminated in the electron microscope. The directions of the polishing marks and of the incident electron beam are indicated by the arrow (A). There are also several cross lines (B) rendered visible by the contamination shadowing effect. Such lines correspond to changes in surface level which may in some cases be as small as 20 Å. This has been established by stripping the contamination layer from the surface and examining it at high magnification as a low angle shadowed replica in the transmission electron microscope. The most likely explanation of these lines seems to be that they are due to crystallographic slip occurring during polishing. Extremely high local pressures must be produced whilst polishing and these may well be large enough to initiate plastic deformation (the Knoop indentation hardness of diamond is 5 500–6 950 kg/sq. mm).

Three polished diamonds have been examined. They are all of type I and x-ray and electron diffraction photographs show no evidence of macroscopic twinning. In each case the mean direction of the cross lines follows the trace of a $\{111\}$ plane. There is, however, a spread of several degrees in their direction and this could be due to cross-slip. The lines only follow one set of $\{111\}$ planes on each stone and, asssuming a glide direction $[110]$, these are the octahedral planes of greatest resolved shear stress (Schmid criterion). On one diamond the face which had been examined was repolished in the same direction as before, the thickness of the layer removed being less than $25\,\mu$. Examination of the same field before and after this second polish showed that, although the lines were visible in each case, there was no detailed correspondence between them. The stone was then repolished again but this time in a completely different direction. Lines were visible on a new set of {111} planes and the old cross lines could not be detected. It would seem unlikely, therefore, that the lines could arise from some lamellar growth structure within the diamond or from cracking of the surface. Moreover, the lines do not follow the traces of octahedron planes of greatest resolved normal breaking stress (Sohncke criterion).

Further confirmation that the lines are not due to cracking has been obtained by examining a gross scratch produced on a polished dodecahedron face by a hard octahedron apex (fig 2). The gross white lines extending a short distance from the scratch follow the {111} planes of greatest breaking stress and are certainly cracks. The second set of lines (B) are the polish marks and there is a third set (C) following traces of another set of {111} planes, which could be slip lines.

Williams (1932) has suggested that some of the lines observed on natural diamonds might be due to slip and Tolansky and Omar (1953) have described a case of possible slip on opposite octahedron faces of a twinned diamond, as mined. The present observations suggest that plastic deformation may be produced in the act of polishing diamond. This would have an important bearing on theories of the mechanism of the polishing of diamond.

We wish to thank Dr. F. P. Bowden for his advice and encouragement, Mr. J. A. Chapman for taking electron diffraction photographs. Mr. A. Kelly of the Cavendish Laboratory for taking back reflection Laue photographs, Mr. A. R. Barringer of Imperial College for assistance in mounting the specimens and Mr. P. Grodzinski for repolishing the diamonds. Our thanks are also due to Messrs. Industrial Distributors (1946) Ltd., for a maintenance grant (M. S.) and for the loan of the diamonds and to the Managers of the I.C.I. Fellowship Fund for the award of a Fellowship (J. W. M.).

References

von Borries, B., 1940, *Z. Physik*, **116,** 370.
Ennos, A. E., 1953, *Brit. J. Appl. Phys.*, **4,** 101.
Menter, J. W., 1952, *J. Inst. Metals*, **81,** 163 ; 1953, *J. Phot. Sci.*, **1,** 12.
Tolansky, S., and Omar, M., 1953, *Phil. Mag.*, **44,** 514.
Williams, A. F., 1932, *The Genesis of Diamond* (London: Benn), p. 462.

Fig. 1

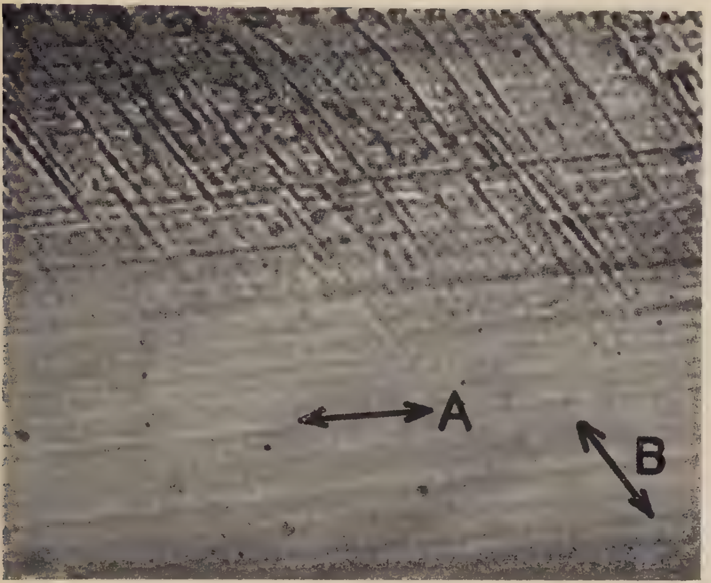

Optical micrograph of contaminated diamond surface. A=direction of polishing marks and incident beam, B=lines probably due to slip. ×850

Fig. 2

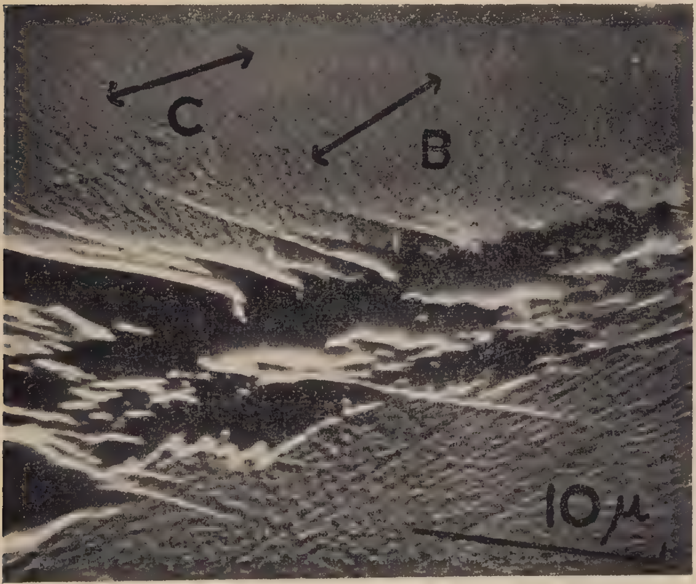

Reflection electron micrograph of gross scratch on diamond. B=polish marks, C=lines probably due to slip.

CL. *Notices of New Books and Periodicals received*

The Stability of Rotating Liquid Masses. By R. A. Lyttleton. [Pp. vii+150.] (Cambridge University Press.) Price 35*s.*

The forms of gravitating fluid masses in steady rotation and their stability have been the subject of many monumental papers. The present book explains the leading principles and results, while referring to the original papers for some of the details of the calculation. The theory of the exchange of stabilities, developed by Poincaré for these problems, has much wider application, and the account of it here is the clearest yet given. The account of ellipsoidal harmonics, though much shorter than those in the original papers and in Hobson's book, is full enough for the purpose and should be useful to specialists in other fields.

The outstanding results of the theory are that of Poincaré, that the triaxial ellipsoid becomes secularly unstable at a certain speed of rotation; that of Liapounoff and Jeans, that when this speed is slightly exceeded there is no neighbouring configuration that is secularly stable; and that of Cartan, that when the Jacobi figure becomes secularly unstable it simultaneously becomes ordinarily unstable. Jeans had overlooked this possibility, saying that secular instability must always occur first. The importance of Cartan's result was first noticed by Lyttleton. Ordinary instability implies that a small disturbance will increase rapidly without oscillation, and further examination shows that the only possible final state is one where the fragments separate with a hyperbolic velocity. A star acquiring too high a rotation as it condenses cannot become a binary star; it would become two independent stars. The fission theory of the formation of binary stars must be abandoned.

The original papers, apart from their unavoidable difficulty, are obscure in some places and inconsistent in others, and Lyttleton's careful study of their interpretation is a valuable clarification.

H. J.

Luminescence and the Scintillation Counter. By S. C. Curran, F.R.S. (Butterworths Scientific Publications, London, 1953.) [Pp. 205+xciii.] Price 32*s.* 6*d.*

The extensive development and use of the scintillation counter in nuclear physics has for some time warranted a detailed treatment of the counter and its principles. The present volume amply fulfills that need. The author is well qualified for the task. He was one of the first physicists to 'modernize' the spinthariscope by inclusion of a photoelectric multiplier to record the emission due to single alpha particles. One of the features of the text is that it treats both the operational characteristics and the fundamental processes in each component of the counter in some detail, prefaced by a valuable chapter on the interaction of the various nuclear particles and high energy radiation with matter. Such subjects as limiting sensitivity and time and energy resolution of the counter and the detailed characteristics of inorganic and organic phosphors, inclusive of liquid and plastic scintillators, are given full discussion. A comprehensive though brief account of applications of the counter to radiation detection and energy measurement is given in a later chapter. As additional topics the text includes a description of the application of photomultipliers to direct detection of particles and a treatment of some electrical circuits involved in the use of scintillation counters, such as those for short time resolution, fast scaling and pulse magnitude discriminators and analysers. Full and up to date references are given at the end of each chapter and name and subject indices at the end of the text. There is no doubt that this volume will be a valuable asset to every nuclear physics laboratory, since within its compass it includes information which up to the present has been widely scattered in original papers. Its value is also enhanced by the proper connection it makes between the physics of constituent parts of the scintillation counter and the application of the whole, a conjunction which will greatly assist in assessing the possibilities of the counter for any specific use.

G. F. J. G.

Modern Radiochemical Practice. By G. B. Cook and J. F. Duncan. (Oxford: Clarendon Press, 1952.) [Pp. xx+407.] Price 42*s*.

This book by two members on the staff of the Atomic Energy Research Establishment at Harwell is a good example of the impossibility of separating, in the science of radioactivity, the spheres of interest of chemists and physicists. It is called *Modern Radiochemical Practice*, but a very considerable part is devoted to the discussion of subjects which a chemist of the old school would consider as pure physics, as, for instance, the radiations emitted by radioactive material, the methods of their measurement and the determination of their energy, and the description of very special electronic equipment. However, the authors are certainly right in assuming that no laboratory interested in radiochemical work can be confident of obtaining reliable results unless at least one of the workers—perhaps, best of all, a physicist—is fully acquainted with the theory and practice of the measuring apparatus, and nobody will, therefore, object to the inclusion of this material, even if the title of the book seems to restrict its contents to 'radiochemical' practice. (The further qualification, 'modern', might well have been omitted; surely no one would suspect that a publication by two Harwell men and the Clarendon Press, appearing in first edition in 1952, might be old-fashioned.)

The book is meant principally as a guide for those who want to apply 'radioelements as indicators', as one used to say in earlier days, or 'isotopes as tracers', as the modern parlance prefers. The substitution of the word 'tracer' for 'indicator' seems to be an advantage because the new term is more restricted and precise; on the other hand the meaning of 'isotopes' as understood by the authors is hardly to be recommended as it is bound to lead to contradictions. This technical term was coined by F. Soddy to denote two different species of atoms belonging to the same element and thus occupying 'the same place' in the Periodic System; but the authors have adopted the recent loose habit of calling every radioactive species an isotope; so for instance when they append to the text of their book a table, not of 'atomic species' or 'nuclides', but of 'isotopes', or when they speak of 'isotopes of the same element'. In other places, however, they are quite aware of the strict meaning of isotopes; e.g. if they discuss the 'separation of isotopes', or explain the method of 'isotopic dilution'. Let us hope that the term 'nuclide', now widely accepted in the U.S.A., will also in the English literature replace the use of 'isotope' in the broader sense, thus restoring this indispensable term to its accurate original meaning.

A special feature of the book is the last chapter, 'Suggested experiments with radioactive material'. Here thirty very different experiments are described in sufficient detail for the introduction of beginners who will be grateful for the many practical hints included. It is obvious that the wide experience of the authors has enabled them to produce a book which will be found very valuable by scientists in many fields who intend to use radioelements as tracers.

F. A. P.

Fluorescence of Solutions. By E. J. Bowen and F. Wokes. (Longmans, Green & Co., Ltd.) [Pp. 90.] Price 25*s*. net.

This book takes the form of a useful monograph for students and practical workers who need an elementary introduction to the subject. It avoids detailed mathematical proofs and devotes considerable space to the methods and practical side of measurements.

[*The Editors do not hold themselves responsible for the views expressed by their correspondents.*]

INDEX TO VOL. 44.

ABSORPTION, gases, high saturations (Bowers), 467, 485.
Alkali halides, instability and melting (Thompson), 131.
—— ——, polarization fields etc., (Krishnan and Roy), 19.
Alpha particles from $^{10}B+D$ (Treacy), 325.
—— —— from $^7Li(p, \alpha)$ (Cartwright *et al.*), 1307.
α (Al–Fe–Si), x-ray examination (Robinson and Black), 1392.
$^{27}Al(\alpha, p)^{30}Si$, p^{31} levels (Roy and Godeau), 1184.
Ambler (E.), Grace (M. A.), Halban (H.), Kurti (N.), Durand (H.), Johnson (C. E.) and Lemmer (H. R.), nuclear polarization of cobalt 60, 216.
Amelinckx (S.), growth of crystals, 337.
——, slip lines and etchpits, 1048.
——, *see* Dekeyser, 1142.
Appelbe (B.), *see* Kay, 105.
Armenteros (R.), Barker (K. H.), Butler (C. C.), Coates (M. S.) and Sowerby (M. G.), mass of V_1^0-particle, 861.
As, β–γ correlation (Rose), 739.
^{79}As–^{79m}Se, in slow neutron fission (Cuninghame), 900.
Astbury (J. P.), Buchanan (J. S.), Chippindale (P.), Millar (D. D.), Newth (J. A.), Page (D. I.), Rytz (A.) and Sahiar (A. B.), charged V-particles, mean life, 242.
—— ——, James (G. D.), Millar (D. D.), Newth (J. A.), Page (D. I.), Sahiar (A. B.) and Rytz (A.), neutral V-particle, 352.
Atmospheric wave-forms (Morrison), 980.
Baltensperger (W.), conduction in impurity bands, 1355.
Barium titanite single crystals, properties (Cross), 1161.
Barker (J. R.), Dobbs (E. R.) and Jones (G. O.), elasticity of solid argon, 1182.
Barker (K. H.), Sard (R. D.) and Sowerby (M. G.), V-particle decays, use of neutron counters, 46.
——, *see* Armenteros, 861.
Barkla (H. M.) and Finlayson (D. M.), properties of KH_2PO_4 below Curie point, 109.
Bartlett (M. S.), statistical estimation of mean life-times, 249.
——, mean lifetimes from multiplate cloud chamber tracks, 1407.
Basinski (Z. S.) and Christian (J. W.), cobalt, martensitic transformation, 791.
Bauschinger effect in cubic metals (Woolley), 597.
Bell (G. M.), regular binary assemblies, second neighbour interaction, 65.
Bellamy (E. H.) and Smith (K. F.), nuclear spins and magnetic moments, alkali elements, 33.
Beryllium, conductivities (Powell), 645.
——, specific heat, low temperatures (Hill and Smith), 636.
Bijl (D.) and Rose-Innes (A. C.), paramagnetic resonance absorption, temperature change, 1187.
Bijvoet (J. M.) and Lonsdale (K.), ionic state of LiH, 204.
Bilby (B. A.), mutual transformation of lattices, 782.
Bird (L.), *see* Salter, 1305.
Bishop (J. F. W.), plastic deformation of crystals by glide, 51.
Black (F. A.), decay in fluorescence on irradiation by particles and photons, 263.
Black (P. J.), see Robinson, 1392.
Bombardment of Cu_3Au (Dixon, Meechan and Brinkman), 449.

Books, new :—Batchelor, Theory of homogeneous turbulence, 675 ; Beck, Method of Descartes, 564 ; Bickley *et al.*, Mathematical tables (Vol. X), 564 ; Blatt and Weisskopf, Theoretical nuclear physics, 356 ; Bosworth, Heat transfer phenomena, 676 ; Bowen and Wokes, Fluorescence of solutions, 1412 ; Chalmers, Progress in metal physics, 108 ; Cook and Duncan, Modern radiochemical practice, 1412 ; Curran, Luminescence and the scintillation counter, 1411 ; Ditchburn, Light, 356 ; Feather, Nuclear stability rules, 231 ; Frisch, Progress in nuclear physics, 794 ; Glasstone and Edlund, Nuclear reactor theory, 924 ; Grew and Ibbs, Thermal diffusion in Gases, 564 ; Hill and Baldwin, Journal of Mechanics, 231 ; Hume-Rothery, Christian and Pearson, Metallurgical equilibrium diagrams, 108 ; Jones, Short table Bessel functions, 108 ; Kolsky, Stress waves in solids, 793 ; Lyttleton, Stability of rotating liquid masses, 1411 ; Pankhurst and Holder, Wind tunnel technique, 232 ; Reports on progress in physics, 924 ; Riemann, Vacuum technique, 794 ; Rosenhead, Compressible flow, tables, 232 ; Shoenburg, Superconductivity, 793 ; Stanley and Wilkes, Table, reciprocal Gamma function, 676 ; Sutton, Micrometeorology, 795 ; Tintner, Econometrics, 108 ; Urey, The planets, 107 ; Weyl, Symmetry, 675.

Boron, bombardment by α-particles (Shire *et al.*), 1197.

Bose–Einstein condensation in helium films (Ziman), 548.

Bowe (P. W. A.), radio atmospherics received simultaneously, 833.

Bowers (R.), absorption of gases at high saturations, 467, 485.

——, helium II film, saturated, thickness, 1309.

Boyle (A. J. F.), *see* Inall, 1081.

Bradfield (G.) and Pursey (H.), preferred orientation in elasticity, 437.

Breitenberger (E.), single-channel kicksorter, 987.

Brewer (D. F.) and Mendelssohn (K.), formation of helium film, 340.

—— ——, helium II, anomalous surface tension, 559.

—— —— ——, absorption, 789.

Brickstock (A.) and Pople (J. A.), spatial correlation of electrons in atoms and molecules, 697, 705.

Brinkman (J. A.), *see* Dixon, 449.

Buchanan (J. S.), *see* Astbury, 242, 352.

Budden (K. G.), propagation of very low frequency radiowaves, 504.

Burcham (W. E.), protons of intermediate energy, range–energy in air, 211.

Burton (W. K.) and Touschek (B. F.), commutation relations in Lagrangian Q mechanics, 161.

—— ——, Schwinger's dynamical principle, 1180.

Butcher (P. N.), multi-stream electrodynamic field equations, 971.

Butement (F. D. S.), μ-meson capture by carbon, spectrum of radiation, 208.

Butler (C. C.), *see* Armenteros, 861.

Campbell (I. J.), wave motion in annular tank, 845.

Caro (D. E.) and Hibbard (L. U.), Synchrotron control, 964.

Cartwright (D. K.), Green (L. L.) and Willmott (J. C.), α particles from ^{7}Li(p, α), 1307.

Carver (J. H.), Edge (R. D.) and Wilkinson (D. H.), reaction ^{181}Ta(γ, 2n)^{179}Ta, 404.

—— and Hay (H. J.), ^{181}Ta(γn)^{180}Ta, cross section at 17·6 Mev, 1191.

Cassels (J. M.), *see* Randle, 425.

Cauchois (Y.), L spectrum of nickel and copper, 173.

Cerium magnesium nitrate.—I (Cooke, Duffus and Wolf), 623.

—— ——.—II (Daniels and Robinson), 630.

Chamberlain (A. C.), iodine 131, deposition from airstream, 1145.

Chandrasekhar (S.), convection by thermal instability in spherical shells, 233, (correction) 1129.

Charlesby (A.), long-chain polymers, equations of state, 578.

Chester (P. F.) and Jones (G. O.), superconductivity at very high pressures, 1281.

Chippindale (P.), *see* Astbury, 242.

Christian (J. W.), *see* Basinski, 791.

Clarebrough (L. M.), Hargreaves (M. E.) and West (G. W.), deformed nickel, released energy, 913.

Clegg (A. B.), *see* Wilkinson, 1269.

Clegg (J. A.), *see* Closs, 313.

Closs (R. L.), Clegg (J. A.) and Kaiser (T. R.), meteor trails, radio reflections, 313.

Coates (M. S.), *see* Armenteros, 861.

Cobalt, martensitic transformation (Basinski and Christian), 791.

Cohen (A. V.), proton bombardment of ^{18}O, 583.

—— and French (A. P.), proton bombardment of ^{15}N, α distribution, 1259.

Cole (D. G.), *see* Gillam, 999.

Coles (B. R.), transition metals in alloys, electronic structure, 915.

Conduction in impurity bands (Baltensperger), 1355.

Convection in spherical shells (Chandrasekhar), 233, 1129.

Cooke (A. H.), Duffus (H. J.) and Wolf (W. P.), cerium magnesium nitrate above 1°K, 623.

Cosmic radiation, penetrating component (Pullar and Dymond), 565.

Cosmic rays underground.—I (Kannangara and Zivkovic), 797.

—— —— ——.—II (Goldsack and Kannangara), 811.

—— —— ——.—III (Kannangara and Shrikantia), 1091.

Cottrell (A. H.), Portevin–Le Chatelier effect, 829.

——, Hunter (S. C.) and Nabarro (F. R. N.), dislocation and solute atom, interaction, 1064.

Counters, stochastic problem (Ramakrishnan and Mathews), 1122.

Croft (A. J.), Faulkner (E. A.), Hatton (J.) and Seymour (E. F. W.), electrical resistance, gold, very low temperatures, 289.

Cross (L. E.), barium titanite single crystals, properties, 1161.

Crystallographic slip in diamond (Seal and Menter), 1408.

Crystal growth, dislocation (Amelinckx), 337.

Crystals, plastic deformation by guide (Bishop), 51.

Cuninghame (J. G.), ^{79}As–^{79m}Se in slow neutron fission, 900.

Cunliffe (A.) and Gould (R. N.), inverse perturbation, 785.

Dalitz (R. H.), nature of τ-meson, 1068.

Daniel (V.) and Turner (C.), nucleation in a dielectric, 1371.

Daniels (J. M.) and Robinson (F. N. H.), cerium magnesium nitrate below 1°K, 630.

Danysz (M.) and Pniewski (J.), delayed disintegration of nuclear fragment, 348.

Davis (G.), *see* Tidman, 350.

Debye specific heat, surface contribution (Stratton), 519.

Decay in fluorescence by irradiation (Black), 263.

Decock (H. J.), *see* Roy, 1189.

Deformed nickel, release of energy (Clarebrough, Hargreaves and West), 913.

Dekeyser (W.), Amelinckx (S.), Votava (E.) and Vandermeerssche (G.), 111 faces of ZnS crystals, 1142.

Delayed disintegration of nuclear fragment (Danysz and Pniewski), 348.

—— —— (Tidman *et al.*), 350.

Diffusion problems in crystal growth (Seeger), 1.

Dipolar lattice, polarization (Pople), 1276.

Disintegrations by 50–125 Mev protons (Hodgson), 1113.

Dislocation and solute atom, interaction (Cottrell, Hunter and Nabarro), 1064.

Dislocations, stable (Frank and Nicholas), 1213.

Dissanaike (G. A.), helium ions in metals, charge exchange, 1051.

Dixon (C. E.), Meechan (C. J.) and Brinkman (J. A.), ordered Cu$_3$Au, bombardment, 449.

Dobbs (E. R.), *see* Barker, 1182.

Duffus (H. J.), *see* Cooke, 623.

Dungey (J. W.), electrical discharges in astrophysical systems, 725.

Durand (D.), *see* Ambler, 216.

Dymond (E. G.), *see* Pullar, 565.
Edge (R. D.), *see* Carver, 404.
Elasticity of solid argon (Barker, Dobbs and Jones), 1182.
Electrical discharges, astrophysical (Dungey), 725.
Electrical resistance, gold, very low temperatures (Croft *et al.*), 289.
Electrical resistivity of liquid iron (Powell), 772.
Electrodynamic field equations (Butcher), 971.
E. M. Radiation from radium E (Martin and Parry), 344.
Estimation of mean lifetimes from multiplate cloud chamber tracks (Bartlett), 1407.
Exchange energy, nearly free electrons in metals (Wohlfarth), 281.
Fatigue cracks, growth (Head), 925.
Faulkner (E. A.), *see* Croft, 289.
Feather (N.), shell model of the nucleus, a new parameter, 103.
Ferguson (A. T. G.) and Lewis (G. M.), annihilation of positrons in solids, 1339.
——, *see* Lewis, 1011.
Finlayson (D. M.), *see* Barkla, 109.
Frank (F. C.), tin whiskers, 854.
—— and Nicholas (J. F.), stable dislocations in lattices, 1213.
Fremlin (J. H.), helium 3 reactions, 141.
French (A. P.), *see* Cohen, 1259.
Friedel (J.), rigidity, copper alloys, anomaly, 444.
Galbraith (W.) and Whitehouse (W. J.), negative μ-mesons, interaction with uranium, 77.
——, *see* Jelley, 619.
γ rays from ${}^{19}\mathrm{F}(\mathrm{p}, \alpha\gamma){}^{16}\mathrm{O}$ (Sanders), 1302.
γ-rays, use in low temperature colorimetry (Kurti and Simon), 501.
Gayther (D. B.), τ-meson, decay in flight, 1297.
Germanium diodes, thermal properties (Tillman and Henderson), 677.
Gibson (W. M.), Reaction ${}^{11}\mathrm{B}(\mathrm{d}, \mathrm{n}){}^{12}\mathrm{C}$, 297.
Gillam (E.) and Cole (D. G.), continuous phase transformations, 999.
Godeau (C.), *see* Roy, 1184.
Goldsack (S. J.) and Kannangara (M. L. T.), cosmic rays underground.—II, 811.
Gould (R. N.), *see* Cunliffe, 785.
Grace (M. A.), *see* Ambler, 216.
Green (L. L.), Scanlon (J. P.) and Willmott (J. C.), stripping at low energy, 919.
Green (L. L.), *see* Cartwright, 1307.
Gurari (M.), slow electrons in polar materials, self energy, 329.
Halban (H.), *see* Ambler, 216.
Ham (A. C.) and Jackson (L. C.), helium II film, visual observations, formation of bulk liquid, 214.
—— ——, rate of extension of the helium II film, 1403.
Hanbury Brown (R.) and Hazard (C.), radio-frequency radiation from the galaxy, 939.
Hargreaves (M. E.), *see* Clarebrough, 913.
Hatton (J.), *see* Croft, 289.
Hay (H. J.), *see* Carver, 1191.
Hazard (C.), *see* Hanbury Brown, 939.
Head (A. K.), dislocations and boundaries, 92.
——, growth of fatigue cracks, 925.
Heat conductivities of superconducting metals (Mendelssohn and Renton), 776.
Heating from γ-rays, low temperatures (Platzman), 497.
Hedges (J. M.) and Mitchell (J. W.), silver bromide, polyhedral substructures in crystals, 223.
—— ——, experiments in photographic sensitivity, 357.
Helium II, absorption (Long and Meyer), 788, (Brewer and Mendelssohn), 789.
——, anomalous surface tension (Brewer and Mendelssohn), 559.
——, film (Jackson and Henshaw), 14.
——, —— (Ham and Jackson), 214.
——, —— (Brewer and Mendelssohn), 340.
——, —— (Bowers), 1309.
Helium ions in metals, charge exchange (Dissanaike), 1051.
——, solid, thermal conductivity at high densities (Webb and Wilks), 664.
—— 3 reactions (Fremlin), 141.

Henderson (J. C.), *see* Tillman, 677.
Henshaw (D. G.), *see* Jackson, 14.
Herz (A. J.), Hodgson (P. E.) and Tennant (R. M.), production of τ-mesons in ice, 85.
Herz (A. J.), *see* Tidman, 350.
High energy bremsstrahlung, polarization (Phillips), 169.
Hill (R. W.) and Smith (P. L.), beryllium, specific heat at low temperatures, 636.
Hitchcock (A. J. M.), pairing energy in $j-j$ coupling, 766.
Hodgson (P. E.), disintegrations by 50–125 MEV protons, 1113.
——, *see* Herz, 85.
Holtebekk (T.), Isachsen (N.) and Sörensen (S. O.), nuclear explosions, helium isotopes, 1037.
Hooper (J. E.), photon component, 70 000 feet, 871.
Hughes, (J. B.), paper by Tzou, 1300.
Hume-Rothery (W.), metallic carbides and nitrides of type MX, 1154.
Hunter (S. C.), *see* Cottrell, 1064.
Illingworth (C. R.), laminar boundary layer, rotating body, 389.
Inall (E. K.) and Boyle (A. J. F.), γ-rays from ^{7}Li(pγ) ^{8}Be(α) ^{4}He, 1081.
Interaction of dislocations and boundaries (Head), 92.
—— of negative μ-mesons with uranium (Galbraith and Whitehouse), 77.
Inverse perturbation (Cunliffe and Gould), 785.
Iodine 131, deposition (Chamberlain), 1145.
Ionic state of LiH (Bijvoet and Lonsdale), 204.
Ionized gas, collisional effects (Westfold), 712.
Isachsen (N.), Vangen (V.) and Sörensen (S. O.), direct production of κ-mesons, 224.
——, *see* Holtebekk, 1037.
Isotopic spin selection rules.—I (Wilkinson and Jones), 542.
—— —— ——.—II (Wilkinson), 1019.
—— —— ——.—III (Wilkinson and Clegg), 1269, 1322.
Jackson (L. C.) and Henshaw (D. G.), helium II film, further observations, 14.
——, *see* Ham, 214, 1403.
j–j Coupling, pairing energy (Hitchcock), 766.
James (G. D.), *see* Astbury, 352.
Jelley (J. V.) and Galbraith (W.), light pulses from night sky, 619.
Johnson (C. E.), see Ambler, 216.
Jones (G. A.), *see* Wilkinson, 542.
Jones (G. O.), *see* Barker, 1182.
——, *see* Chester, 1281.
Jones (H.), valency of transition metals in alloys, 907.
Kaiser (T. A.), *see* Closs, 313.
Kannangara (M. L. T.) and Shrikantia (G. S.), Cosmic rays underground.—III, 1091.
——, and Zivkovic (M.), cosmic rays underground.—I, 797.
——, *see* Goldsack, 811.
κ-mesons direct production (Isachsen, Vangen and Sörensen), 224.
κ_1-meson, mass (Kristiansson), 268.
Kay (H. F.) and Applebe (B.), surface of beryl and cadmium iodide crystals, 105.
Keith (H. D.) and Mitchell (J. W.), reduction of silver bromide crystals, 877.
Kicksorter, precision (Breitenberger), 987.
Krishnan (Sir K. S.) and Roy (S. K.), polarization fields and resonance frequencies, alkali halides, 19.
Kristiansson (K.), mass of κ_1-meson, 268.
Kurti (N.) and Simon (F. E.), γ-rays in low temperature colorimetry, 501.
——, *see* Ambler, 216.
Lagasse (A.), *see* Roy, 1189.
Lagrangian Q mechanics, commutation relations (Burton and Touschek), 161.
Laminar boundary layer (Illingworth), 389.
Lawson (J. D.), transparency of nuclei to neutrons (diffraction effect), 102.
Lees (C. F.), Morrison (G. C.), Muirhead (H.) and Rosser (W. G. V.), star production by 130 MEV protons, 304.

Lemmer (H. R.), *see* Ambler, 216.
Leontic (B.) and Wolfendale (A. W.), μ-mesons in lead, anomalous scattering, 1101.
Lewis (G. M.) and Ferguson (A. T. G.), positrons, annihilation, 1011, 1339.
Light pulses from night sky (Jelley and Galbraith), 619.
Lindhard (J.), resistance-independent absorption of light by metals, 916.
Lindsay-Jones (G.), *see* Shire, 1197.
^{7}Li(pγ) ^{8}Be(α) ^{4}He, γ-rays, (Inall and Boyle), 1081.
Long (E.) and Meyer (L.), adsorption of helium on glass, 788.
Lonsdale (K.), *see* Bijvoet, 204.
Lundén (A.), *see* Shire, 1197.
MacDonald (D. K. C.) and Roy (S. K.), thermoelectric power of monovalent metals at high temperature, 1364.
Magneto-hydrodynamic channel flow (Murgatroyd), 1348.
Mandl (F.) and Skyrme (T. H. R.), neutron cross sections, energy dependence, 1028.
March (N. H.), virial theorem in free electron and Thomas–Fermi models, 346.
——, Thomas–Fermi model, exchange, 1193.
Martin (D. G. E.) and Parry (G.), radiation from radium E, 344.
Mass estimation, range-scattering (Menon and O'Ceallaigh), 1291.
Mathews (P. M.), *see* Ramakrishnan, 1122.
Mean life-times, statistical estimation (Bartlett), 249.
Meechan (C. J.), *see* Dixon, 449.
Mendelssohn (K.), *see* Brewer, 340, 559, 789.
——, and Renton (C. A.), superconductive metals, heat conductivities, 776.
Menon (M. G. K.) and O'Ceallaigh (C.), mass estimation, range-scattering method, 1291.
Menter (J. W.), *see* Seal, 1408.
Metallic carbides and nitrides (Hume-Rothery), 1154.
Meteor trails, radio reflections (Closs, Clegg and Kaiser), 313.
Meyer (L.), *see* Long, 788.
Millar (D. D.) and Page (D. I.), Ω^0 decay, an unusual, 1049.
——, *see* Astbury, 242, 352.
Mitchell (J. W.), *see* Hedges, 223, 357.
——, *see* Keith, 877.
Morrison (G. C.), Muirhead (H.) and Rosser (W. G. V.), nuclear disintegrations by high energy protons, 1326.
——, *see* Lees, 304.
Morrison (R. B.), atmospheric waveforms, variation with distance, 980.
Mott (B. W.) and Williams (J.), thermal etching of uranium, 841.
Mott (N. F.), electronic structure of transition metals, 187.
——, work-hardening of metal (theory).—II, 742.
μ-meson capture by carbon, spectrum of radiation (Butement), 208.
μ-mesons in lead, anomalous scattering (Leontic and Wolfendale), 1101.
Muirhead (H.), *see* Lees, 304.
——, *see* Morrison, 1326.
Murgatroyd (W.), magneto-hydrodynamic channel flow, 1348.
Mutual transformation of lattices (Bilby), 782.
^{23}Na(p, $\alpha\gamma$) ^{20}Ne, angular correlations (Seed), 921.
Nabarro (F. R. N.), *see* Cottrell, 1064.
Neutrons by high energy protons (Randle *et al.*), 425.
Neutron cross sections (Mandl and Skyrme), 1028.
—— ——, 30–153 Mev (Taylor and Wood), 95.
Newth (J. A.), *see* Astbury, 242, 352.
Nicholas (J. F.), *see* Frank, 1213.
Nickel and copper, L spectrum (Cauchois), 173.
Nuclear disintegrations by protons (Morrison, Muirhead and Rosser), 1326.
—— explosions, helium isotopes, mass (Holtebekk, Isachsen and Sörensen), 1037.
—— polarization of cobalt 60 (Ambler *et al.*), 216.
—— spins and magnetic moments, alkali elements (Bellamy and Smith), 33.

Nucleation in a dielectric (Daniel and Turner), 1371.
O'Ceallaigh (C.), *see* Menon, 1291.
Omar (M.), *see* Tolansky, 514.
Ordered Cu_3Au, bombardment by electrons (Dixon, Meechan and Brinkman), 449.
Pack (D. C.) and Roberts (L.), flow of supersonic jet past wedge, 561.
Page (D. I.), *see* Astbury, 242, 352.
——, *see* Millar, 1049.
Paper by Tzou (Hughes), 1300.
Paramagnetic resonance, solutions (Bijl and Rose-Innes), 1187.
Parry (G.), *see* Martin, 344.
Phase transformations, continuous (Gillam and Cole), 999.
Phillips (K.), polarization of high energy bremsstrahlung, 169.
——, reaction ^{63}Cu (γn) ^{62}Cu, multiple resonances, 533.
Photographic sensitivity (Hedges and Mitchell), 357.
Photon component, 70 000 feet (Hooper), 871.
Pickavance (T. G.), *see* Randle, 425.
Planetary convection (Urey), 227.
Platzman (R. L.), heating from γ-rays at low temperatures, 497.
Pniewski (J.), *see* Danysz, 348.
Poole (M. J.), inelastic scattering of neutrons, 1398.
Polymers, equations of state (Charlesby), 578.
Pople (J. A.), dipolar lattice, polarization, 1276.
——, *see* Brickstock, 697, 705.
Portevin–Le Chatelier effect (Cottrell), 829.
Positrons, annihilation (Lewis and Ferguson), 1011.
——, —— (Ferguson and Lewis), 1339.
Powell (C. F.), tracks of charged particles, use of stripped emulsions, 219.
Powell (R. W.), beryllium, thermal and electrical conductivities, 645.
——, resistivity of liquid iron, 772.
Preferred orientation, elasticity (Bradfield and Pursey), 437.
Properties of KH_2PO_4 below Curie point (Barkla and Finlayson), 109.
Proton bombardment of ^{15}N, α distribution (Cohen and French), 1259.
—— —— of ^{16}O (Cohen), 583.
——, multiple scattering in thin foils (Skyrme), 191.
——, range-energy in air (Burcham), 211.
Pullar (J. D.) and Dymond (E. G.), cosmic radiation in upper atmosphere, penetrating component, 565.
Pursey, *see* Bradfield, 437.
Quantum dynamical principle (Schwinger), 1171.
Radiative width, dipole transitions (Wilkinson), 450.
Radio atmospherics (Bowe), 833.
Radio-frequency radiation, galaxy (Brown and Hazard), 939.
Radio waves, very low frequency, propagation (Budden), 504.
Ramakrishnan (A.) and Mathews (P. M.), counters, stochastic problem, 1122.
Randle (T. C.), Cassels (J. M.), Pickavance (T. G.) and Taylor (A. E.), neutrons by high energy protons, 425.
Rate of extension, method for the determination, of the helium II film (Ham and Jackson), 1403.
Reaction $^{11}B(d, n)^{12}C$ (Gibson), 297.
—— ^{9}Be (p, p2n) ^{7}Be (Salter and Bird), 1305.
—— ^{63}Cu (γn) ^{62}Cu, multiple resonances (Phillips), 533.
—— ^{18}O ($p\alpha$) ^{15}N (Roy, Lagasse and Decock), 1189.
—— ^{181}Ta (γ, 2n) ^{179}Ta, (Carver, Edge and Wilkinson), 404.
Regular binary assemblies, second order interactions (Bell), 65.
Renton (C. A.), *see* Mendelssohn, 776.
Resistance-independent absorption of light by metals (Lindhard), 916.
Rigidity, copper alloys, anomaly (Friedel), 444.
Roberts (L.), *see* Pack, 561.
Robinson (F. N. H.), *see* Daniels, 630.
Robinson (K.) and Black (P .J.), α(Al–Fe–Si), x-ray examination, 1392.
Rose (H.), ^{76}As, β–γ correlation, 739.

Rose-Innes (A. C.), *see* Bijl, 1187.
Rosser (W. G. V.), *see* Lees, 304.
——, *see* Morrison, 1326.
Roy (R. R.) and Godeau (C.), Al (α, p) Si, width of levels p^{31}, 1184.
Roy (R. R.), Lagasse (A.) and Decock (M. J.), reaction ^{18}O (p α) ^{15}N, 1189.
Roy (S. K.), *see* Krishnan, 19.
——, *see* MacDonald, 1364.
Rudstam (S. G.), spallation of vanadium, manganese and cobalt, 1131.
Rytz (A.), *see* Astbury, 242, 352.
Sahiar (A. B.), *see* Astbury, 242, 352
Salter (D. C.) and Bird (L.), reaction ^{9}Be (p, p2n) ^{7}Be, 1305.
Sanders (J. E.), γ rays from ^{19}F (p, $\alpha\gamma$) ^{16}O, 1302.
Sard (R. D.), *see* Barker, 46.
Scanlon (J. P.), *see* Green, 919.
Schwinger (J.), quantum dynamical principle, 1171.
Schwinger's dynamical principle (Burton and Touschek), 1180.
Seal (M.) and Menter (J. W.), crystallographic slip in diamond, 1408.
Seed (J.), angular correlations, ^{23}Na (p, $\alpha\gamma$) ^{20}Ne, 921.
Seeger (A.), diffusion in crystal growth from dilute solution, 1.
Seymour (E. F. W.), *see* Croft, 289.
Shell model of the nucleus, a new parameter (Feather), 103.
Shire (E. S.), Wormald (J. R.), Lindsay-Jones (G.), Lundén (A.) and Stanley (A. G.), bombardment of boron by alpha-particles, 1197.
Shrikantia (G. S.), *see* Kannangara, 1091.
Silver bromide crystals, reduction (Keith and Mitchell), 877.
—— —— ——, sub-structures (Hedges and Mitchell), 223.
Simon (F. E.), *see* Kurti, 501.
Skyrme (D. M.), multiple scattering of protons in thin foils, 191.
Skyrme (T. H. R.), *see* Mandl, 1028.
Slip lines and etchpits (Amelinckx), 1048.
Slip in diamond (Tolansky and Omar), 514.
Slow electrons in polar materials, self energy (Gurari), 329.
Smith (A. D. N.), Young's modulus of copper, cold work, 453.
Smith (K. F.), *see* Bellamy, 33.
Smith (P. L.), *see* Hill, 636.
Sörensen (S. O.), *see* Isachsen, 224.
——, *see* Holtebekk, 1037.
Sowerby (M. G.), *see* Barker, 46.
——, *see* Armenteros, 861.
Spallation of Va, Mn and Co (Rudstam), 1131.
Spatial correlation of electrons in molecules (Brickstock and Pople), 697, 705.
Star production by 130 Mev, cross section (Lees *et al.*), 304.
Stanley (A. G.), *see* Shire, 1197.
Stratton (R.), Debye specific heat, surface contribution, 519.
——, surface free energy of metal, 1236; superconducting, 1247.
Stripping reaction at low energy (Green, Scanlon and Willmott), 919.
Superconductivity at very high pressures (Chester and Jones), 1281.
Supersonic jet past wedge (Pack and Roberts), 561.
Surface free energy of metal (Stratton), 1236, 1247.
Surface of beryl and cadmium iodide crystals (Kay and Appelbe), 105.
Synchrotron control (Caro and Hibbard), 964.
^{181}Ta (γn) ^{180}Ta, cross section (Carver and Hay), 1191.
τ-meson, decay in flight (Gayther), 1297.
——, nature (Dalitz), 1068.
——, production in ice (Herz, Hodgson and Tennant), 85.
Taylor (A. E.) and Wood (E.), neutron cross sections, 30–153 Mev, 95.
——, *see* Randle, 425.
Tennant (R. M.), *see* Herz, 85.
——, *see* Tidman, 350.
Thermal etching of uranium (Mott and Williams), 841.
Thermoelectric power at high temperature (MacDonald and Roy), 1364.
Thomas–Fermi model, exchange (March), 1193.
Thompson (J. H. C.), alkali halides, instability and melting, 131.

Tolansky (S.) and Omar (M.), slip found in diamond, 514.
Tin whiskers (Frank), 854.
Tidman (D. A.), Davis (G.), Herz (A. J.) and Tennant (R. M.), delayed disintegration of nuclear fragment, 350.
Tillman (J. R.) and Henderson (J. C.), thermal properties of germanium diodes, 677.
Touschek (B. F.), *see* Burton, 161, 1180.
Tracks of charged particles, stripped emulsions (Powell), 219.
Transition metals, electronic structure (Mott), 187.
—— —— in alloys (Coles), 915.
Transparency of nuclei to neutrons, diffraction effect (Lawson), 102.
Treacy (P. B.), alpha particles from $^{10}B+D$, 325.
Turner (C.), *see* Daniel, 1371.
Unusual Ω^0 decay (Millar and Page), 1049.
Urey (H. C.), planetary convection applied to the earth, 227.
V-particle decay, use of neutron counters (Barker, Sard and Sowerby), 46.
——, charged, mean life (Astbury *et al.*), 242.
——, neutral (Astbury *et al.*), 352.
$V_1{}^0$-particle, mass (Armenteros *et al.*), 861.
Valency of metals in alloys (Jones), 907.
Vandermeerssche (G.), *see* Dekeyser, 1142.
Vangen (V.), *see* Isachsen, 224.
Velocities of fundamental particles (Whyte), 1303.
Virial theorem in models (March), 346.
Votava (E.), *see* Dekeyser, 1142.
Wave motion in annular tank (Campbell), 845.
Webb (F. J.) and Wilks (J.), solid helium, thermal conductivity at high densities, 664.
West (G. W.), *see* Clarebrough, 913.
Westfold (K. C.), collisional effects in ionized gas, 712.
Whitehouse (W. J.), *see* Galbraith, 77.
Whyte (L. L.), velocities of fundamental particles, 1303.
Wilkinson (D. H.), radiative width, dipole transitions, light elements, 450.
——, *see* Carver, 404.
——, isotopic spin selection rules, 1019; with Jones (G. A.), 542; with Clegg (A. B.), 1269, 1322.
Wilks (J.), *see* Webb, 664.
Williams (J.), *see* Mott (B. W.), 841.
Willmott (J. C.), *see* Cartwright, 1307.
——, *see* Green, 919.
Wohlfarth (E. P.), exchange energy of nearly free electrons in metals, 281.
Wolfendale (A. W.), *see* Leontic, 1101.
Wolf (W P.), *see* Cooke, 623.
Wood (E.), *see* Taylor, 95.
Woolley (R. L.), Bauschinger effect in cubic metals, 597.
Work-hardening of metals, theory (Mott), 742.
Wormald (J. R.), *see* Shire, 1197.
Young's modulus, cold work, (Smith), 453.
Zivkovic (M.), *see* Kannangara, 797.
Ziman (J. M.), Bose–Einstein condensation in helium films, 548.
ZnS crystals, 111 faces (Dekeyser *et al.*), 1142.

END OF THE FORTY-FOURTH VOLUME

Printed by Taylor & Francis, Ltd.
Red Lion Court, Fleet Street, London, E.C.4

U. of Haw.